

Dear Dr Schymanski,

Thank you again for your comments. We have addressed them and those of the reviewer, particularly with reference to the interdependence of air temperature and LW radiation and the effect this will have on the calculation of PET. We have tabulated the response to your comments below.

We decided against reformulating the second attribution using net LW (and net SW) and instead have expanded the discussion of the validity of the use of air temperature to approximate surface temperature. This is largely because calculation of net radiation requires information about the surface (albedo and emissivity), which are parameters that are chosen when defining the surface for which the PET is calculated. We are rather interested in how the particular chosen PET is dependent on purely meteorological variables. We also think that the discussion of the use of air temperature to approximate surface temperature reads better when considering the upwelling LW as a function of temperature, rather than as a driving variable.

Regards,

Emma Robinson on behalf of the authors

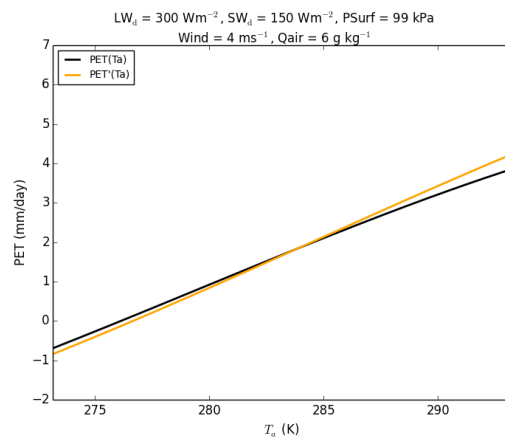
Editor comment	Author response
I am not sure I would agree with the referee's strong opinion about relative humidity being constant as the climate warms, as this may only apply over the oceans (see the wording in Schneider et al., 2010). However, I do agree that it is difficult to separate the effects of air temperature and humidity and therefore I wonder if it might be beneficial for the reader to see attribution based on assuming constant absolute and relative humidity as well as constant vapour pressure deficit, accompanied by a short discussion of the interdependency between air temperature and humidity.	After reflection we decided not to add any extra attributions to the paper, but we have expanded the discussion of the interdependency of air temperature and humidity. As part of this we have added discussion of expected trends in Rh (that it's expected not to change much overall, but that this may vary regionally over land) and references as requested by the reviewer. (Section 4.4)
I would like to re-emphasise the reviewer's point about inconsistent consideration of air temperature effects in the radiative component. On L347-350, you explain that the available energy (A) is computed as absorbed shortwave plus absorbed downwelling longwave minus emitted longwave, assuming that surface temperature is equal to air temperature. Obviously, replacement of surface temperature by air temperature is a gross simplification and it needs to be pointed out clearly that this may lead to artefacts. For example, on L591, you explain that increasing air temperature "decreases the radiative component (due to	The assumption that the upwelling LW can be calculated with air temperature as an approximation of surface temperature is indeed a strong simplification and may lead to artefacts. When the air temperature is greater than (less than) the surface temperature, the outgoing LW is over (under) estimated, therefore the net radiation is under (over) estimated, and so the radiative component of the PET is under (over) estimated.  In the absence of information about the surface temperature, a more thorough treatment is to linearise the net radiation as well as the latent and sensible heat fluxes, resulting in an adjusted

**Editor comment**

increasing outgoing LW radiation)", whereas a few lines later you clarify that "downward LW radiation is also proportional to the air temperature so that increases in downward LW broadly cancel the increasing outgoing LW radiation". My impression is that the net effect of air temperature on the radiative component in your analysis is likely an artefact of the simplifications inherent in your estimation of incoming and outgoing longwave. Although it may be justifiable, in the context of previous studies, to present the results as you did, I would urge you to mention this problem prominently in the description of the results (e.g. L633) and in the discussion. See also the referee's comment about L562-563, and his proposed way of considering the problem in hess-520-referee-report-1.pdf, attached to his review. I quite like the idea of first presenting results based on common methods and then present a new set of results based on an improved method, accompanied by a critical discussion of the approach. I leave the choice up to you, but the paper definitely needs an adequate discussion of the deficiencies in the longwave calculations due to lacking knowledge about surface temperature.

**Author response**

Penman-Monteith equation which implicitly solves the surface energy balance by including the net radiation (Monteith, 1981; Thompson et al., 1981). This effectively has an extra resistance,  $r_R$ , which represents the resistance to LW radiative transfer between the surface and the measurement height, and the net radiation is still calculated using air temperature to find an "isothermal flux density" – the net radiation which would be received if surface temperature were equal to air temperature (Monteith, 1981). As we are using the air temperature to calculate upwelling LW in this study, ideally this adjusted PM equation should have been used and for future studies we will look into implementing it fully. However, for the present study, the difference between the two is relatively small. For typical UK conditions we find that it makes a difference of a few percent to the calculated PET, see the figure below for an example, which shows the PM equation as we have calculated it in the paper (black) and the adjusted PM equation (orange) for typical UK conditions and for daily mean air temperature between 0C and 20C. We find a slightly stronger dependence of the adjusted PET on air temperature, so we may be underestimating the effect of temperature change on PET, although this is likely to be small.



We have added a brief discussion of this to the text (Section 3 after Eq 8, Section 4.3).

In addition, we have added further discussion of the effect of treating the LWdown as an independent variable and LWup as a function of temperature, as recommended by the reviewer. (Section 4.3)

Editor comment	Author response
<p>I am also a bit puzzled about the derivatives in Appendix C, as mentioned below. Could you please check that they are correct (especially wind speed) and explain in the paper how they were obtained? If they are not verifiably correct, this could shed doubt on the whole attribution section.</p>	<p>I have written a summary which gives more details of the steps in the calculation of these derivatives. This can be found after the response to the reviewer below. As part of our study we also verified them by comparing with numerical approximations of the derivatives and are satisfied that they are correct.</p>

Additional editor comments	Author response
<p>L323: double word: "that that"</p>	<p>This has been fixed</p>
<p>L 589-592: I would firstly remove the comment that increased air temperature increases the aerodynamic component of PET "as it makes the air more able to hold water", and secondly clarify that the decrease of the radiative component is due to the assumption that surface temperature equals air temperature, which is a gross simplification. The effect of air temperature on PET (or ET) is through the surface energy balance, by its effect on sensible heat flux, as explained in Schymanski &amp; Or (2016, PCE 39(7): 1448-1459). Given the simplifications about the surface energy balance in this study, I would be careful not to over-interpret the results. It is probably too late now to suggest removing the distinction between radiative and aerodynamical components, but I really think that the reader would benefit from a critical discussion of this distinction given the simplifications used here and elsewhere in the literature.</p>	<p>Yes, we have removed the comment that increased air temperature increases the aerodynamic component of PET "as it makes the air more able to hold water".</p> <p>As mentioned above, ideally when using air temperature as an input to calculating net radiation, the adjusted Penman-Monteith PET (Monteith, 1981) would be used. In this adjusted formulation, the net radiation is included as part of solving the surface energy balance. Within this framework, the surface temperature is implicitly proportional to air temperature, plus a correction which is a function of air temperature plus other atmospheric variables.</p> <p>The current paper assumes that the difference between surface and air temperature is negligible, which is, as you point out, a gross assumption. Relaxing this would incur a different dependence of PET on air temperature, through the extra resistance term <math>r_R</math>. The adjusted PM equation is implicitly assuming a relationship between air temperature and surface temperature, so the radiative component is still a function of air temperature.</p> <p>For typical conditions in the UK, the difference between the two variants of PET is small. However, we do note that the assumption that surface and air temperature are equal is very strong and may lead to artefacts in this analysis, so we have added text to point this out. (Section 4.3)</p>

Additional editor comments	Author response
L471: You mentioned that you would adopt the wording proposed by G.P. Weedon here, but have not done so. Was this forgotten?	The discussion at L471 in the current draft (“...while in drier regions (England, English lowlands) the mean PET and PETI are higher than the precipitation for much of the summer...”) was not mentioned by GP Weedon. However, assuming that this comment is referring to the discussion of how the confidence intervals were calculated (at L477-481) then G P Weedon suggested that the text be changed to “the 95% confidence intervals of the slope were calculated specifically allowing for the non-zero lag-1 autocorrelation...”, which has already been implemented in the manuscript submitted in response to the initial reviews (8 <sup>th</sup> July 2016). (Section 4.1) Please let us know if there is something else we should change.
L614: "... to consider relative humidity (R_h) as the independent variable." I propose to add "as" so that the sentence does not imply that RH is indeed an independent variable.	Yes, we have changed this. (Section 4.4)
L628: The reference to Jenkins and Dai is probably misplaced here, as the reviewer pointed out.	We had put in a comparison with the relative humidity trends in Jenkins and Dai here, but moved it to the discussion without deleting the references. These have now been deleted.
L700: Echoing comment by G.P. Weedon: Please mention the magnitude (and confidence interval) of the trends seen in this data set.	I have added the trend in the MORECS sunshine hours to the previous paragraph. (Section 5)
L720: As the referee pointed out, something went wrong here with the references. Please fix this.	Yes, we have deleted these
L833: Eq. C1 appears wrong to me, as $r_a$ is a function of the square root of wind speed, so the derivative is not complete. Could you also describe the steps that led to the derivatives in C2-C7? I wasn't able to follow the derivations.	In Eq 10 we define aerodynamic resistance following Allen et al. (1998), so that it is a function of $1/\text{wind speed}$ . This is applicable for ET from vegetated surfaces in neutral conditions, and we use the specific parameters for the reference crop. The derivative is correct for this aerodynamic resistance formulation. As mentioned above, I have attached a summary of the calculations to illustrate this.

## References

- Allen, R. G., Pereira, L. S., Raes, D., and Smith, M.: Crop evapotranspiration - Guidelines for computing crop water requirements, Food and Agriculture Organization of the United Nations, Rome, Italy, FAO Irrigation and Drainage Paper, 1998.
- Monteith, J. L.: Evaporation and surface temperature, Quarterly Journal of the Royal Meteorological Society, 107, 1-27, 10.1002/qj.49710745102, 1981.

Thompson, N., Barrie, I. A., and Ayles, M.: The Meteorological Office rainfall and evaporation calculation system: MORECS, Meteorological Office, Bracknell, 1981.

Dear reviewer #2

Thank you once again for your invaluable input and suggestions for the paper. Although an interesting suggestion, we have decided not to re-implement the attribution with net LW but rather made the suggested changes to the text. We have tabulated the details of our response below.

Regards,

Emma Robinson on behalf of the authors

<b>Reviewer comment</b>	<b>Author response</b>
<p>This revision soundly implements my major RH vs. qa suggestion from last round and largely fixes the minor issues as well. The results are quite interesting in the new framework, and correspond rather well to the recent Spain results of Vicente-Serrano (this should perhaps be noted.) I recommend acceptance pending the following minor revisions. Almost all of these are just writing suggestions or typos stemming from the new revisions, and should be quick to address.</p>	<p>Thank you for the Rh suggestion, we believe that it has been a valuable addition to the paper. Ultimately we decided against using LWnet (and SWnet) in the second attribution section, and focus just on the relative humidity. However, we have amended the text in places to more fully discuss this interdependence of LW radiation and air temperature. We also have implemented your suggestions for text revisions and typo fixes.</p> <p>We have added a reference to the V-S paper. (Section 5)</p>
<p>Since several of the writing suggestions toward the end come from the decision to keep the temperature dependence of longwave radiation artificially split between the temperature and Ld contributions, I also remind the authors that they could still use net longwave if they choose... I still think this would simplify their story a lot. Again this would only be for attribution purposes, not for the main part of the paper. Eq C2 would be exactly the same, but it would now get multiplied by the trend in net longwave rather than the trend in Ld (so I guess it would be named <math>dEp/dLn</math> not <math>dEp/Ld</math>.) And Eqs C5,C7 would just be missing the term involving <math>-4\sigma T^3</math>. Other than that, exact same procedure. This would take a bit longer than just changing the writing, but could still be considered.</p> <p>Thanks again for this huge effort and excellent study!</p>	<p>We have decided to keep the downwelling LW as the variable in the second attribution. Therefore we have extended the discussion of the split between the LWup and LWdown components – details are in the responses below.</p>

Minor comments	Author response
243-244: Should change the text here to clarify that it makes a negligible difference in the calculated *PET and PETI*, not just the specific humidity. You explained this to me in your written response, but did not change the text to reassure the reader.	We have edited the text to include this. (End of Section 2.2)
(Why are there no lines numbered 339 through 369 - is a page missing?)	We have checked and there is no content missing. This must have been an error in the line numbering introduced when producing the marked up version in Word.
558-559 vs. 576-577: This should still be re-arranged for the reader's sake. Right now the reader sees "t is the time in days since a rain event" at 558-559 and is very confused because they just read that this whole thing is only done *on* rain days. So you should say the equivalent of 576-577 right away afterward, and further explain that t is always a fractional value less than 1 (i.e. number of hours since rain divided by 24) rather than a proper number of days (e.g. 3.7 or 6 or 10.2), which is how it reads right now. That has to be made clear for the procedure to make sense.	Yes, we have amended the text to clarify this. (Section 3.1)
765-768 or 758-759 (optional): It may be good here to stick in a reference to the Held and Soden (2006) or Schneider et al (2010) papers I cited in the previous comments, which both argue on theoretical grounds that RH shouldn't be affected as much as qa by climate change. Schneider et al have a particularly nice and transparent derivation, though I suppose it's only valid over ocean.	We have added these references (Section 4.4)
773: Fig B3 is not actually taken from Jenkins or Dai, so what sentence(s) of yours are citing these two papers? Is there a missing intended sentence or two before this citation? (should the citation even be in this location?)	This is a mistake – the text which required these references has been moved to the Discussion but the references were left behind here. This has now been rectified.
779: You mean "aerodynamic component to increase" - need to fix this typo. (Ta bars in Fig 15c are all positive, as they should be!) To show the contrast with the qa framework, you should also add something like ", but much less than before" after the parenthetical remark at 780.	Yes, we have edited the text as requested (End of Section 4.4)

Minor comments	Author response
<p>Section 4.4 in general: I think you need to explain the method just a bit more... you need to explicitly say here that you computed <math>R_h</math> and <math>T_a</math> derivatives of your new eq. 19 and multiplied them by the <math>R_h</math> and <math>T_a</math> trends, analogous to the beginning of 4.3. Otherwise the reader might be a little confused, particularly as to how the <math>T_a</math> piece of EPA change here could be different in magnitude from the <math>T_a</math> piece already presented. (I totally get it of course, but just making sure a third-party reader does!) An effective way to do this might be to write another simple equation like eq 18 but with <math>dE_p/dR_h</math> instead of <math>dE_p/dq_a</math>, and also explicitly noting that <math>dE_p/dT_a</math> is now taken at constant <math>R_h</math> rather than constant <math>q_a</math>. In the last (results) paragraph you could also explain that the <math>T_a</math> piece of EPA is now smaller because it now implicitly includes a constant-<math>R_h</math> rise in <math>q_a</math> (this is connected with the previous comment about 780). You don't have to do all of these steps but even doing some of them would help.</p>	<p>These are all useful suggestions and we have implemented these. (Section 4.4)</p>



Minor comments	Author response
<p>Fig B3b: A bit odd that the local Rh trend is significant over almost all of GB, but the trend in the area-average back at Fig 14c (leftmost symbol) is not significant. Are these significances defined consistently?</p>	<p>Thank you for noticing this – the maps were in fact plotted using the wrong CIs. As part of the process of analysis we calculated CIs based on a simple linear regression, as well as the CIs allowing for the non-zero lag-1 autocorrelation. The latter are the ones that have been used throughout the analysis, but we mistakenly used the former to calculate the significant regions of the trend maps (Figures B1, B2 and B3b). The simple linear regression CIs are less conservative and more restrictive, so make it appear that more of the area of the UK has significant trends. This was the case for all the variables, although most noticeable for the relative humidity. Now that we have remade the plots using the correct CIs, they are consistent with the rest of the analysis, and show smaller regions for which the trends are significant. For the relative humidity this leaves only a few small regions with significant trends, and this is consistent with the area means having non-significant trends as well. Note that the trends shown in the maps are unchanged, just the regions that are grey (for non-significant trends) have increased. (Figures B1, B2 and B3b)</p>
<p>810 (and perhaps 777 and/or 951 as well?) It would be good to remind the reader that the Ta piece only looks so “negligible” because the modest positive part from EPA gets canceled by that funny negative contribution from the EPR term, which as you now explain at 736-742 is kind of “unfair” anyway. And that, thus, the real physical contribution of Ta in the Rh framework is probably not so negligible, and is roughly equal to the EPA part. But agreed, even this is still way smaller than the qa-based result!</p> <p>A clear way to see this using the Great Britain row of Fig 15 is to assume the Ta bar in the middle column is fictitious, and mentally add its negative to the near-zero Ta bar in the left column. The result is now as big or bigger than the Sd bar in the left column! (The Ld bars would also be assumed to be fictitious in this estimate, so the total would still be the same.)</p>	<p>Yes, we have added this. (Section 5, also Section 6).</p>

Minor comments	Author response
908-914: Similarly, if LW didn't unfairly include the temperature-driven downward but not upward part, these conclusions would also be quite different (the numbers would be way smaller.)	Again, we have added text to point this out. (Section 5)
And similar to the 773 comment, what's up with the "ghost" references at the very beginning of the paragraph?	Again, this seems to be to do with moving chunks of text around – the references get copied to the new location, but also abandoned in the original place. They have now been deleted from this paragraph.
Table 1, specific humidity row: The constant air pressure is 100 kPa, not 1 kPa (right?)	Yes, this has been changed
Table 5 caption: needs to include a "when relative humidity is used" clause, like Table 6 caption. (Unless I misunderstand what Table 5 actually is??)	Yes, this has been changed
Also, Table 5 still has a stray "Specific Humidity" heading in part c... this should be changed to "Relative Humidity" unless I misunderstand. (Are the numbers in Table 5c still Rh numbers, or are they accidentally qa numbers?)	Yes, this was an oversight in the column heading and has been changed. The numbers are the Rh numbers, not qa, so have not been altered.

## Summary of derivatives calculated for Appendix C

### Wind speed

The aerodynamic resistance is inversely proportional to the wind speed (not a function of the square root). If we substitute the aerodynamic resistance (Eq 10) into the PET (Eq 4), then we have

$$E_P = \frac{t_d \Delta A + \frac{c_p \rho_a u_{10}}{278} (q_s - q_a)}{\lambda \left( \Delta + \gamma \left( 1 + \frac{r_s u_{10}}{278} \right) \right)} \quad (S1)$$

We differentiate this (using the quotient rule) to get

$$\frac{\partial E_P}{\partial u_{10}} = \frac{t_d}{\lambda} \left( \frac{\frac{c_p \rho_a}{278} (q_s - q_a)}{\Delta + \gamma \left( 1 + \frac{r_s}{r_a} \right)} - \frac{\frac{\gamma r_s}{278} \left( \Delta A + \frac{c_p \rho_a u_{10}}{278} (q_s - q_a) \right)}{\left( \Delta + \gamma \left( 1 + \frac{r_s}{r_a} \right) \right)^2} \right) \quad (S2)$$

We can then rearrange this to get

$$\frac{\partial E_P}{\partial u_{10}} = \frac{\frac{t_d}{\lambda} \frac{c_p \rho_a}{r_a} (q_s - q_a) (\Delta + \gamma) - \frac{t_d}{\lambda} \frac{\Delta A}{\Delta + \gamma \left( 1 + \frac{r_s}{r_a} \right)} \frac{\gamma r_s}{r_a}}{u_{10} \left( \Delta + \gamma \left( 1 + \frac{r_s}{r_a} \right) \right)} \quad (S3)$$

And notice that the numerator can be simplified by replacing  $E_{PA}$  and  $E_{PR}$  to get

$$\frac{\partial E_P}{\partial u_{10}} = \frac{(\Delta + \gamma) E_{PA} - \gamma \frac{r_s}{r_a} E_{PR}}{u_{10} \left( \Delta + \gamma \left( 1 + \frac{r_s}{r_a} \right) \right)} \quad (S4)$$

### Downward shortwave radiation

Using the equation for available energy (Eq 8), the PET is

$$E_P = \frac{t_d \Delta \left( (1 - \alpha) S_d + \varepsilon (L_d - \sigma T_*^4) \right) + \frac{c_p \rho_a}{r_a} (q_s - q_a)}{\lambda \left( \Delta + \gamma \left( 1 + \frac{r_s}{r_a} \right) \right)} \quad (S5)$$

Differentiating this with respect to downward shortwave gives

$$\frac{\partial E_P}{\partial S_d} = \frac{t_d}{\lambda} \frac{\Delta (1 - \alpha)}{\Delta + \gamma \left( 1 + \frac{r_s}{r_a} \right)} \quad (S6)$$

Which is equal to

$$\frac{\partial E_P}{\partial S_d} = \frac{t_d}{\lambda} \frac{\Delta A}{\Delta + \gamma \left( 1 + \frac{r_s}{r_a} \right)} \frac{(1 - \alpha)}{A} \quad (S7)$$

Again, we can simplify by replacing  $E_{PR}$  to get

$$\frac{\partial E_P}{\partial S_d} = E_{PR} \frac{(1 - \alpha)}{A} \quad (S8)$$

Note that in the paper we were using  $R_n$  rather than  $A$ , but have changed this to make the notation consistent with the rest of the paper.

In practice, when coding we would tend to use the expanded version (Eq S6), rather than this final version (Eq S8), as having available energy in the denominator is badly behaved as  $A$  becomes small.

### Downward longwave radiation

Similarly to the shortwave, we use the available energy equation and then differentiate Eq S5 with respect to the downward longwave to get

$$\frac{\partial E_P}{\partial L_d} = \frac{t_d}{\lambda} \frac{\Delta \varepsilon}{\Delta + \gamma \left(1 + \frac{r_s}{r_a}\right)} \quad (\text{S9})$$

Which rearranges to

$$\frac{\partial E_P}{\partial L_d} = \frac{t_d}{\lambda} \frac{\Delta A}{\Delta + \gamma \left(1 + \frac{r_s}{r_a}\right)} \frac{\varepsilon}{A} \quad (\text{S10})$$

Which is equivalent to

$$\frac{\partial E_P}{\partial L_d} = E_{PR} \frac{\varepsilon}{A} \quad (\text{S11})$$

### Specific humidity

Differentiating the PET (Eq 4) with respect to specific humidity gives

$$\frac{\partial E_P}{\partial q_a} = \frac{t_d}{\lambda} \frac{-\frac{c_p \rho_a}{r_a}}{\Delta + \gamma \left(1 + \frac{r_s}{r_a}\right)} \quad (\text{S12})$$

Which is equivalent to

$$\frac{\partial E_P}{\partial q_a} = \frac{t_d}{\lambda} \frac{-1}{(q_s - q_a)} \frac{\frac{c_p \rho_a}{r_a} (q_s - q_a)}{\Delta + \gamma \left(1 + \frac{r_s}{r_a}\right)} \quad (\text{S13})$$

Which simplifies to

$$\frac{\partial E_P}{\partial q_a} = \frac{E_{PA}}{q_a - q_s} \quad (\text{S14})$$

### Air temperature

This is more complicated, as many of the variables in the standard PET equation are functions of air temperature, namely specific humidity and its derivative, available energy and air density. Using the quotient rule, we can calculate the derivative of the PET to be

$$\frac{\partial E_P}{\partial T_a} = \frac{t_d}{\lambda} \left( \frac{\Delta \frac{\partial A}{\partial T_a} + A \frac{\partial \Delta}{\partial T_a} + \frac{c_p}{r_a} \left( \rho_a \frac{\partial q_s}{\partial T_a} + (q_s - q_a) \frac{\partial \rho_a}{\partial T_a} \right)}{\Delta + \gamma \left( 1 + \frac{r_s}{r_a} \right)} - \frac{\left( \Delta A + \frac{c_p \rho_a}{r_a} (q_s - q_a) \right) \frac{\partial \Delta}{\partial T_a}}{\left( \Delta + \gamma \left( 1 + \frac{r_s}{r_a} \right) \right)^2} \right) \quad (S15)$$

We then substitute the derivatives

$$\frac{\partial A}{\partial T_a} = -4 \varepsilon \sigma T_a^3 \quad (S16)$$

$$\frac{\partial \rho_a}{\partial T_a} = \frac{-p_*}{r T_a^2} = \frac{-\rho_a}{T_a} \quad (S17)$$

$$\frac{\partial q_s}{\partial T_a} = \Delta \quad (S18)$$

$$\frac{\partial \Delta}{\partial T_a} = \Delta \left( \frac{T_{sp}}{T_a^2} \frac{\sum_{i=1}^4 i(i-1)a_i \left( 1 - \frac{T_{sp}}{T_a} \right)^{i-2}}{\sum_{i=1}^4 i a_i \left( 1 - \frac{T_{sp}}{T_a} \right)^{i-1}} + \Delta \frac{p_* + (1-\varepsilon)e_s}{p_* q_s} - \frac{2}{T_a} \right) \quad (S19)$$

And rearrange, substituting  $E_{PA}$  and  $E_{PR}$  as necessary, to get

$$\frac{\partial E_P}{\partial T_a} = E_{PR} \left[ \left( 1 - \frac{\Delta}{\Delta + \gamma \left( 1 + \frac{r_s}{r_a} \right)} \right) \left( \frac{T_{sp}}{T_a^2} \frac{\sum_{i=1}^4 i(i-1)a_i \left( 1 - \frac{T_{sp}}{T_a} \right)^{i-2}}{\sum_{i=1}^4 i a_i \left( 1 - \frac{T_{sp}}{T_a} \right)^{i-1}} + \Delta \frac{p_* + (1-\varepsilon)e_s}{p_* q_s} - \frac{2}{T_a} \right) - \frac{4\varepsilon \sigma T_a^3}{R_n} \right] + E_{PA} \left[ \frac{\Delta}{q_s - q_a} - \frac{1}{T_a} - \frac{\Delta}{\Delta + \gamma \left( 1 + \frac{r_s}{r_a} \right)} \left( \frac{T_{sp}}{T_a^2} \frac{\sum_{i=1}^4 i(i-1)a_i \left( 1 - \frac{T_{sp}}{T_a} \right)^{i-2}}{\sum_{i=1}^4 i a_i \left( 1 - \frac{T_{sp}}{T_a} \right)^{i-1}} + \Delta \frac{p_* + (1-\varepsilon)e_s}{p_* q_s} - \frac{2}{T_a} \right) \right] \quad (S20)$$

### Relative humidity

When we look at the problem in terms of relative humidity instead of specific humidity, the PET is

$$E_P = \frac{t_d}{\lambda} \frac{\Delta A + \frac{c_p \rho_a}{r_a} q_s (1 - R_h)}{\Delta + \gamma \left( 1 + \frac{r_s}{r_a} \right)} \quad (S21)$$

In this case, the derivative with respect to relative humidity is reasonably straightforward, giving

$$\frac{\partial E_P}{\partial R_h} = \frac{t_d}{\lambda} \frac{-\frac{c_p \rho_a}{r_a} q_s}{\Delta + \gamma \left( 1 + \frac{r_s}{r_a} \right)} \quad (S22)$$

Which is equivalent to

$$\frac{\partial E_P}{\partial R_h} = \frac{t_d}{\lambda} \frac{-1}{1-R_h} \frac{c_p \rho_a}{r_a} q_s (1-R_h) \quad (S23)$$

Which can be rewritten

$$\frac{\partial E_P}{\partial R_h} = \frac{E_{PA}}{R_h - 1} \quad (S24)$$

### Air temperature when using relative humidity

In this case, the derivative of PET with respect to air temperature is

$$\frac{\partial E_P}{\partial T_a} = \frac{t_d}{\lambda} \left( \frac{\Delta \frac{\partial A}{\partial T_a} + A \frac{\partial \Delta}{\partial T_a} + \frac{c_p}{r_a} (1-R_h) \left( \rho_a \frac{\partial q_s}{\partial T_a} + q_s \frac{\partial \rho_a}{\partial T_a} \right)}{\Delta + \gamma \left( 1 + \frac{r_s}{r_a} \right)} - \frac{\left( \Delta A + \frac{c_p \rho_a}{r_a} q_s (1-R_h) \right) \frac{\partial \Delta}{\partial T_a}}{\left( \Delta + \gamma \left( 1 + \frac{r_s}{r_a} \right) \right)^2} \right) \quad (S25)$$

We use the same substitutions as before for the derivatives of specific humidity (Eq S18) and its derivative (Eq S19), available energy (Eq S16) and air density (Eq S17), and rearrange, substituting  $E_{PA}$  and  $E_{PR}$  as necessary, to get

$$\frac{\partial E_P}{\partial T_a} = E_{PR} \left[ \left( 1 - \frac{\Delta}{\Delta + \gamma \left( 1 + \frac{r_s}{r_a} \right)} \right) \left( \frac{T_{sp}}{T_a^2} \frac{\sum_{i=1}^4 i(i-1) a_i T_r^{i-2}}{\sum_{i=1}^4 i a_i T_r^{i-1}} + \Delta \frac{p_* + (1-\varepsilon) e_s}{p_* q_s} - \frac{2}{T_a} \right) - \frac{4 \varepsilon \sigma T_a^3}{R_n} \right] + E_{PA} \left[ \frac{\Delta}{q_s} - \frac{1}{T_a} - \frac{\Delta}{\Delta + \gamma \left( 1 + \frac{r_s}{r_a} \right)} \left( \frac{T_{sp}}{T_a^2} \frac{\sum_{i=1}^4 i(i-1) a_i T_r^{i-2}}{\sum_{i=1}^4 i a_i T_r^{i-1}} + \Delta \frac{p_* + (1-\varepsilon) e_s}{p_* q_s} - \frac{2}{T_a} \right) \right] \quad (S26)$$

1 **Trends in atmospheric evaporative demand in Great Britain**  
2 **using high-resolution meteorological data**

3

4 **Emma L. Robinson<sup>1</sup>, Eleanor M. Blyth<sup>1</sup>, Douglas B. Clark<sup>1</sup>, Jon Finch<sup>1</sup> and Alison**  
5 **C. Rudd<sup>1</sup>**

6 [1]{Centre for Ecology and Hydrology, Maclean Building, Benson Lane, Crowmarsh Gifford,  
7 Wallingford OX10 8BB}

8 Correspondence to: Emma L. Robinson (emrobi@ceh.ac.uk)

9

10 **Abstract**

11 Observations of climate are often available on very different spatial scales from observations  
12 of the natural environments and resources that are affected by climate change. In order to help  
13 bridge the gap between these scales using modelling, a new dataset of daily meteorological  
14 variables was created at 1 km resolution over Great Britain for the years 1961-2012, by  
15 interpolating coarser resolution climate data and including the effects of local topography.  
16 These variables were used to calculate atmospheric evaporative demand (AED) at the same  
17 spatial and temporal resolution. Two functions that represent AED were chosen: one is a  
18 standard form of Potential Evapotranspiration (PET) and the other is a derived PET measure  
19 used by hydrologists that includes the effect of water intercepted by the canopy (PETI).  
20 Temporal trends in these functions were calculated, with PET found to be increasing in all  
21 regions, and at an overall rate of  $0.021 \pm 0.021 \text{ mm d}^{-1} \text{ decade}^{-1}$  in Great Britain. PETI was found  
22 to be increasing at a rate of  $0.019 \pm 0.020 \text{ mm d}^{-1} \text{ decade}^{-1}$  in Great Britain, but this was not  
23 statistically significant. However, there was a trend in PETI in England of  $0.023 \pm 0.023 \text{ mm d}^{-1}$   
24  $\text{decade}^{-1}$ . The trends were found to vary by season, with spring PET increasing by  
25  $0.043 \pm 0.019 \text{ mm d}^{-1} \text{ decade}^{-1}$  ( $0.038 \pm 0.018 \text{ mm d}^{-1} \text{ decade}^{-1}$  when the interception correction  
26 is included) in Great Britain, while there is no statistically significant trend in other seasons.  
27 The trends were attributed analytically to trends in the climate variables; the overall positive  
28 trend was predominantly driven by rising air temperature, although rising specific humidity  
29 had a negative effect on the trend. Recasting the analysis in terms of relative humidity revealed  
30 that the overall effect is that falling relative humidity causes the PET to rise. Increasing  
31 downward short- and longwave radiation made an overall positive contribution to the PET  
32 trend, while decreasing wind speed made a negative contribution to the trend in PET. The trend  
33 in spring PET was particularly strong due to a strong decrease in relative humidity and increase  
34 in downward shortwave radiation in the spring.  
35



## 36 1 Introduction

37 There are many studies showing the ways in which our living environment is changing over  
38 time: changing global temperatures (IPCC, 2013), radiation (Wild, 2009) and wind speeds  
39 (McVicar et al., 2012) can have significant impacts on ecosystems and human life (IPCC,  
40 2014a). While there are overall global trends, the impacts can vary between regions (IPCC,  
41 2014b). In the UK, wildlife surveys of both flora (Wood et al., 2015; Evans et al., 2008) and  
42 fauna (Pocock et al., 2015) show a shift in patterns and timing (Thackeray et al., 2010). In  
43 addition, the UK natural resources of freshwater (Watts et al., 2015), soils (Reynolds et al.,  
44 2013; Bellamy et al., 2005) and vegetation (Berry et al., 2002; Hickling et al., 2006; Norton et  
45 al., 2012) are changing. The UK is experiencing new environmental stresses on the land and  
46 water systems through changes in temperature and river flows (Crooks and Kay, 2015; Watts  
47 et al., 2015; Hannaford, 2015), which are part of a widespread global pattern of temperature  
48 increase and circulation changes (Watts et al., 2015).

49 To explain these changes in terms of climate drivers, there are several gridded meteorological  
50 datasets available at global and regional scales. Global datasets can be based on observations  
51 – for example the 0.5° resolution Climate Research Unit time series 3.21 (CRU TS 3.21) data  
52 (Jones and Harris, 2013; Harris et al., 2014) – while some are based on global meteorological  
53 reanalyses bias-corrected to observations – for example the WATCH Forcing Data (WFD, 0.5°;  
54 Weedon et al. (2011)), the WATCH Forcing Data methodology applied to ERA-Interim  
55 reanalysis product (WFDEI, 0.5°; Weedon et al. (2014)) and the Princeton Global  
56 Meteorological Forcing Dataset (0.25°–1°; Sheffield et al. (2006)). At the regional scale in  
57 Great Britain (GB), there are datasets that are derived directly from observations – for example  
58 the Met Office Rainfall and Evaporation Calculation System (MORECS) dataset at 40 km  
59 resolution (Thompson et al., 1981; Hough and Jones, 1997; Field, 1983) and the UKCP09  
60 observed climate data at 5 km resolution (Jenkins et al., 2008).

61 However, while regional observations of carbon, methane and water emissions from the land  
62 (Baldocchi et al., 1996), the vegetation cover (Morton et al., 2011) and soil properties  
63 (FAO/IIASA/ISRIC/ISS-CAS/JRC, 2012) are typically made at the finer landscape scale of  
64 100 m to 1000 m, most of these long-term gridded meteorological datasets are only available  
65 at a relatively coarse resolution of a few tens of km. These spatial scales may not be  
66 representative of the climate experienced by the flora and fauna being studied, and it has also  
67 been shown that input resolution can have a strong effect on the performance of hydrological

68 models (Kay et al., 2015). In addition, the coarse temporal resolution of some datasets, for  
69 example the monthly CRU TS 3.21 data (Harris et al., 2014; Jones and Harris, 2013), can miss  
70 important sub-monthly extremes.

71 Regional studies are important to identify drivers and impacts of changing meteorology that  
72 may or may not be reflected in trends in global means. For example, in Canada (Vincent et al.,  
73 2015) and Europe (Fleig et al., 2015), high resolution meteorological data have been used to  
74 identify the impacts of changing circulation patterns, while in Australia wind speed data have  
75 been used to quantify the effects of global stilling in the region (McVicar et al., 2008). While  
76 there are datasets available at finer spatial and temporal resolutions for the UK (such as  
77 UKCP09 (Jenkins et al., 2008)), these often do not provide all the variables needed to identify  
78 the impacts of changing climate.

79 To address this, we have created a meteorological dataset for Great Britain at 1 km resolution:  
80 the Climate Hydrology and Ecology research Support System meteorology dataset for Great  
81 Britain (1961-2012) (CHESS-met; Robinson et al. (2015b)). It is derived from the observation-  
82 based MORECS dataset (Thompson et al., 1981; Hough and Jones, 1997), and then downscaled  
83 using information about topography. This is augmented by an independent precipitation dataset  
84 – Gridded Estimates of daily and monthly Areal Rainfall for the United Kingdom (CEH-  
85 GEAR; Tanguy et al. (2014); Keller et al. (2015)) – along with variables from two global  
86 datasets – WFD and CRU TS 3.21 – to produce a comprehensive, observation-based, daily  
87 meteorological dataset at 1 km × 1 km spatial resolution.

88 In order to understand the effect of meteorology on the water cycle, a key variable in  
89 hydrological modelling is the atmospheric evaporative demand (AED), which is determined by  
90 meteorological variables (Kay et al., 2013). It has been shown that water-resource and  
91 hydrological model results are largely driven by how this property is defined and used  
92 (Haddeland et al., 2011). The AED can be expressed in several ways, for instance the  
93 evaporation from a wet surface, from a well-watered but dry uniform vegetated cover, or from  
94 a hypothetical well-watered but dry version of the actual vegetation. Metrics such as the Palmer  
95 Drought Severity Index (PDSI; Palmer (1965)) use potential evapotranspiration (PET) as an  
96 input to represent AED, while many hydrological models such as Climate and Land use  
97 Scenario Simulation in Catchments (CLASSIC; Crooks and Naden (2007)) or Grid-to-Grid  
98 (G2G; Bell et al. (2009)), which also require an input representing AED, use a distinct form of  
99 the PET which includes the intercepted water from rainfall (this is described later in the text)  
100 which we hereby name PETI. While hydrological models can make use of high resolution

101 topographic information and precipitation datasets, they are often driven with PET calculated  
102 at a coarser resolution (Bell et al., 2011; Bell et al., 2012; Kay et al., 2015). Therefore, we have  
103 also created a 1 km × 1 km resolution dataset, the Climate Hydrology and Ecology research  
104 Support System Potential Evapotranspiration dataset for Great Britain (1961-2012) (CHESS-  
105 PE; Robinson et al. (2015a)), consisting of estimates of PET and PETI, which can be used to  
106 run high-resolution hydrological models.

107 Other regional studies have created gridded estimates of AED in Austria (Haslinger and  
108 Bartsch, 2016) and Australia (Donohue et al., 2010). Regional studies of trends in AED have  
109 seen varied results, with increasing AED seen in Romania (Paltineanu et al., 2012), Serbia  
110 (Gocic and Trajkovic, 2013), Spain (Vicente-Serrano et al., 2014), some regions of China (Li  
111 and Zhou, 2014) and Iran (Azizzadeh and Javan, 2015; Hosseinzadeh Talaei et al., 2013;  
112 Tabari et al., 2012), decreasing AED in north east India (Jhajharia et al., 2012) and regions in  
113 China (Yin et al., 2009; Song, 2010; Shan et al., 2015; Zhao et al., 2015; Zhang et al., 2015;  
114 Lu et al., 2016) and regional variability in Australia (Donohue et al., 2010) and China (Li et  
115 al., 2015). In order to understand this variability, it is important to quantify the relative  
116 contributions of the changing meteorological variables to trends in AED and regional studies  
117 often find different drivers of changing AED (see McVicar et al. (2012) for a review). Relative  
118 humidity has been shown to drive AED in the Canary Islands (Vicente-Serrano et al., 2016),  
119 wind speed and air temperature were shown to have nearly equal but opposite effects in  
120 Australia (Donohue et al., 2010), while in China sunshine hours (Li et al., 2015), wind speed  
121 (Yin et al., 2009) or a combination of the two (Lu et al., 2016) have been shown to drive trends.  
122 Rudd and Kay (2015) investigated projected changes in PET using a regional climate model,  
123 but little has been done to investigate historical trends of AED in the UK.

124 The objectives of this paper are (i) to evaluate the trends in key meteorological variables in  
125 Great Britain over the years 1961-2012; (ii) to evaluate the AED in Great Britain over the same  
126 time period using PET; (iii) to investigate the effect of including interception in the formulation  
127 of PET called PETI; (iv) to evaluate trends in PET over the time period of interest; and (v) to  
128 attribute the trends in PET to trends in meteorological variables. To address these objectives,  
129 the paper is structured as follows. Section 2 presents the calculation of the meteorological  
130 variables. Section 3 presents the calculation of PET and PETI from the meteorological  
131 variables and assesses the difference between PET and PETI. In Section 4 the trends of the  
132 meteorological variables and AED are calculated and the trends in PET are attributed to trends

133 in meteorological variables. In Section 5 the results are discussed and conclusions are presented  
134 in Section 6.

## 135 **2 Calculation of meteorological variables**

136 The meteorological variables included in this new dataset (Robinson et al., 2015b) are daily  
137 mean values of air temperature, specific humidity, wind speed, downward longwave (LW) and  
138 shortwave (SW) radiation, precipitation and air pressure, plus daily temperature range (Table  
139 1). These variables are important drivers of near-surface conditions, and, for instance, are the  
140 full set of variables required to drive the JULES land surface model (LSM) (Best et al., 2011;  
141 Clark et al., 2011), as well as other LSMs.

142 The data were derived primarily from MORECS, which is a long-term gridded dataset starting  
143 in 1961 and updated to the present (Thompson et al., 1981; Hough and Jones, 1997). It  
144 interpolates five variables from synoptic stations (daily mean values of air temperature, vapour  
145 pressure and wind speed, daily hours of bright sunshine and daily total precipitation) to a 40  
146 km × 40 km resolution grid aligned with the Ordnance Survey National Grid. There are  
147 currently 270 stations reporting in real time, while a further 170 report the daily readings on a  
148 monthly basis, but numbers have varied throughout the run. The algorithm interpolates a  
149 varying number of stations (up to nine) for each square, depending on data availability (Hough  
150 and Jones, 1997). The interpolation is such that the value in each grid square is the effective  
151 measurement of a station positioned at the centre of the square and at the grid square mean  
152 elevation, averaged from 00:00 GMT to 00:00 GMT the next day. MORECS is a consistent,  
153 quality-controlled time series, which accounts for changing station coverage. The MORECS  
154 variables were used to derive the air temperature, specific humidity, wind speed, downward  
155 LW and SW radiation and air pressure in the new dataset. The WFD and CRU TS 3.21 datasets  
156 were used for surface air pressure and daily temperature range respectively, as they could not  
157 be calculated solely from MORECS. Additionally precipitation was obtained from the CEH-  
158 GEAR data, which is a product directly interpolated to 1 km from the station data (Keller et  
159 al., 2015).

160 The spatial coverage of the dataset was determined by the spatial coverage of MORECS, which  
161 covers the majority of Great Britain, but excludes some coastal regions and islands at the 1 km  
162 scale. For most of these points, the interpolation was extended from the nearest MORECS  
163 squares, but some outlying islands (in particular Shetland and the Scilly Isles) were excluded  
164 when the entire island was further than 40 km from the nearest MORECS square.

165 **2.1 Air temperature**

166 Air temperature,  $T_a$  (K), was derived from the MORECS air temperature. The MORECS air  
167 temperature was reduced to mean sea level, using a lapse rate of  $-0.006 \text{ K m}^{-1}$  (Hough and  
168 Jones, 1997). A bicubic spline was used to interpolate from 40 km resolution to 1 km resolution,  
169 then the temperatures were adjusted to the elevation of each 1 km square using the same lapse  
170 rate. The 1 km resolution elevation data used were aggregated from the Integrated Hydrological  
171 Digital Terrain Model (IHDTM) – a 50 m resolution digital terrain model (Morris and Flavin,  
172 1990).

173 **2.2 Specific humidity**

174 Specific humidity,  $q_a$  ( $\text{kg kg}^{-1}$ ), was derived from the MORECS vapour pressure,  $e_M$  (Pa),  
175 which was first reduced to mean sea level, using the equation

176 
$$e_{sea} = e_M \left( 1 - \frac{L_e}{100} h_M \right) \quad (1)$$

177 where  $L_e$  is the lapse rate of  $-0.025 \text{ \% m}^{-1}$  and  $h$  is the elevation of the MORECS square  
178 (Thompson et al., 1981). The actual lapse rate of humidity will, in general, vary according to  
179 atmospheric conditions. However, calculating this would require more detailed information  
180 than is available in the input data used. Any method of calculating the variation of specific  
181 humidity with height will involve several assumptions, but the method used here is well-  
182 established and is used by the Met Office in calculating MORECS (Thompson et al., 1981).  
183 The value of the vapour pressure lapse rate is chosen to keep relative humidity approximately  
184 constant with altitude, rather than assuming that the vapour pressure itself is constant.

185 A bicubic spline was used to interpolate vapour pressure to 1 km resolution then the values  
186 were adjusted to the 1 km resolution elevation using the IHDTM elevations and using the same  
187 lapse rate, such that

188 
$$e = e_{sea,1km} \left( 1 + \frac{L_e}{100} h_{1km} \right), \quad (2)$$

189 where  $e_{sea,1km}$  is the sea-level vapour pressure at 1 km resolution and  $h_{1km}$  is the 1 km resolution  
190 elevation.

191 Finally the specific humidity was calculated, using

192 
$$q_a = \frac{\epsilon e}{p_* - (1 - \epsilon)e}, \quad (3)$$

193 where  $e$  is the vapour pressure (Pa) and  $\epsilon = 0.622$  is the mass ratio of water to dry air (Gill,  
194 1982). The air pressure,  $p^*$ , in this calculation was assumed to have a constant value of 100000  
195 Pa because this was prescribed in the computer code. It would be better to use a varying air  
196 pressure, as calculated in Section 2.8, but this makes a negligible difference (of a few percent)  
197 to the calculated specific humidity, and to the PET and PETI calculated in Section 3. and a  
198 constant  $p^*$  was retained.

### 199 **2.3 Downward shortwave radiation**

200 Downward SW radiation,  $S_d$  ( $\text{W m}^{-2}$ ), was derived from the MORECS hours of bright sunshine  
201 (defined as the total number of hours in a day for which solar irradiation exceeds  $120 \text{ W m}^{-2}$   
202 (WMO, 2013)). The value calculated is the mean SW radiation over 24 hours. The sunshine  
203 hours were used to calculate the cloud cover factor,  $C_f = n/N$ , where  $n$  is the number of hours  
204 of bright sunshine in a day, and  $N$  is the total number of hours between sunrise and sunset  
205 (Marthews et al., 2011). The cloud cover factor was interpolated to 1 km resolution using a  
206 bicubic spline. The downward SW solar radiation for a horizontal plane at the Earth's surface  
207 was then calculated using the solar angle equations of Iqbal (1983) and a form of the Ångström-  
208 Prescott equation which relates hours of bright sunshine to solar irradiance (Ångström, 1918;  
209 Prescott, 1940), with empirical coefficients calculated by Cowley (1978). They vary spatially  
210 and seasonally and effectively account for reduction of irradiance with increasing solar zenith  
211 angle, as well as implicitly accounting for spatially- and seasonally-varying aerosol effects.  
212 However, they do not vary interannually and thus do not explicitly include long-term trends in  
213 aerosol concentration.

214 The downward SW radiation was then corrected for the average inclination and aspect of the  
215 surface, assuming that only the direct beam radiation is a function of the inclination and that  
216 the diffuse radiation is homogeneous. It was also assumed that the cloud cover is the dominant  
217 factor in determining the diffuse fraction (Muneer and Munawwar, 2006). The aspect and  
218 inclination were calculated using the IHDTM elevation at 50 m resolution, following the  
219 method of Horn (1981), and were then aggregated to 1 km resolution. The top of atmosphere  
220 flux for horizontal and inclined surfaces was calculated following Allen et al. (2006) and the  
221 ratio used to scale the direct beam radiation.

## 222 **2.4 Downward longwave radiation**

223 Downward LW radiation,  $L_d$  ( $\text{W m}^{-2}$ ), was derived from the 1 km resolution air temperature  
224 (Sect. 2.1), vapour pressure (Sect. 2.2) and cloud cover factor (Sect. 2.3). The downward LW  
225 radiation for clear sky conditions was calculated as a function of air temperature and  
226 precipitable water using the method of Dilley and O'Brien (1998), with precipitable water  
227 calculated from air temperature and humidity following Prata (1996). The additional  
228 component due to cloud cover was calculated using the equations of Kimball et al. (1982),  
229 assuming a constant cloud base height of 1000 m.

## 230 **2.5 Wind speed**

231 The wind speed at a height of 10 m,  $u_{10}$  ( $\text{m s}^{-1}$ ), was derived from the MORECS 10 m wind  
232 speed, which were interpolated to 1 km resolution using a bicubic spline and adjusted for  
233 topography using a 1 km resolution dataset of mean wind speeds produced by the UK Energy  
234 Technology Support Unit (ETSU; Newton and Burch (1985); Burch and Ravenscroft (1992)).  
235 This used Numerical Objective Analysis Boundary Layer (NOABL) methodology combined  
236 with station wind measurements over the period 1975-84 to produce a map of mean wind speed  
237 over the UK. To calculate the topographic correction, the ETSU wind speed was aggregated to  
238 40 km resolution, then the difference between each 1 km value and the corresponding 40 km  
239 mean found. This difference was added to the interpolated daily wind speed. In cases where  
240 this would result in a negative wind speed, the wind speed was set to zero.

## 241 **2.6 Precipitation**

242 Precipitation rate,  $P$  ( $\text{kg m}^{-2} \text{s}^{-1}$ ), is taken from the daily CEH-GEAR dataset (Tanguy et al.,  
243 2014; Keller et al., 2015), scaled to the appropriate units. The CEH-GEAR methodology uses  
244 natural neighbour interpolation (Gold, 1989) to interpolate synoptic station data to a 1 km  
245 resolution gridded daily dataset of the estimated precipitation in 24 hours between 09:00 GMT  
246 and 09:00 GMT the next day.

## 247 **2.7 Daily temperature range**

248 Daily temperature range (DTR),  $D_T$  (K), was obtained from the CRU TS 3.21 monthly mean  
249 daily temperature range estimates on a  $0.5^\circ$  latitude  $\times$   $0.5^\circ$  longitude grid, which is interpolated  
250 from monthly climate observations (Harris et al., 2014; Jones and Harris, 2013). There is no  
251 standard way to correct DTR for elevation, so these data were reprojected to the 1 km grid with

252 no interpolation and the monthly mean used to populate the daily values in each month.  
253 Although DTR is not required in the calculation of AED, it is a required input of the JULES  
254 LSM, in order to run at sub-daily timestep with daily input data.

## 255 **2.8 Surface air pressure**

256 Surface air pressure,  $p^*$  (Pa), was derived from the WFD, an observation-corrected reanalysis  
257 product, which provides 3 hourly meteorological data for 1958-2001 on a  $0.5^\circ$  latitude  $\times$   $0.5^\circ$   
258 longitude resolution grid (Weedon et al., 2011). Mean monthly values of WFD surface air  
259 pressure and air temperature were calculated for each  $0.5^\circ$  grid box over the years 1961-2001.  
260 These were reprojected to the 1 km grid with no interpolation, then the lapse rate of air  
261 temperature (Sect. 2.1) used to calculate the integral of the hypsometric equation (Shuttleworth,  
262 2012), in order to obtain the air pressure at the elevation of each 1 km grid. The mean monthly  
263 values were used to populate the daily values in the full dataset, thus the surface air pressure in  
264 the new dataset does not vary interannually, but does vary seasonally. This is reasonable as the  
265 trend in surface air pressure in the WFD is negligible (Weedon et al., 2011).

## 266 **2.9 Spatial and seasonal patterns of meteorological variables**

267 Long-term mean values of the meteorological variables were calculated for each 1 km square  
268 over the whole dataset, covering the years 1961-2012 (Fig. 1). Four sub-regions of interest  
269 were defined (Fig. 2); three of these regions correspond to nations (England, Wales and  
270 Scotland), while the fourth is the ‘English lowlands’, a subset of England, covering south-  
271 central and south-east England, East Anglia and the East Midlands (Folland et al., 2015). Mean-  
272 monthly climatologies were calculated over the whole of Great Britain (GB), and over these  
273 four regions of interest (Fig. 3).

274 The maps clearly show the effect of topography on the variables (Fig. 1), with an inverse  
275 correlation between elevation and temperature, specific humidity, downward LW radiation and  
276 surface air pressure and a positive correlation with wind speed. The precipitation has an east-  
277 west gradient due to prevailing weather systems and orography. The fine-scale structure of the  
278 downward SW radiation is due to the aspect and elevation of each grid cell, with more spatial  
279 variability in areas with more varying terrain. As no topographic correction has been applied  
280 to DTR, it varies only on a larger spatial scale. Although specific humidity is inversely  
281 proportional to elevation, relative humidity is not, as the saturated specific humidity will also  
282 be inversely proportional to elevation due to the decrease in temperature with height. The



283 strong correlation between wind speed and elevation means that it is very variable over short  
284 spatial scales, particularly in Scotland.

285 The mean-monthly climatologies (Fig. 3) demonstrate the differences between the regions,  
286 with Scotland generally having lower temperatures and more precipitation than the average,  
287 and England (particularly the English lowlands) being warmer and drier.

## 288 **2.10 Validation of meteorology**

289 The precipitation dataset, CEH-GEAR, has previously been validated against observations  
290 (Keller et al., 2015). Other studies discuss the uncertainties in the CRU TS 3.21 daily  
291 temperature range data (Harris et al., 2014) and WFDEI air pressure data (Weedon et al., 2014).

292 For the other variables, the MORECS data set is ultimately derived from the synoptic stations  
293 around the UK which represent most of the available observed meteorological data for the  
294 country. The only way to validate the gridded meteorology presented here is to compare it to  
295 independently observed data, which are available at a few sites where meteorological  
296 measurement stations that are not part of the synoptic network are located. Here we carry out  
297 a validation exercise with data from four sites from the UK, which have meteorological  
298 measurements available for between 5 and 10 years. Details of the sites and data are in  
299 Appendix A. Fig. 4 shows the comparison of data set air temperature with the observed air  
300 temperature at each of the four sites. This shows a strong correlation ( $r^2$  between 0.94 and 0.97)  
301 between the data set and the observations. Fig. 5 shows the mean-monthly climatology  
302 calculated from both the data set and from the observations (only for times for which  
303 observations were available) and demonstrates that the data set successfully captures the  
304 seasonal cycle. This has been repeated for downward SW radiation and for an estimate of the  
305 mixing ratio of water vapour, 10 m wind speed and surface air pressure (Appendix A). The air  
306 temperature, downward SW radiation and mixing ratio all have high correlations and represent  
307 the seasonal cycle well. The downward SW is overestimated at Auchencorth Moss, which may  
308 be due to local factors (e.g. shading, or the siting of the station within the grid square). The  
309 wind speed is overestimated by the derived data set at two sites, which is likely to be due to  
310 land cover effects. The modelling which produced the ETSU dataset uses topography but not  
311 land cover (Burch and Ravenscroft, 1992; Newton and Burch, 1985), so at sites with tall  
312 vegetation the wind speed is likely to be less than the modelled value. The air pressure has a  
313 low correlation because the data set contains a mean-monthly climatological value. However,

314 the mean bias is low and the RMSE is small, confirming that it is reasonable to use a  
 315 climatological value in place of daily data.

### 316 **3 Calculation of potential evapotranspiration (PET)**

317 There are several ways to assess the evaporative demand of the atmosphere. Pan evaporation  
 318 can be modelled using the Pen-Pan model (Rotstayn et al., 2006), or open-water evaporation  
 319 can be modelled with the Penman equation (Penman, 1948). However, neither of these account  
 320 for the fact that in general the evaporation is occurring from a vegetated surface. A widely used  
 321 model is the Penman-Monteith PET,  $E_P$  (mm d<sup>-1</sup>, equivalent to kg m<sup>-2</sup> d<sup>-1</sup>), which is a  
 322 physically-based formulation of AED (Monteith, 1965), including the effect of stomatal  
 323 resistance. It provides an estimate of AED dependent on the atmospheric conditions but  
 324 allowing for the fact that ~~that~~ the water is evaporating through the surface of leaves and thus  
 325 the resistance is higher. It can be calculated from the daily meteorological variables using the  
 326 equation

$$327 \quad E_P = \frac{t_d}{\lambda} \frac{\Delta A + \frac{c_p \rho_a}{r_a} (q_s - q_a)}{\Delta + \gamma \left(1 + \frac{r_s}{r_a}\right)}, \quad (4)$$

328 where  $t_d = 86400$  s d<sup>-1</sup> is the length of a day,  $\lambda = 2.5 \times 10^6$  J kg<sup>-1</sup> is the latent heat of evaporation,  
 329  $q_s$  is saturated specific humidity (kg kg<sup>-1</sup>),  $\Delta$  is the gradient of saturated specific humidity with  
 330 respect to temperature (kg kg<sup>-1</sup> K<sup>-1</sup>),  $A$  is the available energy (W m<sup>-2</sup>),  $c_p = 1010$  J kg<sup>-1</sup> K<sup>-1</sup> is the  
 331 specific heat capacity of air,  $\rho_a$  is the density of air (kg m<sup>-3</sup>),  $q_a$  is specific humidity (kg kg<sup>-1</sup>),  
 332  $\gamma = 0.004$  K<sup>-1</sup> is the psychrometric constant,  $r_s$  is stomatal resistance (s m<sup>-1</sup>) and  $r_a$  is aerodynamic  
 333 resistance (s m<sup>-1</sup>) (Stewart, 1989).

334 The saturated specific humidity,  $q_s$  (kg kg<sup>-1</sup>), is calculated from saturated vapour pressure,  $e_s$   
 335 (Pa), using Eq. 3. The saturated vapour pressure is calculated using an empirical fit to air  
 336 temperature

$$337 \quad e_s = p_{sp} \exp\left(\sum_{i=1}^4 a_i \left(1 - \frac{T_{sp}}{T_a}\right)^i\right), \quad (5)$$

338 where  $p_{sp} = 101325$  Pa is the steam point pressure,  $T_{sp} = 373.15$  K is the steam point temperature  
 339 and  $a = (13.3185, -1.9760, -0.6445, -0.1299)$  are empirical coefficients (Richards, 1971).

340 The derivative of the saturated specific humidity with respect to temperature,  $\Delta$  (kg kg<sup>-1</sup> K<sup>-1</sup>),  
 341 is therefore

$$342 \quad \Delta = \frac{T_{sp}}{T_a^2} \frac{p_{sp} q_s}{p_{sp} - (1-\epsilon)e_s} \sum_{i=1}^4 i a_i \left(1 - \frac{T_{sp}}{T_a}\right)^{i-1}, \quad (6)$$

343 where the air pressure used is the spatially varying air pressure calculated in Sect.2.8.

344 The available energy,  $A$  ( $\text{W m}^{-2}$ ), is the energy balance of the surface,

$$345 \quad A = R_n - G, \quad (7)$$

346 where  $R_n$  is the net radiation ( $\text{W m}^{-2}$ ) and  $G$  is the soil heat flux ( $\text{W m}^{-2}$ ). The net soil heat flux  
347 is negligible at the daily timescale (Allen et al., 1998), so the available energy is equal to the  
348 net radiation, such that

$$349 \quad A = (1 - \alpha)S_d + \varepsilon(L_d - \sigma T_s^4), \quad (8)$$

350 where  $\sigma$  is the Stefan-Boltzmann constant,  $\alpha$  is the albedo and  $\varepsilon$  the emissivity of the surface  
351 and  $T_s$  is the surface temperature (Shuttleworth, 2012). For this study we make the simplifying  
352 assumption that the surface temperature is ~~approximated by using~~approximately equal to the  
353 air temperature,  $T_a$  and use the latter in Eq. 8.

354 The air density,  $\rho_a$  ( $\text{kg m}^{-3}$ ), is a function of air pressure and temperature,

$$355 \quad \rho_a = \frac{p_a}{rT_a}, \quad (9)$$

356 where  $r = 287.05 \text{ J kg}^{-1} \text{ K}^{-1}$  is the gas constant of air and the air pressure used is the spatially  
357 varying air pressure calculated in Sect. 2.8.

358 The stomatal and aerodynamic resistances are strongly dependent on land cover due to  
359 differences in roughness length and physiological constraints on transpiration of different  
360 vegetation types. In addition, the albedo and emissivity are also dependent on the land cover.  
361 In order to investigate the effect of meteorology on AED, as distinct from land use effects, the  
362 PET was calculated for a single land cover type over the whole of the domain. If necessary,  
363 this can be adjusted to give an estimate of PET specific to the local land cover, for example  
364 using regression relationships (Crooks and Naden, 2007). As a standard, the Food and  
365 Agriculture Organization of the United Nations (FAO) calculate reference crop evaporation for  
366 a hypothetical reference crop, which corresponds to a well-watered grass (Allen et al., 1998).  
367 Following this, the PET in the current study was calculated for a reference crop of 0.12 m  
368 height, with constant stomatal resistance,  $r_s = 70.0 \text{ s m}^{-1}$ , an albedo of 0.23 and emissivity of  
369 0.92 over the whole of Great Britain. This study therefore neglects the effect of land-use on  
370 evaporation, which could be investigated in future by calculating PET for different land surface  
371 types, with different coverage for each year of the dataset.

372 In general, aerodynamic resistance is a function of wind speed and canopy height. Following  
373 Allen et al. (1998), the aerodynamic resistance,  $r_a$  ( $s\ m^{-1}$ ), of a reference crop of 0.12 m height  
374 is a function of the 10 m wind speed

$$375 \quad r_a = \frac{278}{u_{10}}.$$

376 (10)

377 Note that, since the wind speed is likely to be biased high at sites with tall vegetation (Sect.  
378 2.10), this implies that the aerodynamic resistance is likely to be biased low, leading to an  
379 overestimate of PET. However, the estimate of PET here is for a reference crop over the whole  
380 of the dataset, and does not consider the effect of tall vegetation, so the wind speed is  
381 appropriate.

382 Thus the PET is a function of six of the meteorological variables: air temperature, specific  
383 humidity, downward LW and SW radiation, wind speed and surface air pressure.

384 To explore the role of the different meteorological variables in the AED, it is helpful to split  
385 the radiative component (the first part of the numerator in Eq. 4) from the wind component (the  
386 second part). Formally, this is defined as follows (Doorenbos, 1977):

387 The radiative component,  $E_{PR}$ ,

$$388 \quad E_{PR} = \frac{t_d}{\lambda} \frac{\Delta A}{\Delta + \gamma \left(1 + \frac{r_s}{r_a}\right)},$$

389 (11)

390 and the aerodynamic component,  $E_{PA}$ ,

$$391 \quad E_{PA} = \frac{t_d}{\lambda} \frac{c_p \rho_a (q_s - q_a)}{\Delta + \gamma \left(1 + \frac{r_s}{r_a}\right)},$$

392 (12)

393 such that  $E_P = E_{PR} + E_{PA}$ .

### 394 **3.1 Potential evapotranspiration with interception (PETI)**

395 When rain falls, water is intercepted by the canopy. The evaporation of this water is not  
396 constrained by stomatal resistance but is subject to the same aerodynamic resistance as  
397 transpiration (Shuttleworth, 2012). At the same time, transpiration is inhibited in a wet canopy.  
398 Suppression of transpiration is well observed both by comparing eddy-covariance fluxes and  
399 observations of sap flow (Kume et al., 2006; Moors, 2012), and by observing stomatal and

400 photosynthesis response to wetting (Ishibashi and Terashima, 1995). For plants which have at  
401 least some of their stomata on the upper surface of the leaves, this can be due to water directly  
402 blocking the stomata. However, in GB most plants have stomata only on the underside of the  
403 leaves, so the transpiration is inhibited by other mechanisms.

404 Physically, the suppression may be due to the fact that energy is used in evaporating the  
405 intercepted water, so less is available for transpiration or that the increased humidity of the air  
406 decreases the evaporative demand (Bosveld and Bouten, 2003). It may also be due to the  
407 presence of water on the leaf surface causing stomatal closure through physiological reactions,  
408 which can be observed even when the stomata are on the underside of a leaf and the water is  
409 lying on the upper side (Ishibashi and Terashima, 1995).

410 In the short term after a rain event, potential water losses due to evaporation may be  
411 underestimated if only potential transpiration is calculated, and therefore overall rates  
412 underestimated. As transpiration is inhibited over the wet fraction of the canopy (Ward and  
413 Robinson, 2000), the PET over a grid box will be a linear combination of the potential  
414 interception and potential transpiration, each weighted by the fraction of the canopy that is wet  
415 or dry. This can be accounted for by introducing an interception term to the calculation of PET,  
416 giving PETI. This is modelled as an interception store, which is (partially) filled by rainfall,  
417 proportionally inhibiting the transpiration. As the interception store dries, the relative  
418 contribution of interception is decreased and the transpiration increases. In this dataset, this  
419 correction is applied on days with precipitation, while on days without precipitation the  
420 potential is equal to the PET defined in Eq. 4. Although an unconventional definition of PET,  
421 a similar interception correction is applied to the PET provided at 40 km resolution by  
422 MORECS (Thompson et al., 1981) which is used widely by hydrologists.

423 This method implicitly assumes that the water is liquid, however snow lying on the canopy will  
424 also inhibit transpiration, and will be depleted by melting as well as by sublimation. The rates  
425 may be slower, and the snow may stay on the canopy for longer than one day. However, the  
426 difference of accounting for canopy snow as distinct from canopy water will have a small effect  
427 on large-scale averages, as the number of days with snow cover in GB is relatively low, and  
428 they occur during winter when the PET is small.

429 The PETI is a weighted sum of the PET,  $E_p$ , (as calculated in Eq 2.) and potential interception,  
430  $E_I$ , which is calculated by substituting zero stomatal resistance,  $r_s=0 \text{ s m}^{-1}$ , into Eq. 4. To  
431 calculate the relative proportions of interception and transpiration, it is assumed that the wet

432 fraction of the canopy is proportional to the amount of water in the interception store. The  
 433 interception store,  $S_I$  ( $\text{kg m}^{-2}$ ), decreases through the day according to an exponential dry down  
 434 (Rutter et al., 1971), such that

$$435 \quad S_I(t) = S_o e^{-\frac{E_I}{S_{tot}}t},$$

436 (13)

437 where  $E_I$  is the potential interception,  $S_{tot}$  is the total capacity of the interception store ( $\text{kg m}^{-2}$ ),  $S_o$  is the precipitation that is intercepted by the canopy ( $\text{kg m}^{-2}$ ) and  $t$  is the time (in days) since a rain event. We assume that the interception component is only significant on the day in which rainfall occurs, and that it is negligible on subsequent days, so the calculation is only carried out for days of non-zero rainfall. Thus  $t$  is a positive fraction between zero and one.

442 The total capacity of the interception store is calculated following Best et al. (2011), such that

$$443 \quad S_{tot} = 0.5 + 0.05\Lambda,$$

444 (14)

445 where  $\Lambda$  is the leaf area index (LAI). For the FAO standard grass land cover the LAI is 2.88 (Allen et al., 1998). The fraction of precipitation intercepted by the canopy is also found following Best et al. (2011), assuming that precipitation lasts for an average of 3 hours.

448 The wet fraction of the canopy,  $C_{wet}$ , is proportional to the store size, such that

$$449 \quad C_{wet}(t) = \frac{S(t)}{S_{tot}}.$$

450 (15)

451 The total PETI is the sum of the interception from the wet canopy and the transpiration from the dry canopy,

$$453 \quad E_{PI}(t) = E_I C_{wet}(t) + E_P(1 - C_{wet}(t)).$$

454 (16)

455 This is integrated over one day (from  $t=0$  to  $t=1$ ) to find the total PETI,  $E_{PI}$  ( $\text{mm d}^{-1}$ ), to be

$$456 \quad E_{PI} = S_o \left(1 - e^{-\frac{E_I}{S_{tot}}}\right) + E_P \left(1 - \frac{S_o}{E_I} \left(1 - e^{-\frac{E_I}{S_{tot}}}\right)\right).$$

(17)

457 This calculation is only carried out for days on which rainfall occurs. On subsequent days it is  
 458 assumed that the canopy has sufficiently dried out that the interception component is zero.

Formatted: Space Before: 12 pt

459 The PETI is a function of the same six meteorological variables as the PET, plus the  
460 precipitation.

### 461 **3.2 Spatial and seasonal patterns of PET and PETI**

462 Both PET and PETI have a distinct gradient from low in the north-west to high in the south-  
463 east, and they are both inversely proportional to the elevation (Fig. 6), reflecting the spatial  
464 patterns of the meteorological variables. The PETI is 8 % higher than the PET overall but this  
465 difference is larger in the north and west, where precipitation rates, and therefore interception,  
466 are higher (Fig. 6). In Scotland, the higher interception and lower AED mean that this increase  
467 is a larger proportion of the total, with the mean PETI being 11 % larger than the PET (in some  
468 areas the difference is more than 25%). In the English lowlands the difference is smaller, at 6  
469 %, but this is a more water limited region where hydrological modelling can be sensitive to  
470 even relatively small adjustments to PET (Kay et al., 2013).

471 The seasonal climatology of both PET and PETI follow the meteorology (Fig. 7), with high  
472 values in the summer and low in the winter. Although the relative difference peaks in winter,  
473 the absolute difference between PET and PETI is bimodal, with a peak in March and a smaller  
474 peak in October (September in Scotland) (Fig. 7), because in winter the overall AED is low,  
475 while in summer the amount of precipitation is low, so the interception correction is small. The  
476 seasonal cycle of PET is driven predominantly by the radiative component, which has a much  
477 stronger seasonality than the aerodynamic component (Fig. 8).

478 On a monthly or annual timescale, the ratio of PET to precipitation is an indicator of the wet-  
479 or dryness of a region (Oldekop, 1911; Andréassian et al., 2016). Low values of PET relative  
480 to precipitation indicate wet regions, where evaporation is demand-limited, while high values  
481 indicate dry, water-limited regions. In the wetter regions (Scotland, Wales) mean-monthly PET  
482 and PETI (Fig. 7) are on average lower than the mean-monthly precipitation (Fig. 3) throughout  
483 the year, while in drier regions (England, English lowlands) the mean PET and PETI are higher  
484 than the precipitation for much of the summer, highlighting the regions' susceptibility to  
485 hydrological drought (Folland et al., 2015).

## 486 4 Decadal trends

### 487 4.1 Meteorological Variables

488 Annual means of the meteorological variables (Fig. 9) and the PET and PETI (Fig. 10) were  
489 calculated for each region. The trends in these annual means were calculated using linear  
490 regression; the significance ( $P$  value) and 95% confidence intervals (CI) of the slope are  
491 calculated specifically allowing for the non-zero lag-1 autocorrelation, to account for possible  
492 correlations between adjacent data points (Zwiers and von Storch, 1995; von Storch and  
493 Zwiers, 1999). The annual trends can be seen in Table 2. In addition, seasonal means were  
494 calculated, with the four seasons defined to be Winter (December-February), Spring (March-  
495 May), Summer (June-August) and Autumn (September-November), and trends in these means  
496 were also found.

497 The trends in the annual and seasonal means for all regions are plotted in Fig. 11; trends that  
498 are statistically significant at the 5% level are plotted with solid error bars, those that are not  
499 significant are plotted with dashed lines. The analysis was repeated for each pixel in the 1 km  
500 resolution dataset; maps of these rates of change can be seen in Fig. B1.

501 There was a statistically significant trend in air temperature in the English Lowlands throughout  
502 the year. In the other regions the trends were statistically significant in spring and autumn, and  
503 for the annual means. The trends agree with recent trends in the Hadley Centre Central England  
504 Temperature (HadCET) dataset (Parker and Horton, 2005) and in temperature records for  
505 Scotland (Jenkins et al., 2008) as well as in the CRUTEM4 dataset (Jones et al., 2012). An  
506 increase in winter precipitation in Scotland is seen in the current dataset, which leads to a  
507 statistically significant increase in the annual mean precipitation of GB. However, all other  
508 regions and seasons have no statistically significant trends in precipitation. Long term  
509 observations show that there has been little trend in annual precipitation, but a change in  
510 seasonality with wetting winters and drying summers since records began, although with little  
511 change over the past 50 years (Jenkins et al., 2008). The statistically significant decline in wind  
512 speed in all regions is consistent with the results of McVicar et al. (2012) and Vautard et al.  
513 (2010), who report decreasing wind speeds in the northern hemisphere over the late 20<sup>th</sup>  
514 century.



## 515 4.2 Potential Evapotranspiration

516 The trends of the meteorological variables are interesting in their own right. But for hydrology,  
517 it is the impact that the trends have on evaporation that matters and that depends on their  
518 combination, which can be expressed through PET.

519 The regional trends of annual mean PET and PETI and the radiative and aerodynamic  
520 components of PET can be seen in Table 2, and the trends in the annual and seasonal means  
521 are plotted in Fig. 12 for all regions. Maps of the trends can be seen in Fig. B2. The trend in  
522 the radiative component of PET is positive over the whole of GB. However, the trend in the  
523 aerodynamic component varies; for much of Wales, Scotland and northern England, it is not  
524 significant, or is slightly negative, while in south-east England and north-west Scotland it is  
525 positive. This leads to a positive trend in PET over much of GB, but no significant trend in  
526 southern Scotland and northern England. There is a statistically significant increase in annual  
527 PET in all regions except Wales; the GB trend ( $0.021 \pm 0.021 \text{ mm d}^{-1} \text{ decade}^{-1}$ ) is equivalent to  
528 an increase of  $0.11 \pm 0.11 \text{ mm d}^{-1}$  ( $8.3 \pm 8.1 \%$  of the long term mean) over the whole dataset.  
529 Increases in PETI are only statistically significant in England ( $0.023 \pm 0.023 \text{ mm d}^{-1} \text{ decade}^{-1}$ )  
530 and English lowlands ( $0.028 \pm 0.025 \text{ mm d}^{-1} \text{ decade}^{-1}$ ), where the increases over the whole  
531 dataset are  $0.12 \pm 0.12 \text{ mm d}^{-1}$  ( $8.0 \pm 8.0 \%$  of the long term mean) and  $0.15 \pm 0.13 \text{ mm d}^{-1}$  ( $9.7 \pm 8.8$   
532  $\%$  of the long term mean) respectively. There is a difference in trend between different seasons.  
533 In winter, summer and autumn there are no statistically significant trends in PET or PETI, other  
534 than the English lowlands in autumn, but the spring is markedly different, with very significant  
535 trends ( $P < 0.0005$ ) in all regions. The GB spring trends in PET ( $0.043 \pm 0.019 \text{ mm d}^{-1} \text{ decade}^{-1}$ )  
536 and PETI ( $0.038 \pm 0.018 \text{ mm d}^{-1} \text{ decade}^{-1}$ ) are equivalent to an increase of  $0.22 \pm 0.10 \text{ mm d}^{-1}$   
537 ( $13.8 \pm 6.2 \%$  of the long-term spring mean) and  $0.20 \pm 0.09 \text{ mm d}^{-1}$  ( $11.2 \pm 5.3 \%$  of the long-  
538 term spring mean) over the length of the dataset respectively. The radiative component of PET  
539 has similarly significant trends in spring, while the aerodynamic component has no significant  
540 trends in any season, except the English Lowlands in autumn (Fig. 12).

541 There are few studies of long-term trends in AED in the UK. MORECS provides an estimate  
542 of Penman-Monteith PET with interception correction calculated directly from the 40 km  
543 resolution meteorological data (Hough and Jones, 1997; Thompson et al., 1981), and increases  
544 can be seen over the dataset (Rodda and Marsh, 2011). But as the PET and PETI in the current  
545 dataset are ultimately calculated using the same meteorological data (albeit by different  
546 methods), it is not unexpected that similar trends should be seen. Site-based studies suggest an  
547 increase over recent decades (Burt and Shahgedanova, 1998; Crane and Hudson, 1997), but it

548 is difficult to separate climate-driven trends from local land-use trends. A global review paper  
 549 (McVicar et al., 2012) identified a trend of decreasing AED in the northern hemisphere, driven  
 550 by decreasing wind speeds, however they also reported significant local variations on trends in  
 551 pan evaporation, including the increasing trend observed by Stanhill and Möller (2008) at a  
 552 site in England after 1968. Matsoukas et al. (2011) identified a statistically significant increase  
 553 in PET in several regions of the globe, including southern England, between 1983 and 2008,  
 554 attributing it predominantly to an increase in the radiative component of PET, due to global  
 555 brightening. However, these results were obtained using reanalysis data, which is limited in its  
 556 ability to capture trends in wind speed. This limitation has been documented in both northern  
 557 (Pryor et al., 2009) and southern (McVicar et al., 2008) hemispheres.

558 Regional changes in actual evaporative losses can be estimated indirectly using regional  
 559 precipitation and runoff or river flow. Using a combination of observations and modelling,  
 560 Marsh and Dixon (2012) identified an increase in evaporative losses in Great Britain from  
 561 1961-2011. Hannaford and Buys (2012) note seasonal and regional differences in trends in  
 562 observed river flow, suggesting that decreasing spring flows in the English lowlands are  
 563 indicative of increasing AED. However, changing evaporative losses can also be due to  
 564 changing supply through precipitation, so it is important to formally attribute the trends in PET  
 565 to changing climate, in order to understand changing evapotranspiration.

### 566 4.3 Attribution of trends in potential evapotranspiration

567 In order to attribute changes in PET to changes in climate, the rate of change of PET,  $dE_p/dt$   
 568 ( $\text{mm d}^{-1} \text{ decade}^{-1}$ ), can be calculated as a function of the rate of change of each input variable  
 569 (Roderick et al., 2007),

$$570 \frac{dE_p}{dt} = \frac{dE_p}{dT_a} \frac{dT_a}{dt} + \frac{dE_p}{dq_a} \frac{dq_a}{dt} + \frac{dE_p}{du_{10}} \frac{du_{10}}{dt} + \frac{dE_p}{dL_d} \frac{dL_d}{dt} + \frac{dE_p}{dS_d} \frac{dS_d}{dt} . \quad (18)$$

571 Note that we exclude the surface air pressure, because this dataset uses a mean-monthly  
 572 climatology as the interannual variability of air pressure is negligible. The derivative of the  
 573 PET with respect to each of the meteorological variables can be found analytically (Appendix  
 574 C). The derivatives are calculated from the daily meteorological data at 1 km resolution.  
 575 Substituting the slopes of the linear regressions of the gridded annual means (Appendix B) for  
 576 the rate of change of each variable with time, and the overall time-average of the derivatives  
 577 of PET with respect to the meteorological variables, the contribution of each variable to the  
 578 rate of change of PET can be calculated at 1 km resolution. These are then averaged over the

579 regions of interest. The same ~~can~~is also ~~be~~ applied to the radiative and aerodynamic  
580 components independently.

581 Note that this can also be applied to the regional means of the derivatives of PET and the  
582 regional trends in the meteorological variables. The results are compared in Table 3 and the  
583 two approaches are consistent. For the regional analysis, we also quote the 95% CI. However,  
584 for the gridded values, there is such high spatial coherence that combining the 95% CI over the  
585 region results in unreasonably constrained results. We therefore use the more conservative CI  
586 obtained from the regional analysis. Also note that this method assumes that the rate of change  
587 of the variables with respect to time is constant over the seasonal cycle (and thus the product  
588 of the means is equal to the mean of the products), and indeed this is how it is often applied  
589 (Donohue et al., 2010; Lu et al., 2016). The effect of this assumption was investigated by  
590 repeating the analysis with seasonal trends and means, but this makes negligible difference to  
591 the results.

592 Figure 13 shows the contribution of each meteorological variable to the rate of change of the  
593 annual mean PET and to the radiative and aerodynamic components and compares the total  
594 attributed trend to that obtained by linear regression. The percentage contribution is in Table  
595 4, calculated as a fraction of the fitted trend. The final column shows the total attributed trend  
596 (i.e. the sum of the previous columns) as a percentage of the fitted trend, to demonstrate the  
597 success of the attribution at recovering the fitted trends. For the PET trend and for the trend in  
598 the radiative component, these values generally sum to the linear regression to within a few  
599 percent. However, for the aerodynamic component, the fitted trends are much smaller than the  
600 statistical uncertainty. This means that there can be a large and/or negative percentage  
601 difference between the attributed and fitted trends, even when the absolute difference is  
602 negligible.

603 The largest overall contribution to the rate of change of PET comes from increasing air  
604 temperature, which has the effect of increasing the aerodynamic component (~~as it makes the~~  
605 ~~air more able to hold water), but it decreases the radiative component (due to increasing~~  
606 ~~outgoing LW radiation), but decreasing the radiative component. The latter effect is due to~~  
607 approximating the surface temperature with the air temperature in the calculation of upwelling  
608 LW radiation. This assumption is applied as it simplifies the surface energy balance but it may  
609 introduce artefacts into the calculation of PET. A more thorough formulation of PET, which  
610 linearises the net radiation in the derivation of the Penman-Monteith equation, can be  
611 calculated to allow for a non-negligible difference between air and surface temperature

612 (Monteith, 1981; Thompson et al., 1981), but the difference between the more thorough  
613 formulation and the formulation used here is small, particularly for the temperature range of  
614 GB.

615 Note that in this calculation we are assuming that air temperature and downward LW radiation  
616 vary independently, while in reality (and implicit in the calculation of downward LW in Sect.  
617 2.4), downward LW radiation is also ~~proportional to a function of~~ the air temperature so that  
618 increases in downward LW may broadly cancel the increasing ~~outgoing upwelling~~ LW  
619 radiation. If we instead ~~used~~ were to use net LW radiation as the independent variable, it is  
620 likely that dependence of the rate of change of the radiative component on air temperature  
621 would be reduced in magnitude and compensated by the rate of change of net LW radiation.

622 Overall the next largest increases are caused by increasing downward SW radiation,  
623 particularly in the English regions in the spring, as it increases the radiative component of PET.  
624 However, in Scotland and Wales, the increasing downward LW radiation is also important.  
625 Increasing specific humidity strongly decreases the PET by decreasing the aerodynamic  
626 component, while the decreasing wind speed has the effect of increasing the radiative  
627 component, but more strongly decreasing the aerodynamic component, so overall it tends to  
628 cause a decrease in PET. Since the increasing air temperature and downward LW and SW  
629 radiation have the effect of increasing PET, but the increasing specific humidity and decreasing  
630 wind speed tend to decrease it, then the overall trend is positive, but smaller than the trend due  
631 to air temperature alone.

#### 632 **4.4 Relative humidity**

633 The increase in PET due to increasing air temperature is largely cancelled by the decrease due  
634 to increasing specific humidity; ~~so that the overall trend is smaller than the contribution to the~~  
635 increase from air temperature alone. However, although we have assumed that specific  
636 humidity and air temperature are independent variables, they are in fact coevolving ~~as part of~~ in  
637 a warming atmosphere. ~~As~~ As air temperature increases, the saturated specific humidity  
638 increases according to the Clausius-Clapeyron relation (Schneider et al., 2010). However, since  
639 evaporation also increases with rising temperature, the increased water flux into the atmosphere  
640 ensures that specific humidity also increases and it can be shown that there is likely to be little  
641 change in global relative humidity even with significant change in global temperature (Held  
642 and Soden, 2006; Schneider et al., 2010), although this may vary regionally over land (Dai,  
643 2006). Although it is not completely independent of air temperature, an alternative way of

644 assessing the drivers of AED is to consider relative humidity,  $R_h$ , as the independent humidity  
 645 variable. In this case, the PET can be recast in terms of relative humidity, such that

$$646 \quad E_P = \frac{t_d}{\lambda} \frac{\Delta A + \frac{c_p \rho_a}{r_a} q_s (1 - R_h)}{\Delta + \gamma \left(1 + \frac{r_s}{r_a}\right)}. \quad (19)$$

648 Relative humidity can be calculated from the specific humidity using

$$649 \quad R_h = \frac{q_a}{q_s}. \quad (20)$$

651 Although in this case relative humidity is a function of air temperature, through the saturated  
 652 specific humidity, in reality they are often found to behave as independent variables. It has  
 653 been shown that there is little cancellation of the air temperature and relative humidity terms  
 654 when studying both historical data (Vicente Serrano et al., 2016) and future climate projections  
 655 (Scheff and Frierson, 2014).

656 The relative humidity annual means, mean-monthly climatology and seasonal trends can be  
 657 seen in Fig. 14. We find ~~that there is~~ a statistically significant negative trend in relative  
 658 humidity, in the spring and autumn (except Wales in the autumn) but no overall negative trend  
 659 in winter or summer, ~~or for~~ and no significant trend in the annual means. Maps of the overall  
 660 mean relative humidity and ~~its~~ the trend in the annual mean are in Fig B3. (Jenkins et al., 2008;  
 661 Dai, 2006). There are only small regions in the west of Scotland and the east and south west of  
 662 England where there are significant trends in the annual mean.

663 We calculate an alternative attribution using relative humidity as a variable, rather than specific  
 664 humidity, such that

$$665 \quad \frac{dE_P}{dt} = \frac{dE_P}{dT_a} \frac{dT_a}{dt} + \frac{dE_P}{dR_h} \frac{dR_h}{dt} + \frac{dE_P}{du_{10}} \frac{du_{10}}{dt} + \frac{dE_P}{dL_d} \frac{dL_d}{dt} + \frac{dE_P}{dS_d} \frac{dS_d}{dt}. \quad (21)$$

666 We then calculate the derivative of the PET with respect to relative humidity and the derivatives  
 667 with respect to air temperature and pressure are now taken at constant  $R_h$  rather than constant  
 668  $q_a$ , so these are also recalculated. See Appendix C for details.

669 Figure 15 shows the contribution of the different variables to the rate of change of PET with  
 670 this alternative formulation. The total attributed change is nearly the same as that in Fig. 13,  
 671 although there are small differences due to statistical uncertainty in the fits. ~~The contribution~~  
 672 ~~of air temperature to the rate of change is significantly reduced, so much as to be negligible. It~~

673 ~~causes the radiative component to decrease as before (due to increased outgoing~~ The  
674 contributions of downward SW and LW radiation) and the aerodynamic component to decrease  
675 ~~(because the rising air temperature increases the saturated specific humidity), and of wind~~  
676 speed to the rate of change of PET are unchanged. Although it is not statistically significant,  
677 ~~there is a~~ the negative trend in relative humidity, ~~and this~~ leads to an increase in the aerodynamic  
678 component, which is larger than the increase due to increasing downward SW radiation. The  
679 contribution of air temperature to the rate of change is significantly reduced compared to the  
680 specific humidity formulation. The air temperature-driven decrease in the radiative component  
681 now largely cancels the temperature-driven increase in the aerodynamic component, which is  
682 much smaller than in Sect. 4.3 as it now implicitly includes the rising specific humidity.  
683 However, the effect of air temperature on the radiative component comes through the effect of  
684 air temperature on the upwelling LW radiation in the calculation of net radiation and this is  
685 dependent on the simplifying assumption that the surface temperature is equal to the air  
686 temperature when solving the energy balance. If the fully linearised version of the Penman-  
687 Monteith equation were used (Monteith, 1981), then the dependence on air temperature would  
688 be more complicated as it would account for a non-negligible difference between air and  
689 surface temperature. This may result in a different contribution of air temperature to the  
690 changing PET, although this difference is likely to be small.

## 691 **5 Discussion**

692 These high resolution datasets provide insight into the effect of the changing climate of Great  
693 Britain on AED over the past five decades. There have been significant climatic trends in the  
694 UK since 1961; in particular rising air temperature and specific humidity, decreasing wind  
695 speed and decreasing cloudiness. Although some are positive and some negative, these  
696 meteorological trends combine to give statistically significant trends in PET.

697 Wind speeds have decreased more significantly in the west than the east, and show a consistent  
698 decrease across seasons. Contrary to Donohue et al. (2010) and McVicar et al. (2012), this  
699 study finds that the change in wind speed of the late 20<sup>th</sup> and early 21<sup>st</sup> centuries has not had a  
700 dominant influence on PET over the period of study, although it has mitigated the increasing  
701 trend in PET. However, the previous studies were concerned with open-water Penman  
702 evaporation, which has a simpler (proportional) dependence on wind speed than the Penman-  
703 Monteith PET considered here (Schymanski and Or, 2015).

704 The air temperature trend in this study of  $0.21 \pm 0.15$  K decade<sup>-1</sup> in GB is consistent with  
705 observed global and regional trends (Hartmann et al., 2013; Jenkins et al., 2008). The  
706 temperature trend is responsible for a large contribution to the trend in PET, although the large  
707 negative contribution from the specific humidity (as well as a small negative contribution from  
708 wind speed) means that the overall trend is smaller than the temperature trend alone.

709 When the attribution is recast in terms of relative humidity, the effect of air temperature is  
710 ~~negligible~~ much smaller, supporting the hypothesis that the temperature and specific humidity  
711 components cancel because their changes are part of the same thermodynamic warming  
712 processes. ~~However, although the relative humidity does not have a statistically significant~~  
713 ~~trend (except~~ Much of the increase in the aerodynamic component due to air temperature is  
714 cancelled by the decrease of the radiative component, which is due to the effect of air  
715 temperature on the calculated upwelling LW radiation. However this is because of the  
716 assumption that surface temperature can be approximated with air temperature, thus the real  
717 physical contribution of air temperature in the relative humidity formulation is likely to be  
718 roughly equal to the increase in the aerodynamic component. Although the relative humidity  
719 does not have a statistically significant trend overall (although there are significant trends in  
720 spring and for some regions in autumn), it is large enough that the negative trend in relative  
721 humidity is the largest contribution to the increasing PET, followed by the downward SW  
722 radiation. This corresponds well to recent findings in Spain (Vicente-Serrano et al., 2016).

723 The trend in relative humidity is consistent with that seen in historical regional (Jenkins et al.,  
724 2008) and global (Dai, 2006; Willett et al., 2014) analyses. Although not statistically significant  
725 overall, it contributes to between 57 % and 68 % of the trends in PET (between 39 % and 46  
726 % or the trends in spring PET). Globally trends in relative humidity vary spatially, with mid-  
727 latitudes showing a decrease and the tropics and high-latitudes showing an increase, despite an  
728 overall increase in specific humidity over land, particularly in the Northern Hemisphere (Dai,  
729 2006; Willett et al., 2014). In these global analyses, Great Britain is in a region of transition  
730 between decreasing relative humidity in Western Europe and increasing relative humidity in  
731 Scandinavia, so that small decreasing trends are found, but they are not significant; this is  
732 consistent with our findings. We ~~have~~ found the relative humidity to be decreasing significantly  
733 in spring, which is also when the downward SW is increasing. This is ~~again~~ consistent with  
734 reduced precipitation and cloud cover due to changing weather patterns (Sutton and Dong,  
735 2012).

736 Increasing solar radiation has been shown to increase spring and annual AED, contributing to  
737 between 18 % and 50 % of the fitted trend in annual PET, and to between 43 % and 53 % of  
738 the fitted trend in spring PET. Two main mechanisms can be responsible for changing solar  
739 radiation—: changing cloud cover and changing aerosol concentrations. Changing aerosol  
740 emissions have been shown to have had a significant effect on solar radiation in the 20<sup>th</sup>  
741 century. In Europe, global dimming due to increased aerosol concentrations peaked around  
742 1980, followed by global brightening as aerosol concentrations decreased (Wild, 2009).  
743 Observations of changing continental runoff and river flow in Europe over the 20<sup>th</sup> century  
744 have been attributed to changing aerosol concentrations, via their effect on solar radiation, and  
745 thus AED (Gedney et al., 2014).

746 In this study we use the duration of bright sunshine to calculate the solar radiation, using  
747 empirical coefficients which do not vary with year, so aerosol effects are not explicitly  
748 included- and the trend in downward SW is driven by the increase in sunshine hours in the  
749 MORECS dataset ( $0.088 \pm 0.055 \text{ h d}^{-1} \text{ decade}^{-1}$  over GB). The coefficients used in this study to  
750 convert sunshine hours to radiation fluxes were empirically derived in 1978; the derivation  
751 used data from the decade 1966-75, as this period was identified to be before reductions in  
752 aerosol emissions had begun to significantly alter observed solar radiation (Cowley, 1978).  
753 Despite this, the trend in SW radiation in the current dataset from 1979 onwards ( $1.4 \pm 1.4 \text{ W}$   
754  $\text{m}^{-2} \text{ decade}^{-1}$ ) is consistent, within uncertainties, with that seen over GB in the WFDEI data  
755 ( $0.9 \pm 1.1 \text{ W m}^{-2} \text{ decade}^{-1}$ ), which is bias-corrected to observations and includes explicit aerosol  
756 effects (Weedon et al., 2014).

757 It has been suggested that aerosol effects also implicitly affect sunshine duration since in  
758 polluted areas, there will be fewer hours above the official ‘sunshine hours’ threshold of 120  
759  $\text{Wm}^{-2}$  (Helmes and Jaenicke, 1986). Several regional studies have shown trends in sunshine  
760 hours that are consistent with the periods of dimming and brightening across the globe (eg  
761 Liley, 2009; Sanchez-Lorenzo et al., 2009; Sanchez-Lorenzo et al., 2008; Stanhill and Cohen,  
762 2005), and several have attempted to quantify the relative contribution of trends in cloud cover  
763 and aerosol loading (e.g. Sanchez-Lorenzo and Wild (2012) in Switzerland, see Sanchez-  
764 Romero et al. (2014) for a review). Therefore, it may be that some of the brightening trend seen  
765 in the current dataset is due to the implicit signal of aerosol trends in the MORECS sunshine  
766 duration, although this is likely to be small compared to the effects of changing cloud cover.

767 The trends in the MORECS sunshine duration used in this study are consistent with changing  
768 weather patterns which may be attributed to the Atlantic Multidecadal Oscillation (AMO). The



769 AMO has been shown to cause a decrease in spring precipitation (and therefore cloud cover)  
770 in northern Europe over recent decades (Sutton and Dong, 2012), and the trend in MORECS  
771 sunshine hours is dominated by an increase in the spring mean. This has also been seen in  
772 Europe-wide sunshine hours data (Sanchez-Lorenzo et al., 2008) and is also consistent with  
773 the falling spring relative humidity found in the current study. On the other hand, the effect of  
774 changing aerosols on sunshine hours is expected to be largest in the winter (Sanchez-Lorenzo  
775 et al., 2008). However, it would not be possible to directly identify either of these effects on  
776 the sunshine duration without access to longer data records.

777 The inclusion of explicit aerosol effects in the coefficients of the Ångström-Prescott equation  
778 would be expected to reduce the positive trend in AED in the first two decades of the dataset,  
779 and increase it after 1980. Gedney et al. (2014) attribute a decrease in European solar radiation  
780 of  $10 \text{ W m}^{-2}$  between the periods 1901-10 and 1974-80, and an increase of  $4 \text{ W m}^{-2}$  from 1974-  
781 84 to 1990-99 to changing aerosol contributions. Applying these trends to the current dataset,  
782 with a turning point at 1980, would double the overall increase in solar radiation in Great  
783 Britain, which would lead to a 40 % increase in the overall trend in PET. So, if this effect were  
784 to be included, it would confirm the results found in this paper.

785 ~~(Willett et al., 2014; Dai, 2006; Sutton and Dong, 2012)~~ Although the contribution is generally  
786 smaller (except in Scotland), the trends in LW radiation in these datasets contribute to between  
787 15% and ~~28~~27% of the trends in PET and between 27% and 46% of the trends in the radiative  
788 component. In Scotland the downward LW radiation is the dominant driver of changing PET-  
789 in the relative humidity formulation. Note, however, that this is largely cancelled by the  
790 increasing upwelling LW, which is captured in this study in the effect of air temperature on the  
791 radiative component, and which may be different if the approximation that the difference  
792 between air temperature and surface temperature is negligible were relaxed. Observations of  
793 LW radiation are often uncertain, but the trend in this dataset, although small, is consistent with  
794 observed trends (Wang and Liang, 2009), as well as with trends in the WFDEI bias-corrected  
795 reanalysis product (Weedon et al., 2014).

796 Trends in temperature and cloud cover in the UK are expected to continue into the coming  
797 decades, with precipitation expected to increase in the winter but decrease in the summer  
798 (Murphy et al., 2009). Therefore it is likely that AED will increase, increasing water stress in  
799 the summer when precipitation is lower and potentially affecting water resources, agriculture  
800 and biodiversity. This has been demonstrated for southern England and Wales by Rudd and

801 Kay (2015), who calculated present and future PET using high-resolution RCM output and  
802 included the effects of CO<sub>2</sub> on stomatal opening.

803 The current study is concerned only with the effects of changing climate on AED and has  
804 assumed a constant bulk canopy resistance throughout. However, plants are expected to react  
805 to increased CO<sub>2</sub> in the atmosphere by closing stomata and limiting the exchange of gases,  
806 including water (Kruijt et al., 2008), and observed changes in runoff have been attributed to  
807 this effect (Gedney et al., 2006; Gedney et al., 2014). It is possible that the resulting change of  
808 canopy resistance could partially offset the increased atmospheric demand (Rudd and Kay,  
809 2015) and may impact runoff (Gedney et al., 2006; Prudhomme et al., 2014), but further studies  
810 would be required to quantify this.

## 811 **6 Conclusion**

812 This paper has presented a unique, high-resolution, observation-based dataset of  
813 meteorological variables and AED in Great Britain since 1961. Key trends in the  
814 meteorological variables are (i) increasing air temperature and specific humidity, consistent  
815 with global temperature trends; (ii) increasing solar radiation, particularly in the spring,  
816 consistent with changes in aerosol emissions and weather patterns in recent decades; (iii)  
817 decreasing wind speed, consistent with observations of global stilling; ~~and~~ (iv) increasing  
818 precipitation, driven by increasing winter precipitation in Scotland; and (v) no significant trend  
819 in relative humidity overall, but decreasing relative humidity in the spring. The meteorological  
820 variables were used to evaluate AED in Great Britain via calculation of PET and PETI. It has  
821 been demonstrated that including the interception component in the calculation of PETI gives  
822 a mean estimate that is overall 8% larger than PET alone, with strong seasonality and spatial  
823 variation of the difference. PET was found to be increasing by  $0.021 \pm 0.021$  mm d<sup>-1</sup> decade<sup>-1</sup> in  
824 GB over the study period. With the interception component included, the trend in PETI is  
825 weaker ( $0.019 \pm 0.020$  mm d<sup>-1</sup>), and over GB is not significant at the 5% level. The trend in PET  
826 was analytically attributed to the trends in the meteorological variables, and it was found that  
827 the dominant effect was that increasing air temperature was driving increasing PET, with  
828 smaller increases from increased downward SW and LW radiation. However, the effect of  
829 temperature is largely compensated by the associated increase in specific humidity, while  
830 decreasing wind speed tended to decrease the PET. When the attribution was recast in terms of  
831 relative humidity, temperature was found to have a ~~negligible~~small effect on the trend in PET  
832 due to cancellation between the increase in the aerodynamic component and decrease in the  
833 radiative component, while the decreasing relative humidity caused PET to increase, at a

834 similar rate to the downward SW radiation (and downward LW radiation in Scotland). The  
835 increase in PET due to these variables is mitigated by the observed northern hemisphere wind  
836 stilling, which causes a decrease in PET, however, the overall trend in PET is positive over the  
837 period of study.

838 In addition to providing meteorological data and estimates of AED for analysis, the  
839 meteorological variables provided are sufficient to run LSMs and hydrological models. The  
840 high spatial (1 km) and temporal (daily) resolution will allow this dataset to be used to study  
841 the effects of climate on physical and biological systems at a range of scales, from local to  
842 national.

#### 843 **Data Access**

844 The data can be downloaded from the Environmental Information Platform at the Centre for  
845 Ecology & Hydrology. The meteorological variables (CHESS-met) can be found at  
846 <https://catalogue.ceh.ac.uk/documents/80887755-1426-4dab-a4a6-250919d5020c>,  
847 while the PET and PETI (CHESS-PE) can be accessed at  
848 <https://catalogue.ceh.ac.uk/documents/d329f4d6-95ba-4134-b77a-a377e0755653>.

#### 849 **Author contribution**

850 EB, JF and DBC designed the study. JF, ACR, DBC and ELR developed code to create  
851 meteorological data. ELR created the PET and PETI. ELR and EB analysed trends. ELR, EB,  
852 ACR and DBC wrote the manuscript.

#### 853 **Acknowledgements**

854 The meteorological variables presented are based largely on GB meteorological data under  
855 licence from the Met Office, and those organisations contributing to this national dataset  
856 (including the Met Office, Environment Agency, Scottish Environment Protection Agency  
857 (SEPA) and Natural Resources Wales) are gratefully acknowledged. The CRU TS 3.21 daily  
858 temperature range data were created by the University of East Anglia Climatic Research Unit,  
859 and the WFD air pressure data were created as part of the EU FP6 project WATCH (Contract  
860 036946). Collection of flux data was funded by EU FP4 EuroFlux (Griffin Forest); EU FP5  
861 CarboEuroFlux (Griffin Forest); EU FP5 GreenGrass (Easter Bush); EU FP6 CarboEuropeIP  
862 (Alice Holt, Griffin Forest, Auchencorth Moss, Easter Bush); EU FP6 IMECC (Griffin  
863 Forest); the Forestry Commission (Alice Holt); the Natural Environment Research Council,  
864 UK (Auchencorth Moss, Easter Bush).

865 Fig. 1 ~~and~~, panels a) and b) of Fig. ~~66 and panel a) of Fig. B3~~ were produced with the python  
866 implementation of the cubehelix colour scheme (Green, 2011).  
867 Thanks to Nicola Gedney and Graham Weedon for useful discussions.  
868 Thanks to three anonymous reviewers, who provided insightful and helpful comments.  
869 This work was partially funded by the Natural Environment Research Council in the  
870 Changing Water Cycle programme: NERC Reference: NE/I006087/1.  
871

## 872 **Appendix A: Data validation**

873 Meteorological data were downloaded from the European Fluxes Database Cluster  
874 (<http://gaia.agraria.unitus.it>) for four sites positioned around Great Britain. Two were  
875 woodland sites (Alice Holt (Wilkinson et al., 2012; Heinemeyer et al., 2012) and Griffin Forest  
876 (Clement, 2003)), while two had grass and crop cover (Auchencorth Moss (Billett et al., 2004)  
877 and Easter Bush (Gilmanov et al., 2007; Soussana et al., 2007)). Table A1 gives details of the  
878 data used. The data are provided as half-hourly measurements, which were used to create daily  
879 means, where full daily data coverage was available. The daily means of the observed data  
880 were compared to the daily data from the grid square containing the site and the Pearson  
881 correlation ( $r^2$ ), mean bias and root mean square error (RMSE) were calculated. For each site,  
882 monthly means were calculated where the full month had available data, then a climatology  
883 calculated from available months. The same values were calculated from the relevant grid  
884 squares, using only time periods for which observed data were available.

885 Fig. A1 shows the comparison of the data set downward SW radiation against daily mean air  
886 temperature observed at the four sites. Fig. A2 shows the mean-monthly climatology of the  
887 daily values. The observed values of the mixing ratio of water vapour in air were compared  
888 with values calculated from the meteorological dataset, using the equation

$$889 \quad r_w = q_a \left( \frac{m_a}{m_w} \right)$$

890 (A1)

891 where  $m_a$  is the molecular mass of dry air and  $m_w$  is the molecular mass of water. The  
892 comparisons are shown in Figs. A3 and A4.

893 Table A2 shows the  $r^2$ , mean bias and RMSE for each of the variables included in the validation  
894 exercise. The correlations indicate a good relationship between the dataset variables and the  
895 independent observations at the sites, while the mean-monthly climatologies demonstrate that  
896 the data represent the seasonal cycle well. The data set downward SW in Auchencorth Moss is  
897 biased high compared to the observations, while the wind speed is biased high at two sites.

## 898 **Appendix B: Trend maps**

899 Fig. B1 shows the rate of change of each of the meteorological variables at the 1 km resolution,  
900 while Fig. B2 shows the rate of change of the PET, PETI, and the two components of PET at  
901 the same resolution. This shows that the regional trends are consistent with spatial variation  
902 and are not dominated by individual extreme points.

903 **Appendix C: Derivatives of PET**

904 The wind speed affects the PET through the aerodynamic resistance. The derivative with  
905 respect to wind speed is

$$906 \quad \frac{\partial E_P}{\partial u_{10}} = \frac{(\Delta + \gamma) E_{PA} - \gamma \frac{r_s}{r_a} E_{PR}}{u_{10} \left( \Delta + \gamma \left( 1 + \frac{r_s}{r_a} \right) \right)}.$$

907 (C1)

908 The downward LW and SW radiation affect PET through the net radiation, and the derivatives  
909 are

$$910 \quad \frac{\partial E_P}{\partial L_d} = E_{PR} \frac{\epsilon}{R_n}$$

911 (C2)

$$912 \quad \frac{\partial E_P}{\partial S_d} = E_{PR} \frac{(1 - \alpha)}{R_n}.$$

913 (C3)

914 The derivative of PET with respect to specific humidity is

$$915 \quad \frac{\partial E_P}{\partial q_a} = \frac{E_{PA}}{q_a - q_s}.$$

916 (C4)

917 The air temperature affects PET through the saturated specific humidity and its derivative, the  
918 net radiation and the air density, so that the derivative of PET with respect to air temperature  
919 is

$$920 \quad \frac{\partial E_P}{\partial T_a} = E_{PR} \left[ \left( 1 - \frac{\Delta}{\Delta + \gamma \left( 1 + \frac{r_s}{r_a} \right)} \right) \left( \frac{T_{sp}}{T_a^2} \frac{\sum_{i=1}^4 i(i-1) \alpha_i T_r^{i-2}}{\sum_{i=1}^4 i \alpha_i T_r^{i-1}} + \Delta \frac{p_* + (1 - \epsilon) e_s}{p_* q_s} - \frac{2}{T_a} \right) - \frac{4 \epsilon \sigma T_a^3}{R_n} \right] +$$

$$921 \quad E_{PA} \left[ \frac{\Delta}{q_s - q_a} - \frac{1}{T_a} - \frac{\Delta}{\Delta + \gamma \left( 1 + \frac{r_s}{r_a} \right)} \left( \frac{T_{sp}}{T_a^2} \frac{\sum_{i=1}^4 i(i-1) \alpha_i T_r^{i-2}}{\sum_{i=1}^4 i \alpha_i T_r^{i-1}} + \Delta \frac{p_* + (1 - \epsilon) e_s}{p_* q_s} - \frac{2}{T_a} \right) \right].$$

922 (C5)

923 When calculating the attribution with relative humidity as the dependent variable, the  
924 derivative of PET with respect to relative humidity is

$$925 \quad \frac{\partial E_P}{\partial R_h} = \frac{E_{PA}}{R_h - 1},$$

926 (C6)

927 and the derivative of PET with respect to air temperature is

$$\begin{aligned}
928 \quad \frac{\partial E_P}{\partial T_a} &= E_{PR} \left[ \left( 1 - \frac{\Delta}{\Delta + \gamma \left( 1 + \frac{r_s}{r_a} \right)} \right) \left( \frac{T_{sp}}{T_a^2} \frac{\sum_{i=1}^4 i(i-1) a_i T_r^{i-2}}{\sum_{i=1}^4 i a_i T_r^{i-1}} + \Delta \frac{p_* + (1-\varepsilon) e_s}{p_* q_s} - \frac{2}{T_a} \right) - \frac{4 \varepsilon \sigma T_a^3}{R_n} \right] + \\
929 \quad E_{PA} &\left[ \frac{\Delta}{q_s} - \frac{1}{T_a} - \frac{\Delta}{\Delta + \gamma \left( 1 + \frac{r_s}{r_a} \right)} \left( \frac{T_{sp}}{T_a^2} \frac{\sum_{i=1}^4 i(i-1) a_i T_r^{i-2}}{\sum_{i=1}^4 i a_i T_r^{i-1}} + \Delta \frac{p_* + (1-\varepsilon) e_s}{p_* q_s} - \frac{2}{T_a} \right) \right]. \\
930 \quad &(C7)
\end{aligned}$$

931 The difference between Eq. C7 and Eq. C5 is the factor of  $\Delta/q_s$  instead of  $\Delta/(q_s - q_a)$  in the  
932 second bracket.

## 933 7 References

- 934 Allen, R. G., Pereira, L. S., Raes, D., and Smith, M.: Crop evapotranspiration - Guidelines for  
935 computing crop water requirements, Food and Agriculture Organization of the United  
936 Nations, Rome, Italy, FAO Irrigation and Drainage Paper, 1998.
- 937 Allen, R. G., Trezza, R., and Tasumi, M.: Analytical integrated functions for daily solar  
938 radiation on slopes, [Agric. Agricultural and Forest Meteorol. Meteorology](#), 139, 55-73,  
939 doi:10.1016/j.agrformet.2006.05.012, 2006.
- 940 Andréassian, V., Mander, Ü., and Pae, T.: The Budyko hypothesis before Budyko: The  
941 hydrological legacy of Evald Oldekop, *Journal of Hydrology*, 535, 386-391,  
942 <http://dx.doi.org/10.1016/j.jhydrol.2016.02.002>, 2016.
- 943 Ångström, A.: A study of the radiation of the atmosphere, *Smithsonian Miscellaneous*  
944 *Collections*, 65, 159-161, 1918.
- 945 Azizzadeh, M., and Javan, K.: Analyzing Trends in Reference Evapotranspiration in  
946 Northwest Part of Iran, *Journal of Ecological Engineering*, 16, 1-12,  
947 10.12911/22998993/1853, 2015.
- 948 Baldocchi, D., Valentini, R., Running, S., Oechel, W., and Dahlman, R.: Strategies for  
949 measuring and modelling carbon dioxide and water vapour fluxes over terrestrial ecosystems,  
950 *Global Change Biology*, 2, 159-168, doi:10.1111/j.1365-2486.1996.tb00069.x, 1996.
- 951 Bell, V. A., Kay, A. L., Jones, R. G., Moore, R. J., and Reynard, N. S.: Use of soil data in a  
952 grid-based hydrological model to estimate spatial variation in changing flood risk across the  
953 UK, *Journal of Hydrology*, 377, 335-350, doi:10.1016/j.jhydrol.2009.08.031, 2009.
- 954 Bell, V. A., Gedney, N., Kay, A. L., Smith, R. N. B., Jones, R. G., and Moore, R. J.:  
955 Estimating Potential Evaporation from Vegetated Surfaces for Water Management Impact  
956 Assessments Using Climate Model Output, [Journal of Hydrometeorology](#) *J Hydrometeorol.*,  
957 12, 1127-1136, doi:10.1175/2011jhm1379.1, 2011.
- 958 Bell, V. A., Kay, A. L., Cole, S. J., Jones, R. G., Moore, R. J., and Reynard, N. S.: How  
959 might climate change affect river flows across the Thames Basin? An area-wide analysis  
960 using the UKCP09 Regional Climate Model ensemble, *Journal of Hydrology*, 442-443, 89-  
961 104, doi:10.1016/j.jhydrol.2012.04.001, 2012.
- 962 Bellamy, P. H., Loveland, P. J., Bradley, R. I., Lark, R. M., and Kirk, G. J.: Carbon losses  
963 from all soils across England and Wales 1978-2003, *Nature*, 437, 245-248,  
964 doi:10.1038/nature04038, 2005.
- 965 Berry, P. M., Dawson, T. P., Harrison, P. A., and Pearson, R. G.: Modelling potential impacts  
966 of climate change on the bioclimatic envelope of species in Britain and Ireland, *Global Ecol*

967 ~~Biogeography~~ [Ecology and Biogeography](#), 11, 453-462, doi:~~100~~.1046/j.1466-822x.2002.00304.x,  
968 2002.

969 Best, M. J., Pryor, M., Clark, D. B., Rooney, G. G., Essery, R. L. H., Ménard, C. B.,  
970 Edwards, J. M., Hendry, M. A., Porson, A., Gedney, N., Mercado, L. M., Sitch, S., Blyth, E.,  
971 Boucher, O., Cox, P. M., Grimmond, C. S. B., and Harding, R. J.: The Joint UK Land  
972 Environment Simulator (JULES), model description – Part 1: Energy and water fluxes,  
973 *Geoscientific Model Development*, 4, 677-699, doi:10.5194/gmd-4-677-2011, 2011.

974 Billett, M. F., Palmer, S. M., Hope, D., Deacon, C., Storeton-West, R., Hargreaves, K. J.,  
975 Flechard, C., and Fowler, D.: Linking land-atmosphere-stream carbon fluxes in a lowland  
976 peatland system, *Global Biogeochemical Cycles*, 18, n/a-n/a, 10.1029/2003gb002058, 2004.

977 Bosveld, F. C., and Bouten, W.: Evaluating a Model of Evaporation and Transpiration with  
978 Observations in a Partially Wet Douglas-Fir Forest, *Boundary-Layer Meteorology*, 108, 365-  
979 396, 10.1023/a:1024148707239, 2003.

980 Burch, S. F., and Ravenscroft, F.: Computer modelling of the UK wind energy resource:  
981 Final overview report., AEA Industrial Technology, 1992.

982 Burt, T. P., and Shahgedanova, M.: An historical record of evaporation losses since 1815  
983 calculated using long-term observations from the Radcliffe Meteorological Station, Oxford,  
984 England, *Journal of Hydrology*, 205, 101-111, doi:10.1016/S0022-1694(97)00143-1, 1998.

985 Clark, D. B., Mercado, L. M., Sitch, S., Jones, C. D., Gedney, N., Best, M. J., Pryor, M.,  
986 Rooney, G. G., Essery, R. L. H., Blyth, E., Boucher, O., Harding, R. J., Huntingford, C., and  
987 Cox, P. M.: The Joint UK Land Environment Simulator (JULES), model description – Part 2:  
988 Carbon fluxes and vegetation dynamics, *Geoscientific Model Development*, 4, 701-722,  
989 doi:10.5194/gmd-4-701-2011, 2011.

990 Clement, R. M., J.B.; Jarvis, P.G.: Net carbon productivity of Sitka Spruce forest in Scotland,  
991 *Scottish Forestry*, 5-10, 2003.

992 Cowley, J. P.: The distribution over Great Britain of global solar irradiation on a horizontal  
993 surface, *Meteorological Magazine*, 107, 357-372, 1978.

994 Crane, S. B., and Hudson, J. A.: The impact of site factors and climate variability on the  
995 calculation of potential evaporation at Moel Cynnedd, Plynlimon, *Hydrol. Earth Syst. Sci.*, 1,  
996 429-445, doi:10.5194/hess-1-429-1997, 1997.

997 Crooks, S. M., and Naden, P. S.: CLASSIC: a semi-distributed rainfall-runoff modelling  
998 system, *Hydrol. Earth Syst. Sci.*, 11, 516-531, doi:10.5194/hess-11-516-2007, 2007.

999 Crooks, S. M., and Kay, A. L.: Simulation of river flow in the Thames over 120 years:  
1000 Evidence of change in rainfall-runoff response?, *Journal of Hydrology: Regional Studies*, 4,  
1001 Part B, 172-195, doi:10.1016/j.ejrh.2015.05.014, 2015.

1002 Dai, A.: Recent Climatology, Variability, and Trends in Global Surface Humidity, *Journal of*  
1003 *Climate*, 19, 3589-3606, doi:10.1175/JCLI3816.1, 2006.

1004 Dilley, A. C., and O'Brien, D. M.: Estimating downward clear sky long-wave irradiance at  
1005 the surface from screen temperature and precipitable water, *Quarterly Journal of the Royal*  
1006 *Meteorological Society*, 124, 1391-1401, doi:10.1256/Smsqj.54902, 1998.

1007 Donohue, R. J., McVicar, T. R., and Roderick, M. L.: Assessing the ability of potential  
1008 evaporation formulations to capture the dynamics in evaporative demand within a changing  
1009 climate, *Journal of Hydrology*, 386, 186-197, doi:10.1016/j.jhydrol.2010.03.020, 2010.



- 1010 Doorenbos, J. a. P., W. O.: Crop water requirements. FAO Irrigation and Drainage Paper 24.,  
1011 FAO, Rome, Italy, 1977.
- 1012 Evans, N., Baierl, A., Semenov, M. A., Gladders, P., and Fitt, B. D.: Range and severity of a  
1013 plant disease increased by global warming, *Journal of the Royal Society, Interface / the Royal*  
1014 *Society*, 5, 525-531, doi:10.1098/rsif.2007.1136, 2008.
- 1015 FAO/IIASA/ISRIC/ISS-CAS/JRC: Harmonized World Soil Database, 2012.
- 1016 Field, M.: The meteorological office rainfall and evaporation calculation system —  
1017 MORECS, *Agricultural Water Management*, 6, 297-306, [http://dx.doi.org/10.1016/0378-](http://dx.doi.org/10.1016/0378-3774(83)90017-3)  
1018 [3774\(83\)90017-3](http://dx.doi.org/10.1016/0378-3774(83)90017-3), 1983.
- 1019 Fleig, A. K., Tallaksen, L. M., James, P., Hisdal, H., and Stahl, K.: Attribution of European  
1020 precipitation and temperature trends to changes in synoptic circulation, *Hydrology and Earth*  
1021 *System Sciences*, 19, 3093-3107, 10.5194/hess-19-3093-2015, 2015.
- 1022 Folland, C. K., Hannaford, J., Bloomfield, J. P., Kendon, M., Svensson, C., Marchant, B. P.,  
1023 Prior, J., and Wallace, E.: Multi-annual droughts in the English Lowlands: a review of their  
1024 characteristics and climate drivers in the winter half-year, *Hydrology and Earth System*  
1025 *Sciences*, 19, 2353-2375, doi:10.5194/hess-19-2353-2015, 2015.
- 1026 Gedney, N., Cox, P. M., Betts, R. A., Boucher, O., Huntingford, C., and Stott, P. A.:  
1027 Detection of a direct carbon dioxide effect in continental river runoff records, *Nature*, 439,  
1028 835-838, doi:10.1038/nature04504, 2006.
- 1029 Gedney, N., Huntingford, C., Weedon, G. P., Bellouin, N., Boucher, O., and Cox, P. M.:  
1030 Detection of solar dimming and brightening effects on Northern Hemisphere river flow,  
1031 ~~*Nature Geoscience*~~ *Nat Geosci*, 7, 796-800, doi:10.1038/ngeo2263, 2014.
- 1032 Gill, A. E.: Atmosphere-ocean Dynamics, Academic Press, San Diego, California, USA,  
1033 1982.
- 1034 Gilmanov, T. G., Soussana, J. F., Aires, L., Allard, V., Ammann, C., Balzarolo, M., Barcza,  
1035 Z., Bernhofer, C., Campbell, C. L., Cernusca, A., Cescatti, A., Clifton-Brown, J., Dirks, B. O.  
1036 M., Dore, S., Eugster, W., Fuhrer, J., Gimeno, C., Gruenwald, T., Haszpra, L., Hensen, A.,  
1037 Ibrom, A., Jacobs, A. F. G., Jones, M. B., Lanigan, G., Laurila, T., Lohila, A., G. Manca,  
1038 Marcolla, B., Nagy, Z., Pilegaard, K., Pinter, K., Pio, C., Raschi, A., Rogiers, N., Sanz, M. J.,  
1039 Stefani, P., Sutton, M., Tuba, Z., Valentini, R., Williams, M. L., and Wohlfahrt, G.:  
1040 Partitioning European grassland net ecosystem CO<sub>2</sub> exchange into gross primary productivity  
1041 and ecosystem respiration using light response function analysis, *Agriculture, Ecosystems &*  
1042 *Environment*, 121, 93-120, 10.1016/j.agee.2006.12.008, 2007.
- 1043 Gocic, M., and Trajkovic, S.: Analysis of trends in reference evapotranspiration data in a  
1044 humid climate, *Hydrological Sciences Journal*, 59, 165-180, 10.1080/02626667.2013.798659,  
1045 2013.
- 1046 Gold, C. M.: Surface interpolation, spatial adjacency and GIS, in: *Three Dimensional*  
1047 *Applications in Geographical Information Systems*, edited by: Raper, J., Taylor and Francis,  
1048 London, 1989.
- 1049 Green, D. A.: A colour scheme for the display of astronomical intensity images, *Bulletin of*  
1050 *the Astronomical Society of India*, 39, 2011.
- 1051 Haddeland, I., Clark, D. B., Franssen, W., Ludwig, F., Voß, F., Arnell, N. W., Bertrand, N.,  
1052 Best, M., Folwell, S., Gerten, D., Gomes, S., Gosling, S. N., Hagemann, S., Hanasaki, N.,  
1053 Harding, R., Heinke, J., Kabat, P., Koiraala, S., Oki, T., Polcher, J., Stacke, T., Viterbo, P.,

1054 Weedon, G. P., and Yeh, P.: Multimodel Estimate of the Global Terrestrial Water Balance:  
 1055 Setup and First Results, *Journal of Hydrometeorology*, 12, 869-884, 10.1175/2011jhm1324.1,  
 1056 2011.

1057 Hannaford, J., and Buys, G.: Trends in seasonal river flow regimes in the UK, *Journal of*  
 1058 *Hydrology*, 475, 158-174, doi:10.1016/j.jhydrol.2012.09.044, 2012.

1059 Hannaford, J.: Climate-driven changes in UK river flows: A review of the evidence, *Progress*  
 1060 *in Physical Geography*, 39, 29-48, doi:10.1177/0309133314536755, 2015.

1061 Harris, I., Jones, P. D., Osborn, T. J., and Lister, D. H.: Updated high-resolution grids of  
 1062 monthly climatic observations - the CRU TS3.10 Dataset, *International Journal of*  
 1063 *Climatology*, 34, 623-642, doi:10.1002/Joc.3711, 2014.

1064 Hartmann, D. L., Klein Tank, A. M. G., Rusticucci, M., Alexander, L. V., Brönnimann, S.,  
 1065 Charabi, Y., Dentener, F. J., Dlugokencky, E. J., Easterling, D. R., Kaplan, A., Soden, B. J.,  
 1066 Thorne, P. W., Wild, M., and Zhai, P. M.: Observations: Atmosphere and Surface, in:  
 1067 *Climate Change 2013: The Physical Science Basis. Contribution of Working Group I to the*  
 1068 *Fifth Assessment Report of the Intergovernmental Panel on Climate Change*, edited by:  
 1069 Stocker, T. F., Qin, D., Plattner, G.-K., Tignor, M., Allen, S. K., Boschung, J., Nauels, A.,  
 1070 Xia, Y., Bex, V., and Midgley, P. M., Cambridge University Press, Cambridge, United  
 1071 Kingdom and New York, NY, USA, 159-254, 2013.

1072 Haslinger, K., and Bartsch, A.: Creating long-term gridded fields of reference  
 1073 evapotranspiration in Alpine terrain based on a recalibrated Hargreaves method, *Hydrology*  
 1074 *and Earth System Sciences*, 20, 1211-1223, 10.5194/hess-20-1211-2016, 2016.

1075 Heinemeyer, A., Wilkinson, M., Vargas, R., Subke, J. A., Casella, E., Morison, J. I. L., and  
 1076 Ineson, P.: Exploring the "overflow tap" theory: linking forest soil CO<sub>2</sub> fluxes  
 1077 and individual mycorrhizosphere components to photosynthesis, *Biogeosciences*, 9, 79-95,  
 1078 10.5194/bg-9-79-2012, 2012.

1079 Held, I. M., and Soden, B. J.: Robust Responses of the Hydrological Cycle to Global  
 1080 Warming, *Journal of Climate*, 19, 5686-5699, 10.1175/jcli3990.1, 2006.

1081 Helmes, L., and Jaenicke, R.: Atmospheric turbidity determined from sunshine records,  
 1082 *Journal of Aerosol Science*, 17, 261-263, doi:10.1016/0021-8502(86)90080-7, 1986.

1083 Hickling, R., Roy, D. B., Hill, J. K., Fox, R., and Thomas, C. D.: The distributions of a wide  
 1084 range of taxonomic groups are expanding polewards, *Global Change Biology*, 12, 450-455,  
 1085 doi:10.1111/j.1365-2486.2006.01116.x, 2006.

1086 Horn, B. K. P.: Hill Shading and the Reflectance Map, *Proceedings of the Ieee*, 69, 14-47,  
 1087 doi:10.1109/Proc.1981.11918, 1981.

1088 Hosseinzadeh Talaei, P., Shifteh Some'e, B., and Sobhan Ardakani, S.: Time trend and  
 1089 change point of reference evapotranspiration over Iran, *Theoretical and Applied Climatology*,  
 1090 116, 639-647, 10.1007/s00704-013-0978-x, 2013.

1091 Hough, M. N., and Jones, R. J. A.: The United Kingdom Meteorological Office rainfall and  
 1092 evaporation calculation system: MORECS version 2.0-an overview, *Hydrology and Earth*  
 1093 *System Sciences*, 1, 227-239, doi:10.5194/hess-1-227-1997, 1997.

1094 IPCC: *Climate Change 2013: The Physical Science Basis. Contribution of Working Group I*  
 1095 *to the Fifth Assessment Report of the Intergovernmental Panel on Climate Change*,  
 1096 Cambridge University Press, Cambridge, United Kingdom and New York, NY, USA, 1535  
 1097 pp., 2013.

1098 IPCC: Climate Change 2014: Impacts, Adaptation, and Vulnerability. Part A: Global and  
1099 Sectoral Aspects. Contribution of Working Group II to the Fifth Assessment Report of the  
1100 Intergovernmental Panel on Climate Change [Field, C.B., V.R. Barros, D.J. Dokken, K.J.  
1101 Mach, M.D. Mastrandrea, T.E. Bilir, M. Chatterjee, K.L. Ebi, Y.O. Estrada, R.C. Genova, B.  
1102 Girma, E.S. Kissel, A.N. Levy, S. MacCracken, P.R. Mastrandrea, and L.L. White (eds.)],  
1103 Cambridge University Press, Cambridge, United Kingdom and New York, NY, USA, 1132  
1104 pp., 2014a.

1105 IPCC: Climate Change 2014: Impacts, Adaptation, and Vulnerability. Part B: Regional  
1106 Aspects. Contribution of Working Group II to the Fifth Assessment Report of the  
1107 Intergovernmental Panel on Climate Change [Barros, V.R., C.B. Field, D.J. Dokken, M.D.  
1108 Mastrandrea, K.J. Mach, T.E. Bilir, M. Chatterjee, K.L. Ebi, Y.O. Estrada, R.C. Genova, B.  
1109 Girma, E.S. Kissel, A.N. Levy, S. MacCracken, P.R. Mastrandrea, and L.L. White (eds.)],  
1110 Cambridge University Press, Cambridge, United Kingdom and New York, NY, USA, 688  
1111 pp., 2014b.

1112 Iqbal, M.: An introduction to solar radiation, Academic Press, London, 1983.

1113 Ishibashi, M., and Terashima, I.: Effects of continuous leaf wetness on photosynthesis:  
1114 adverse aspects of rainfall, *Plant, Cell & Environment*, 18, 431-438, 10.1111/j.1365-  
1115 3040.1995.tb00377.x, 1995.

1116 Jenkins, G. J., Perry, M. C., and Prior, M. J.: The climate of the United Kingdom and recent  
1117 trends, Met Office Hadley Centre, Exeter, UK, 2008.

1118 Jhajharia, D., Dinpashoh, Y., Kahya, E., Singh, V. P., and Fakheri-Fard, A.: Trends in  
1119 reference evapotranspiration in the humid region of northeast India, *Hydrological Processes*,  
1120 26, 421-435, 10.1002/hyp.8140, 2012.

1121 Jones, P. D., Lister, D. H., Osborn, T. J., Harpham, C., Salmon, M., and Morice, C. P.:  
1122 Hemispheric and large-scale land-surface air temperature variations: An extensive revision  
1123 and an update to 2010, *Journal of Geophysical Research: Atmospheres*, 117, n/a-n/a,  
1124 doi:10.1029/2011JD017139, 2012.

1125 ~~Jones, P. D., and Harris, I.:~~ CRU TS3.21: Climatic Research Unit (CRU) Time-Series (TS)  
1126 Version 3.21 of High Resolution Gridded Data of Month-by-month Variation in Climate (Jan.  
1127 1901- Dec. 2012). ~~University of East Anglia Climatic Research Unit,~~  
1128 ~~doi:10.5285/D0E1585D-3417-485F-87AE-4FCECF10A992~~, 2013.

1129 Kay, A. L., Bell, V. A., Blyth, E. M., Crooks, S. M., Davies, H. N., and Reynard, N. S.: A  
1130 hydrological perspective on evaporation: historical trends and future projections in Britain,  
1131 *Journal of Water and Climate Change*, 4, 193, doi:10.2166/wcc.2013.014, 2013.

1132 Kay, A. L., Rudd, A. C., Davies, H. N., Kendon, E. J., and Jones, R. G.: Use of very high  
1133 resolution climate model data for hydrological modelling: baseline performance and future  
1134 flood changes, *Climatic Change*, doi:10.1007/s10584-015-1455-6, 2015.

1135 Keller, V. D. J., Tanguy, M., Prosdocimi, I., Terry, J. A., Hitt, O., Cole, S. J., Fry, M.,  
1136 Morris, D. G., and Dixon, H.: CEH-GEAR: 1 km resolution daily and monthly areal rainfall  
1137 estimates for the UK for hydrological and other applications, *Earth Syst. Sci. Data*, 7, 143-  
1138 155, doi:10.5194/essd-7-143-2015, 2015.

1139 Kimball, B. A., Idso, S. B., and Aase, J. K.: A Model of Thermal-Radiation from Partly  
1140 Cloudy and Overcast Skies, *Water Resources Research*, 18, 931-936,  
1141 doi:10.1029/Wr018i004p00931, 1982.

1142 Kruijt, B., Witte, J.-P. M., Jacobs, C. M. J., and Kroon, T.: Effects of rising atmospheric CO<sub>2</sub>  
1143 on evapotranspiration and soil moisture: A practical approach for the Netherlands, *Journal of*  
1144 *Hydrology*, 349, 257-267, doi:10.1016/j.jhydrol.2007.10.052, 2008.

1145 Kume, T., Kuraji, K., Yoshifuji, N., Morooka, T., Sawano, S., Chong, L., and Suzuki, M.:  
1146 Estimation of canopy drying time after rainfall using sap flow measurements in an emergent  
1147 tree in a lowland mixed-dipterocarp forest in Sarawak, Malaysia, *Hydrological Processes*, 20,  
1148 565-578, 10.1002/hyp.5924, 2006.

1149 ~~Lange, O. L., Lösch, R., Schulze, E. D., and Kappen, L.: Responses of stomata to changes in~~  
1150 ~~humidity, *Planta*, 100, 76-86, 10.1007/bf00386887, 1971.~~

1151 Li, B., Chen, F., and Guo, H.: Regional complexity in trends of potential evapotranspiration  
1152 and its driving factors in the Upper Mekong River Basin, *Quaternary International*, 380-381,  
1153 83-94, 10.1016/j.quaint.2014.12.052, 2015.

1154 Li, Y., and Zhou, M.: Trends in Dryness Index Based on Potential Evapotranspiration and  
1155 Precipitation over 1961–2099 in Xinjiang, China, *Advances in Meteorology*, 2014, 1-15,  
1156 10.1155/2014/548230, 2014.

1157 Liley, J. B.: New Zealand dimming and brightening, *Journal of Geophysical Research*, 114,  
1158 doi:10.1029/2008jd011401, 2009.

1159 Lu, X., Bai, H., and Mu, X.: Explaining the evaporation paradox in Jiangxi Province of  
1160 China: Spatial distribution and temporal trends in potential evapotranspiration of Jiangxi  
1161 Province from 1961 to 2013, *International Soil and Water Conservation Research*, 4, 45-51,  
1162 10.1016/j.iswcr.2016.02.004, 2016.

1163 Marsh, T., and Dixon, H.: The UK water balance – how much has it changed in a warming  
1164 world?, 01-05, doi:10.7558/bhs.2012.ns32, 2012.

1165 Marthews, T. R., Malhi, Y., and Iwata, H.: Calculating downward longwave radiation under  
1166 clear and cloudy conditions over a tropical lowland forest site: an evaluation of model  
1167 schemes for hourly data, *Theoretical and Applied Climatology*, 107, 461-477,  
1168 10.1007/s00704-011-0486-9, 2011.

1169 Matsoukas, C., Benas, N., Hatzianastassiou, N., Pavlakis, K. G., Kanakidou, M., and  
1170 Vardavas, I.: Potential evaporation trends over land between 1983–2008: driven by radiative  
1171 fluxes or vapour-pressure deficit?, *Atmospheric Chemistry and Physics*, 11, 7601-7616,  
1172 doi:10.5194/acp-11-7601-2011, 2011.

1173 McVicar, T. R., Van Niel, T. G., Li, L. T., Roderick, M. L., Rayner, D. P., Ricciardulli, L.,  
1174 and Donohue, R. J.: Wind speed climatology and trends for Australia, 1975–2006: Capturing  
1175 the stilling phenomenon and comparison with near-surface reanalysis output, *Geophysical*  
1176 *Research Letters*, 35, n/a-n/a, 10.1029/2008GL035627, 2008.

1177 McVicar, T. R., Roderick, M. L., Donohue, R. J., Li, L. T., Van Niel, T. G., Thomas, A.,  
1178 Grieser, J., Jhajharia, D., Himri, Y., Mahowald, N. M., Mescherskaya, A. V., Kruger, A. C.,  
1179 Rehman, S., and Dinpashoh, Y.: Global review and synthesis of trends in observed terrestrial  
1180 near-surface wind speeds: Implications for evaporation, *Journal of Hydrology*, 416, 182-205,  
1181 doi:10.1016/j.jhydrol.2011.10.024, 2012.

1182 Monteith, J. L.: Evaporation and environment, in: 19th Symposia of the Society for  
1183 Experimental Biology, University Press, Cambridge, 1965.

1184 ~~Monteith, J. L.: Evaporation and surface temperature, *Quarterly Journal of the Royal*~~  
1185 ~~*Meteorological Society*, 107, 1-27, 10.1002/qj.49710745102, 1981.~~

1186 Moors, E.: Water Use of Forests in the Netherlands, PhD, Vrije Universiteit, Amsterdam, the  
1187 Netherlands, 2012.

1188 Morris, D. G., and Flavin, R. W.: A digital terrain model for hydrology. Proceedings of the  
1189 4th International Symposium on Spatial Data Handling, 1, 250-262, 1990.

1190 Morton, D., Rowland, C., Wood, C., Meek, L., Marston, C., Smith, G., Wadsworth, R., and  
1191 Simpson, I. C.: Final Report for LCM2007 - the new UK land cover map, NERC/Centre for  
1192 Ecology & Hydrology 11/07 (CEH Project Number: C03259), 2011.

1193 Muneer, T., and Munawwar, S.: Potential for improvement in estimation of solar diffuse  
1194 irradiance, [Energy Conversion and Management](#), 47, 68-86,  
1195 doi:10.1016/j.enconman.2005.03.015, 2006.

1196 Murphy, J. M., Sexton, D. M. H., Jenkins, G. J., Boorman, P. M., Booth, B. B. B., Brown, C.  
1197 C., Clark, R. T., Collins, M., Harris, G. R., Kendon, E. J., Betts, R. A., Brown, S. J., Howard,  
1198 T. P., Humphrey, K. A., McCarthy, M. P., McDonald, R. E., Stephens, A., Wallace, C.,  
1199 Warren, R., Wilby, R., and Wood, R. A.: UK Climate Projections Science Report: Climate  
1200 change projections, Met Office Hadley Centre, Exeter, 2009.

1201 Newton, K., and Burch, S. F.: Estimation of the UK wind energy resource using computer  
1202 modelling techniques and map data, Energy Technology Support Unit, 50, 1985.

1203 Norton, L. R., Maskell, L. C., Smart, S. S., Dunbar, M. J., Emmett, B. A., Carey, P. D.,  
1204 Williams, P., Crowe, A., Chandler, K., Scott, W. A., and Wood, C. M.: Measuring stock and  
1205 change in the GB countryside for policy--key findings and developments from the  
1206 Countryside Survey 2007 field survey, *Journal of environmental management*, 113, 117-127,  
1207 doi:10.1016/j.jenvman.2012.07.030, 2012.

1208 Oldekop, E.: Evaporation from the surface of river basins, in: *Collection of the Works of*  
1209 *Students of the Meteorological Observatory, University of Tartu-Jurjew-Dorpat, Tartu,*  
1210 *Estonia, 209, 1911.*

1211 Palmer, W. C.: *Meteorological Drought. Res. Paper No.45, Dept. of Commerce, Washington,*  
1212 *D.C., 1965.*

1213 Paltineanu, C., Chitu, E., and Mateescu, E.: New trends for reference evapotranspiration and  
1214 climatic water deficit, *International Agrophysics*, 26, 10.2478/v10247-012-0023-9, 2012.

1215 Parker, D., and Horton, B.: Uncertainties in central England temperature 1878-2003 and  
1216 some improvements to the maximum and minimum series, *International Journal of*  
1217 *Climatology*, 25, 1173-1188, doi:10.1002/joc.1190, 2005.

1218 Penman, H. L.: Natural Evaporation from Open Water, Bare Soil and Grass, *Proceedings of*  
1219 *the Royal Society of London. Series A. Mathematical and Physical Sciences*, 193, 120-145,  
1220 10.1098/rspa.1948.0037, 1948.

1221 Pocock, M. J., Roy, H. E., Preston, C. D., and Roy, D. B.: The Biological Records Centre in  
1222 the United Kingdom: a pioneer of citizen science., *Biological Journal of the Linnean Society*,  
1223 doi:10.1111/bij.12548, 2015.

1224 Prata, A. J.: A new long-wave formula for estimating downward clear-sky radiation at the  
1225 surface, *Quarterly Journal of the Royal Meteorological Society*, 122, 1127-1151,  
1226 doi:10.1002/qj.49712253306, 1996.

1227 Prescott, J. A.: Evaporation from a water surface in relation to solar radiation, *Transaction of*  
1228 *the Royal Society of South Australia*, 64, 114-125, 1940.

- 1229 Prudhomme, C., Giuntoli, I., Robinson, E. L., Clark, D. B., Arnell, N. W., Dankers, R.,  
 1230 Fekete, B. M., Franssen, W., Gerten, D., Gosling, S. N., Hagemann, S., Hannah, D. M., Kim,  
 1231 H., Masaki, Y., Satoh, Y., Stacke, T., Wada, Y., and Wisser, D.: Hydrological droughts in the  
 1232 21st century, hotspots and uncertainties from a global multimodel ensemble experiment,  
 1233 *Proceedings of the National Academy of Sciences*, 111, 3262-3267,  
 1234 doi:10.1073/pnas.1222473110, 2014.
- 1235 Pryor, S. C., Barthelmie, R. J., Young, D. T., Takle, E. S., Arritt, R. W., Flory, D., Gutowski,  
 1236 W. J., Nunes, A., and Roads, J.: Wind speed trends over the contiguous United States, *Journal*  
 1237 *of Geophysical Research: Atmospheres*, 114, n/a-n/a, 10.1029/2008JD011416, 2009.
- 1238 Reynolds, B., Chamberlain, P. M., Poskitt, J., Woods, C., Scott, W. A., Rowe, E. C.,  
 1239 Robinson, D. A., Frogbrook, Z. L., Keith, A. M., Henrys, P. A., Black, H. I. J., and Emmett,  
 1240 B. A.: Countryside Survey: National "Soil Change" 1978–2007 for Topsoils in Great  
 1241 Britain—Acidity, Carbon, and Total Nitrogen Status, *Vadose Zone Journal*, 12, 0,  
 1242 doi:10.2136/vzj2012.0114, 2013.
- 1243 Richards, J. M.: A simple expression for the saturation vapour pressure of water in the range  
 1244 –50 to 140°C, *Journal of Physics D: Applied Physics*, 4, L15, 1971.
- 1245 Robinson, E. L., Blyth, E., Clark, D. B., Finch, J., and Rudd, A. C.: Climate hydrology and  
 1246 ecology research support system potential evapotranspiration dataset for Great Britain (1961-  
 1247 2012) [CHESS-PE], NERC-Environmental Information Data Centre, doi:10.5285/d329f4d6-  
 1248 95ba-4134-b77a-a377e0755653, 2015a.
- 1249 Robinson, E. L., Blyth, E., Clark, D. B., Finch, J., and Rudd, A. C.: Climate hydrology and  
 1250 ecology research support system meteorology dataset for Great Britain (1961-2012) [CHESS-  
 1251 met], NERC-Environmental Information Data Centre, doi:10.5285/80887755-1426-4dab-  
 1252 a4a6-250919d5020c, 2015b.
- 1253 Rodda, J. C., and Marsh, T. J.: The 1975-76 Drought - a contemporary and retrospective  
 1254 review, Wallingford, UK, 2011.
- 1255 Roderick, M. L., Rotstayn, L. D., Farquhar, G. D., and Hobbins, M. T.: On the attribution of  
 1256 changing pan evaporation, *Geophysical Research Letters*, 34, 10.1029/2007gl031166, 2007.
- 1257 Rotstayn, L. D., Roderick, M. L., and Farquhar, G. D.: A simple pan-evaporation model for  
 1258 analysis of climate simulations: Evaluation over Australia, *Geophysical Research Letters*, 33,  
 1259 10.1029/2006gl027114, 2006.
- 1260 Rudd, A. C., and Kay, A. L.: Use of very high resolution climate model data for hydrological  
 1261 modelling: estimation of potential evaporation, *Hydrology Research*, doi:  
 1262 10.2166/nh.2015.028, 2015.
- 1263 Rutter, A. J., Kershaw, K. A., Robins, P. C., and Morton, A. J.: A predictive model of rainfall  
 1264 interception in forests, 1. Derivation of the model from observations in a plantation of  
 1265 Corsican pine, *Agricultural Meteorology*, 9, 367-384, doi:10.1016/0002-1571(71)90034-3,  
 1266 1971.
- 1267 Sanchez-Lorenzo, A., Calbó, J., and Martin-Vide, J.: Spatial and Temporal Trends in  
 1268 Sunshine Duration over Western Europe (1938–2004), *Journal of Climate*, 21, 6089-6098,  
 1269 doi:10.1175/2008jcli2442.1, 2008.
- 1270 Sanchez-Lorenzo, A., Calbó, J., Brunetti, M., and Deser, C.: Dimming/brightening over the  
 1271 Iberian Peninsula: Trends in sunshine duration and cloud cover and their relations with  
 1272 atmospheric circulation, *Journal of Geophysical Research*, 114, doi:10.1029/2008jd011394,  
 1273 2009.

- 1274 Sanchez-Lorenzo, A., and Wild, M.: Decadal variations in estimated surface solar radiation  
 1275 over Switzerland since the late 19th century, *Atmospheric Chemistry and Physics*, 12, 8635-  
 1276 8644, doi:10.5194/acp-12-8635-2012, 2012.
- 1277 Sanchez-Romero, A., Sanchez-Lorenzo, A., Calbó, J., González, J. A., and Azorin-Molina,  
 1278 C.: The signal of aerosol-induced changes in sunshine duration records: A review of the  
 1279 evidence, *Journal of Geophysical Research: Atmospheres*, 119, 4657-4673,  
 1280 doi:10.1002/2013JD021393, 2014.
- 1281 Scheff, J., and Frierson, D. M. W.: Scaling Potential Evapotranspiration with Greenhouse  
 1282 Warming, *Journal of Climate*, 27, 1539-1558, doi:10.1175/JCLI-D-13-00233.1, 2014.
- 1283 [Schneider, T., O'Gorman, P. A., and Levine, X. J.: Water Vapor and the Dynamics of Climate](#)  
 1284 [Changes, \*Reviews of Geophysics\*, 48, 10.1029/2009rg000302, 2010.](#)
- 1285 Schymanski, S. J., and Or, D.: Wind effects on leaf transpiration challenge the concept of  
 1286 "potential evaporation", *Proceedings of the International Association of Hydrological*  
 1287 *Sciences*, 371, 99-107, 10.5194/piahs-371-99-2015, 2015.
- 1288 Shan, N., Shi, Z., Yang, X., Zhang, X., Guo, H., Zhang, B., and Zhang, Z.: Trends in  
 1289 potential evapotranspiration from 1960 to 2013 for a desertification-prone region of China,  
 1290 *International Journal of Climatology*, n/a-n/a, 10.1002/joc.4566, 2015.
- 1291 Sheffield, J., Goteti, G., and Wood, E. F.: Development of a 50-Year High-Resolution Global  
 1292 Dataset of Meteorological Forcings for Land Surface Modeling, *Journal of Climate*, 19,  
 1293 3088-3111, doi:10.1175/JCLI3790.1, 2006.
- 1294 Shuttleworth, W. J.: *Terrestrial Hydrometeorology*, John Wiley & Sons, Ltd, 2012.
- 1295 Song, Z. W. Z., H. L. ; Snyder, R. L. ;Anderson, F. E. ;Chen, F. : Distribution and Trends in  
 1296 Reference Evapotranspiration in the North China Plain, *Journal of Irrigation and Drainage*  
 1297 *Engineering*, 136, 240-247, doi:10.1061/(ASCE)IR.1943-4774.0000175, 2010.
- 1298 Soussana, J. F., Allard, V., Pilegaard, K., Ambus, P., Amman, C., Campbell, C., Ceschia, E.,  
 1299 Clifton-Brown, J., Czobel, S., Domingues, R., Flechard, C., Fuhrer, J., Hensen, A., Horvath,  
 1300 L., Jones, M., Kasper, G., Martin, C., Nagy, Z., Neftel, A., Raschi, A., Baronti, S., Rees, R.  
 1301 M., Skiba, U., Stefani, P., Manca, G., Sutton, M., Tuba, Z., and Valentini, R.: Full accounting  
 1302 of the greenhouse gas (CO<sub>2</sub>, N<sub>2</sub>O, CH<sub>4</sub>) budget of nine European grassland sites,  
 1303 *Agriculture, Ecosystems & Environment*, 121, 121-134, 10.1016/j.agee.2006.12.022, 2007.
- 1304 Stanhill, G., and Cohen, S.: Solar Radiation Changes in the United States during the  
 1305 Twentieth Century: Evidence from Sunshine Duration Measurements, *Journal of Climate*, 18,  
 1306 1503-1512, doi:10.1175/JCLI3354.1, 2005.
- 1307 Stanhill, G., and Möller, M.: Evaporative climate change in the British Isles, *International*  
 1308 *Journal of Climatology*, 28, 1127-1137, doi:10.1002/joc.1619, 2008.
- 1309 Stewart, J. B.: On the use of the Penman-Monteith equation for determining areal  
 1310 evapotranspiration, in: *Estimation of Areal Evapotranspiration (Proceedings of a workshop*  
 1311 *held at Vancouver, B.C., Canada, August 1987)*. edited by: Black, T. A. S., D. L.; Novak, M.  
 1312 D.; Price, D. T., IAHS, Wallingford, Oxfordshire, UK, 1989.
- 1313 Sutton, R. T., and Dong, B.: Atlantic Ocean influence on a shift in European climate in the  
 1314 1990s, *Nature Geosci*, 5, 788-792, doi:10.1038/ngeo1595, 2012.
- 1315 Tabari, H., Nikbakht, J., and Hosseinzadeh Talae, P.: Identification of Trend in Reference  
 1316 Evapotranspiration Series with Serial Dependence in Iran, *Water Resources Management*, 26,  
 1317 2219-2232, 10.1007/s11269-012-0011-7, 2012.

1318 Tanguy, M., Dixon, H., Prosdocimi, I., Morris, D. G., and Keller, V. D. J.: Gridded estimates  
1319 of daily and monthly areal rainfall for the United Kingdom (1890-2012) [CEH-GEAR],  
1320 NERC Environmental Information Data Centre, doi:10.5285/5dc179dc-f692-49ba-9326-  
1321 a6893a503f6e, 2014.

1322 Thackeray, S. J., Sparks, T. H., Frederiksen, M., Burthe, S., Bacon, P. J., Bell, J. R., Botham,  
1323 M. S., Brereton, T. M., Bright, P. W., Carvalho, L., Clutton-Brock, T., Dawson, A., Edwards,  
1324 M., Elliott, J. M., Harrington, R., Johns, D., Jones, I. D., Jones, J. T., Leech, D. I., Roy, D. B.,  
1325 Scott, W. A., Smith, M., Smithers, R. J., Winfield, I. J., and Wanless, S.: Trophic level  
1326 asynchrony in rates of phenological change for marine, freshwater and terrestrial  
1327 environments, *Global Change Biology*, 16, 3304-3313, doi:10.1111/j.1365-  
1328 2486.2010.02165.x, 2010.

1329 Thompson, N., Barrie, I. A., and Ayles, M.: The Meteorological Office rainfall and  
1330 evaporation calculation system: MORECS, Meteorological Office, Bracknell, 1981.

1331 Vautard, R., Cattiaux, J., Yiou, P., Thepaut, J. N., and Ciais, P.: Northern Hemisphere  
1332 atmospheric stilling partly attributed to an increase in surface roughness, *Nature*  
1333 *GeoscienceNat Geosci*, 3, 756-761, doi:10.1038/Ngeo979, 2010.

1334 Vicente-Serrano, S. M., Azorin-Molina, C., Sanchez-Lorenzo, A., Revuelto, J., López-  
1335 Moreno, J. I., González-Hidalgo, J. C., Moran-Tejeda, E., and Espejo, F.: Reference  
1336 evapotranspiration variability and trends in Spain, 1961–2011, *Global and Planetary Change*,  
1337 121, 26-40, 10.1016/j.gloplacha.2014.06.005, 2014.

1338 Vicente-Serrano, S. M., Azorin-Molina, C., Sanchez-Lorenzo, A., El Kenawy, A., Martín-  
1339 Hernández, N., Peña-Gallardo, M., Beguería, S., and Tomas-Burguera, M.: Recent changes  
1340 and drivers of the atmospheric evaporative demand in the Canary Islands, *Hydrology and*  
1341 *Earth System Sciences* ~~Discussions~~, ~~1-35~~, ~~20~~, ~~3393-3410~~, 10.5194/hess-20-3393-2016-15,  
1342 2016.

1343 Vincent, L. A., Zhang, X., Brown, R. D., Feng, Y., Mekis, E., Milewska, E. J., Wan, H., and  
1344 Wang, X. L.: Observed Trends in Canada's Climate and Influence of Low-Frequency  
1345 Variability Modes, *Journal of Climate*, 28, 4545-4560, 10.1175/jcli-d-14-00697.1, 2015.

1346 von Storch, H., and Zwiers, F. W.: *Statistical analysis in climate research*, Cambridge  
1347 University Press, Cambridge ; New York, x, 484 p. pp., 1999.

1348 Wang, K., and Liang, S.: Global atmospheric downward longwave radiation over land  
1349 surface under all-sky conditions from 1973 to 2008, *Journal of Geophysical Research*, 114,  
1350 doi:10.1029/2009jd011800, 2009.

1351 Ward, R. C., and Robinson, M.: *Principles of Hydrology*, McGraw Hill, 2000.

1352 Watts, G., Battarbee, R. W., Bloomfield, J. P., Crossman, J., Daccache, A., Durance, I.,  
1353 Elliott, J. A., Garner, G., Hannaford, J., Hannah, D. M., Hess, T., Jackson, C. R., Kay, A. L.,  
1354 Kernan, M., Knox, J., Mackay, J., Monteith, D. T., Ormerod, S. J., Rance, J., Stuart, M. E.,  
1355 Wade, A. J., Wade, S. D., Weatherhead, K., Whitehead, P. G., and Wilby, R. L.: Climate  
1356 change and water in the UK - past changes and future prospects, *Progress in Physical*  
1357 *Geography*, 39, 6-28, doi:10.1177/0309133314542957, 2015.

1358 Weedon, G. P., Gomes, S., Viterbo, P., Shuttleworth, W. J., Blyth, E., Osterle, H., Adam, J.  
1359 C., Bellouin, N., Boucher, O., and Best, M.: Creation of the WATCH Forcing Data and Its  
1360 Use to Assess Global and Regional Reference Crop Evaporation over Land during the  
1361 Twentieth Century, *Journal of Hydrometeorology* ~~J Hydrometeorol~~, 12, 823-848,  
1362 doi:10.1175/2011jhm1369.1, 2011.



1363 Weedon, G. P., Balsamo, G., Bellouin, N., Gomes, S., Best, M. J., and Viterbo, P.: The  
1364 WFDEI meteorological forcing data set: WATCH Forcing Data methodology applied to  
1365 ERA-Interim reanalysis data, *Water Resources Research*, 50, 7505-7514,  
1366 doi:10.1002/2014WR015638, 2014.

1367 Wild, M.: Global dimming and brightening: A review, *Journal of Geophysical Research*, 114,  
1368 doi:10.1029/2008jd011470, 2009.

1369 Wilkinson, M., Eaton, E. L., Broadmeadow, M. S. J., and Morison, J. I. L.: Inter-annual  
1370 variation of carbon uptake by a plantation oak woodland in south-eastern England,  
1371 *Biogeosciences*, 9, 5373-5389, 10.5194/bg-9-5373-2012, 2012.

1372 Willett, K. M., Dunn, R. J. H., Thorne, P. W., Bell, S., de Podesta, M., Parker, D. E., Jones,  
1373 P. D., and Williams Jr, C. N.: HadISDH land surface multi-variable humidity and  
1374 temperature record for climate monitoring, *Climate of the Past*, 10, 1983-2006, 10.5194/cp-  
1375 10-1983-2014, 2014.

1376 WMO: Manual on the Global Observing System, Secretariat of the World Meteorological  
1377 Organization, Geneva, Switzerland, 2013.

1378 Wood, C. M., Smart, S. M., and Bunce, R. G. H.: Woodland survey of Great Britain 1971–  
1379 2001, *Earth System Science Data Discussions*, 8, 259-277, doi:10.5194/essdd-8-259-2015,  
1380 2015.

1381 Yin, Y., Wu, S., Chen, G., and Dai, E.: Attribution analyses of potential evapotranspiration  
1382 changes in China since the 1960s, *Theoretical and Applied Climatology*, 101, 19-28,  
1383 10.1007/s00704-009-0197-7, 2009.

1384 Zhang, K.-x., Pan, S.-m., Zhang, W., Xu, Y.-h., Cao, L.-g., Hao, Y.-p., and Wang, Y.:  
1385 Influence of climate change on reference evapotranspiration and aridity index and their  
1386 temporal-spatial variations in the Yellow River Basin, China, from 1961 to 2012, *Quaternary*  
1387 *International*, 380-381, 75-82, 10.1016/j.quaint.2014.12.037, 2015.

1388 Zhao, J., Xu, Z.-x., Zuo, D.-p., and Wang, X.-m.: Temporal variations of reference  
1389 evapotranspiration and its sensitivity to meteorological factors in Heihe River Basin, China,  
1390 *Water Science and Engineering*, 8, 1-8, 10.1016/j.wse.2015.01.004, 2015.

1391 Zwiers, F. W., and von Storch, H.: Taking Serial-Correlation into Account in Tests of the  
1392 Mean, *Journal of Climate*, 8, 336-351, doi:10.1175/1520-  
1393 0442(1995)008<0336:Tsciai>2.0.Co;2, 1995.

1394

1395

1396 Table 1. Description of input meteorological variables

Variable (units)	Source data	Ancillary files	Assumptions	Height
Air temperature (K)	MORECS air temperature	IHDTM elevation	Lapsed to IHDTM elevation	1.2 m
Specific humidity (kg kg <sup>-1</sup> )	MORECS vapour pressure	IHDTM elevation	Lapsed to IHDTM elevation  Constant air pressure = <u>+100</u> kPa	1.2 m
Downward LW radiation (W m <sup>-2</sup> )	MORECS air temperature, vapour pressure, sunshine hours	IHDTM elevation	Constant cloud base height	1.2 m
Downward SW radiation (W m <sup>-2</sup> )	MORECS sunshine hours	IHDTM elevation  Spatially-varying aerosol correction	No time-varying aerosol correction	1.2 m
Wind speed (m s <sup>-1</sup> )	MORECS wind speed	ETSU average wind speeds	Wind speed correction is constant	10 m
Precipitation (kg m <sup>-2</sup> s <sup>-1</sup> )	CEH-GEAR precipitation	-	No transformations performed	n/a
Daily temperature range (K)	CRU TS 3.21 daily temperature range	-	No spatial interpolation from 0.5° resolution.  No temporal interpolation (constant values for each month)	1.2 m

Surface air pressure (Pa)	WFD air pressure	IHDTM elevation	Mean-monthly values from WFD used (each year has same values). Lapsed to IHDTM elevation. No temporal interpolation (constant values for each month).	n/a
---------------------------	------------------	-----------------	-------------------------------------------------------------------------------------------------------------------------------------------------------	-----

1397  
1398

1399 Table 2: Rate of change of annual means of meteorological and potential evapotranspiration  
 1400 variables in Great Britain. Bold indicates trends that are significant at the 5% level. The  
 1401 ranges are given by the 95% CI.

Variable	Rate of change $\pm$ 95% CI				
	Great Britain	England	Scotland	Wales	English lowlands
Air temperature (K dec <sup>-1</sup> )	<b>0.21 <math>\pm</math> 0.15</b>	<b>0.23 <math>\pm</math> 0.14</b>	<b>0.17 <math>\pm</math> 0.12</b>	<b>0.21 <math>\pm</math> 0.15</b>	<b>0.25 <math>\pm</math> 0.17</b>
Specific humidity (g kg <sup>-1</sup> dec <sup>-1</sup> )	<b>0.049 <math>\pm</math> 0.037</b>	<b>0.054 <math>\pm</math> 0.04</b>	<b>0.040 <math>\pm</math> 0.036</b>	<b>0.055 <math>\pm</math> 0.037</b>	<b>0.053 <math>\pm</math> 0.044</b>
Downward SW radiation (W m <sup>-2</sup> dec <sup>-1</sup> )	<b>1.0 <math>\pm</math> 0.8</b>	<b>1.3 <math>\pm</math> 1.0</b>	0.5 $\pm$ 0.6	<b>1.1 <math>\pm</math> 0.9</b>	<b>1.5 <math>\pm</math> 1.0</b>
Downward LW radiation (W m <sup>-2</sup> dec <sup>-1</sup> )	<b>0.50 <math>\pm</math> 0.48</b>	0.45 $\pm$ 0.48	<b>0.58 <math>\pm</math> 0.48</b>	0.50 $\pm$ 0.55	0.42 $\pm$ 0.48
Wind speed (m s <sup>-1</sup> dec <sup>-1</sup> )	<b>-0.18 <math>\pm</math> 0.09</b>	<b>-0.16 <math>\pm</math> 0.09</b>	<b>-0.20 <math>\pm</math> 0.10</b>	<b>-0.25 <math>\pm</math> 0.16</b>	<b>-0.13 <math>\pm</math> 0.07</b>
Precipitation (mm d <sup>-1</sup> dec <sup>-1</sup> )	<b>0.08 <math>\pm</math> 0.06</b>	0.04 $\pm$ 0.06	<b>0.14 <math>\pm</math> 0.09</b>	0.08 $\pm$ 0.09	0.03 $\pm$ 0.05
Daily temperature range (K dec <sup>-1</sup> )	-0.06 $\pm$ 0.06	-0.03 $\pm$ 0.06	<b>-0.13 <math>\pm</math> 0.08</b>	0.00 $\pm$ 0.06	-0.04 $\pm$ 0.07
Relative humidity (% dec <sup>-1</sup> )	-0.39 $\pm$ 0.44	-0.43 $\pm$ 0.46	-0.33 $\pm$ 0.33	-0.36 $\pm$ 0.4	-0.50 $\pm$ 0.53
PET (mm d <sup>-1</sup> dec <sup>-1</sup> )	<b>0.021 <math>\pm</math> 0.021</b>	<b>0.025 <math>\pm</math> 0.024</b>	<b>0.015 <math>\pm</math> 0.015</b>	0.017 $\pm$ 0.021	<b>0.03 <math>\pm</math> 0.026</b>
Radiative component of PET (mm d <sup>-1</sup> dec <sup>-1</sup> )	<b>0.016 <math>\pm</math> 0.010</b>	<b>0.018 <math>\pm</math> 0.011</b>	<b>0.013 <math>\pm</math> 0.008</b>	<b>0.020 <math>\pm</math> 0.013</b>	<b>0.018 <math>\pm</math> 0.011</b>
Aerodynamic component of PET (mm d <sup>-1</sup> dec <sup>-1</sup> )	0.007 $\pm$ 0.011	0.009 $\pm$ 0.013	0.004 $\pm$ 0.009	0.001 $\pm$ 0.013	0.015 $\pm$ 0.015
PETI (mm d <sup>-1</sup> dec <sup>-1</sup> )	0.019 $\pm$ 0.020	<b>0.023 <math>\pm</math> 0.023</b>	0.014 $\pm$ 0.014	0.016 $\pm$ 0.020	<b>0.028 <math>\pm</math> 0.025</b>

1402

1403 Table 3. Contributions to the rate of change of PET and its radiative and aerodynamic  
 1404 components. For each variable, the first column shows the contribution calculated using  
 1405 regional averages, along with the associated 95% CI. The second column shows the  
 1406 contribution calculated at 1 km resolution, then averaged over each region. The uncertainty  
 1407 on this value is difficult to calculate as the pixels are highly spatially correlated, so the  
 1408 uncertainty range from the regional analysis is used in Fig. 13.

a) Contribution to rate of change of PET (mm d <sup>-1</sup> decade <sup>-1</sup> )												
	Air temperature		Specific humidity		Wind speed		Downward LW		Downward SW		Total	
	Regional	Pixel	Regional	Pixel	Regional	Pixel	Regional	Pixel	Regional	Pixel	Regional	Pixel
England	<b>0.041</b> ± <b>0.025</b>	0.039	<b>-0.025</b> ± <b>0.019</b>	-0.024	<b>-0.010</b> ± <b>0.005</b>	-0.007	0.005 ± 0.006	0.005	<b>0.013</b> ± <b>0.009</b>	0.012	0.025 ± 0.034	0.024
Scotland	<b>0.029</b> ± <b>0.021</b>	0.023	<b>-0.020</b> ± <b>0.018</b>	-0.017	<b>-0.010</b> ± <b>0.005</b>	-0.007	0.006 ± <b>0.005</b>	0.006	0.005 ± 0.005	0.004	0.010 ± 0.029	0.008
Wales	<b>0.039</b> ± <b>0.028</b>	0.036	<b>-0.026</b> ± <b>0.018</b>	-0.025	<b>-0.011</b> ± <b>0.007</b>	-0.009	0.006 ± 0.006	0.006	<b>0.010</b> ± <b>0.009</b>	0.009	0.017 ± 0.036	0.017
England and lowlands	<b>0.043</b> ± <b>0.029</b>	0.042	<b>-0.024</b> ± <b>0.020</b>	-0.023	<b>-0.008</b> ± <b>0.004</b>	-0.008	0.005 ± 0.006	0.005	<b>0.015</b> ± <b>0.010</b>	0.015	0.031 ± 0.038	0.030
Great Britain	<b>0.037</b> ± <b>0.026</b>	0.031	<b>-0.023</b> ± <b>0.018</b>	-0.022	<b>-0.010</b> ± <b>0.005</b>	-0.007	0.006 ± <b>0.005</b>	0.005	<b>0.010</b> ± <b>0.007</b>	0.007	0.019 ± 0.033	0.014
b) Contribution to rate of change of radiative component of (mm d <sup>-1</sup> decade <sup>-1</sup> )												
	Air temperature		Specific humidity		Wind speed		Downward LW		Downward SW		Total	
	Regional	Pixel	Regional	Pixel	Regional	Pixel	Regional	Pixel	Regional	Pixel	Regional	Pixel
England	<b>-0.009</b> ± <b>0.006</b>	-0.009	n/a	n/a	<b>0.009</b> ± <b>0.005</b>	0.007	0.005 ± 0.006	0.005	<b>0.014</b> ± <b>0.010</b>	0.013	<b>0.018</b> ± <b>0.013</b>	0.016
Scotland	<b>-0.006</b> ± <b>0.005</b>	-0.006	n/a	n/a	<b>0.009</b> ± <b>0.004</b>	0.007	0.006 ± <b>0.005</b>	0.006	0.005 ± 0.005	0.004	0.014 ± <b>0.010</b>	0.012
Wales	<b>-0.007</b> ± <b>0.005</b>	-0.007	n/a	n/a	<b>0.014</b> ± <b>0.009</b>	0.013	0.006 ± 0.006	0.006	<b>0.010</b> ± <b>0.009</b>	0.010	<b>0.023</b> ± <b>0.015</b>	0.022
England and lowlands	<b>-0.010</b> ± <b>0.007</b>	-0.010	n/a	n/a	<b>0.007</b> ± <b>0.004</b>	0.006	0.005 ± 0.006	0.005	<b>0.016</b> ± <b>0.011</b>	0.015	<b>0.017</b> ± <b>0.014</b>	0.017
Great Britain	<b>-0.008</b> ± <b>0.006</b>	-0.007	n/a	n/a	<b>0.009</b> ± <b>0.005</b>	0.007	0.006 ± <b>0.006</b>	0.006	<b>0.010</b> ± <b>0.008</b>	0.008	<b>0.017</b> ± <b>0.012</b>	0.013
c) Contribution to rate of change of aerodynamic component of PET (mm d <sup>-1</sup> decade <sup>-1</sup> )												
	Air temperature		Specific humidity		Wind speed		Downward LW		Downward SW		Total	
	Regional	Pixel	Regional	Pixel	Regional	Pixel	Regional	Pixel	Regional	Pixel	Regional	Pixel
England	<b>0.052</b> ± <b>0.032</b>	0.050	<b>-0.026</b> ± <b>0.020</b>	-0.026	<b>-0.018</b> ± <b>0.010</b>	-0.015	n/a	n/a	n/a	n/a	0.007 ± 0.039	0.009

Scotland	<b>0.037</b> ± <b>0.027</b>	0.033	<b>-0.021</b> ± <b>0.019</b>	-0.019	<b>-0.019</b> ± <b>0.010</b>	-0.015	n/a	n/a	n/a	n/a	-0.003 ± 0.034	-0.001
Wales	<b>0.048</b> ± <b>0.035</b>	0.046	<b>-0.028</b> ± <b>0.019</b>	-0.027	<b>-0.026</b> ± <b>0.016</b>	-0.023	n/a	n/a	n/a	n/a	-0.005 ± 0.042	-0.003
England and Wales	<b>0.056</b> ± <b>0.037</b>	0.055	<b>-0.026</b> ± <b>0.021</b>	-0.025	<b>-0.015</b> ± <b>0.008</b>	-0.014	n/a	n/a	n/a	n/a	0.015 ± 0.044	0.015
Great Britain	<b>0.046</b> ± <b>0.033</b>	0.041	<b>-0.025</b> ± <b>0.019</b>	-0.023	<b>-0.020</b> ± <b>0.010</b>	-0.015	n/a	n/a	n/a	n/a	0.002 ± 0.039	0.003

1409  
1410

1411 Table 4. Contribution of the trend in each variable to the trends in annual mean PET and its  
 1412 radiative and aerodynamic components as a percentage of the fitted trend in PET and its  
 1413 components.

a) Potential evapotranspiration (PET)						
	Air temperature	Specific humidity	Wind speed	Downward LW	Downward SW	Total
England	154 %	-88 %	-22 %	17 %	47 %	108 %
Scotland	150 %	-74 %	-23 %	26 %	18 %	97 %
Wales	200 %	-130 %	-38 %	28 %	50 %	109 %
English lowlands	142 %	-77 %	-20 %	15 %	45 %	105 %
Great Britain	155 %	-87 %	-23 %	19 %	31 %	96 %
b) Radiative component of PET						
	Air temperature	Specific humidity	Wind speed	Downward LW	Downward SW	Total
England	-47 %	n/a	40 %	28 %	71 %	92 %
Scotland	-42 %	n/a	62 %	46 %	36 %	102 %
Wales	-34 %	n/a	69 %	29 %	52 %	116 %
English lowlands	-53 %	n/a	35 %	27 %	86 %	95 %
Great Britain	-44 %	n/a	46 %	31 %	53 %	87 %
c) Aerodynamic component of PET						
	Air temperature	Specific humidity	Wind speed	Downward LW	Downward SW	Total
England	245 %	-115 %	-48 %	n/a	n/a	82 %
Scotland	68 %	-14 %	-33 %	n/a	n/a	21 %
Wales	-135 %	72 %	-42 %	n/a	n/a	-105 %
English lowlands	282 %	-126 %	-47 %	n/a	n/a	109 %
Great Britain	168 %	-76 %	-44 %	n/a	n/a	48 %

1414  
 1415

1416 Table 5. Contributions to the rate of change of PET and its radiative and aerodynamic  
 1417 components- when relative humidity is used. For each variable, the first column shows the  
 1418 contribution calculated using regional averages, along with the associated 95% CI. The  
 1419 second column shows the contribution calculated at 1 km resolution, then averaged over each  
 1420 region. The uncertainty on this value is difficult to calculate as the pixels are highly spatially  
 1421 correlated, so the uncertainty range from the regional analysis is used in Fig. 13.

a) Contribution to rate of change of PET (mm d <sup>-1</sup> decade <sup>-1</sup> )												
	Air temperature		Relative humidity		Wind speed		Downward LW		Downward SW		Total	
	Regional	Pixel	Regional	Pixel	Regional	Pixel	Regional	Pixel	Regional	Pixel	Regional	Pixel
England	<b>-0.002</b> ± <b>0.001</b>	-0.000	0.015 ± 0.016	0.013	<b>-0.010</b> ± <b>0.005</b>	-0.007	0.005 ± 0.006	0.005	<b>0.013</b> ± <b>0.009</b>	0.012	<b>0.021</b> ± <b>0.020</b>	0.023
Scotland	<b>-0.001</b> ± <b>0.001</b>	0.000	0.011 ± 0.011	0.008	<b>-0.010</b> ± <b>0.005</b>	-0.007	<b>0.006</b> ± <b>0.005</b>	0.006	0.005 ± 0.005	0.004	0.010 ± 0.014	0.011
Wales	<b>-0.002</b> ± <b>0.001</b>	-0.000	0.013 ± 0.014	0.012	<b>-0.011</b> ± <b>0.007</b>	-0.009	0.006 ± 0.006	0.006	<b>0.010</b> ± <b>0.009</b>	0.009	0.015 ± 0.019	0.018
English lowlands	<b>-0.003</b> ± <b>0.002</b>	-0.000	0.017 ± 0.018	0.017	<b>-0.008</b> ± <b>0.004</b>	-0.008	0.005 ± 0.006	0.005	<b>0.015</b> ± <b>0.010</b>	0.015	<b>0.026</b> ± <b>0.022</b>	0.028
Great Britain	<b>-0.002</b> ± <b>0.001</b>	0.000	0.013 ± 0.015	0.011	<b>-0.010</b> ± <b>0.005</b>	-0.007	<b>0.006</b> ± <b>0.005</b>	0.005	<b>0.010</b> ± <b>0.007</b>	0.007	0.016 ± 0.018	0.016
b) Contribution to rate of change of radiative component of (mm d <sup>-1</sup> decade <sup>-1</sup> )												
	Air temperature		Relative humidity		Wind speed		Downward LW		Downward SW		Total	
	Regional	Pixel	Regional	Pixel	Regional	Pixel	Regional	Pixel	Regional	Pixel	Regional	Pixel
England	<b>-0.009</b> ± <b>0.006</b>	-0.009	n/a	n/a	<b>0.009</b> ± <b>0.005</b>	0.007	0.005 ± 0.006	0.005	<b>0.014</b> ± <b>0.010</b>	0.013	<b>0.018</b> ± <b>0.013</b>	0.016
Scotland	<b>-0.006</b> ± <b>0.005</b>	-0.006	n/a	n/a	<b>0.009</b> ± <b>0.004</b>	0.007	<b>0.006</b> ± <b>0.005</b>	0.006	0.005 ± 0.005	0.004	<b>0.014</b> ± <b>0.010</b>	0.012
Wales	<b>-0.007</b> ± <b>0.005</b>	-0.007	n/a	n/a	<b>0.014</b> ± <b>0.009</b>	0.013	0.006 ± 0.006	0.006	<b>0.010</b> ± <b>0.009</b>	0.010	<b>0.023</b> ± <b>0.015</b>	0.022
English lowlands	<b>-0.010</b> ± <b>0.007</b>	-0.010	n/a	n/a	<b>0.007</b> ± <b>0.004</b>	0.006	0.005 ± 0.006	0.005	<b>0.016</b> ± <b>0.011</b>	0.015	<b>0.017</b> ± <b>0.014</b>	0.017
Great Britain	<b>-0.008</b> ± <b>0.006</b>	-0.007	n/a	n/a	<b>0.009</b> ± <b>0.005</b>	0.007	<b>0.006</b> ± <b>0.006</b>	0.006	<b>0.010</b> ± <b>0.008</b>	0.008	<b>0.017</b> ± <b>0.012</b>	0.013
c) Contribution to rate of change of aerodynamic component of PET (mm d <sup>-1</sup> decade <sup>-1</sup> )												
	Air temperature		Specific humidity		Wind speed		Downward LW		Downward SW		Total	
	Regional	Pixel	Regional	Pixel	Regional	Pixel	Regional	Pixel	Regional	Pixel	Regional	Pixel
England	<b>0.006</b> ± <b>0.004</b>	0.006	0.015 ± 0.017	0.014	<b>-0.018</b> ± <b>0.010</b>	-0.015	n/a	n/a	n/a	n/a	0.003 ± 0.020	0.004



Scotland	<b>0.004</b> ± <b>0.003</b>	0.004	0.011 ± 0.011	0.009	<b>-0.019</b> ± <b>0.010</b>	-0.015	n/a	n/a	n/a	n/a	-0.004 ± 0.015	-0.002
Wales	<b>0.005</b> ± <b>0.004</b>	0.005	0.013 ± 0.015	0.012	<b>-0.026</b> ± <b>0.016</b>	-0.023	n/a	n/a	n/a	n/a	-0.007 ± 0.022	-0.006
English lowlands	<b>0.007</b> ± <b>0.004</b>	0.006	0.018 ± 0.019	0.017	<b>-0.015</b> ± <b>0.008</b>	-0.014	n/a	n/a	n/a	n/a	0.009 ± 0.021	0.010
Great Britain	<b>0.005</b> ± <b>0.004</b>	0.005	0.014 ± 0.015	0.011	<b>-0.020</b> ± <b>0.010</b>	-0.015	n/a	n/a	n/a	n/a	-0.001 ± 0.019	0.000

1422  
1423

1424 Table 6. Contribution of the trend in each variable to the trends in annual mean PET and its  
 1425 radiative and aerodynamic components as a percentage of the fitted trend in PET and its  
 1426 components when relative humidity is used.

a) Potential evapotranspiration (PET)						
	Air temperature	Relative humidity	Wind speed	Downward LW	Downward SW	Total
England	-0%	57%	-22%	17%	47%	99%
Scotland	0%	65%	-23%	26%	18%	85%
Wales	-0%	68%	-38%	27%	50%	107%
English lowlands	-0%	57%	-20%	15%	45%	97%
Great Britain	0%	60%	-23%	19%	31%	87%
b) Radiative component of PET						
	Air temperature	Relative humidity	Wind speed	Downward LW	Downward SW	Total
England	-47%	n/a	40%	28%	71%	92%
Scotland	-42%	n/a	62%	46%	36%	102%
Wales	-34%	n/a	69%	29%	52%	116%
English lowlands	-53%	n/a	35%	27%	86%	95%
Great Britain	-44%	n/a	46%	31%	53%	87%
c) Aerodynamic component of PET						
	Air temperature	Relative humidity	Wind speed	Downward LW	Downward SW	Total
England	29%	78%	-48%	n/a	n/a	59%
Scotland	8%	14%	-33%	n/a	n/a	-11%
Wales	-15%	-33%	-42%	n/a	n/a	-90%
English lowlands	33%	98%	-47%	n/a	n/a	84%
Great Britain	19%	52%	-44%	n/a	n/a	27%

1427  
 1428

1429 Table A1. Details of sites used for validation of meteorological data.

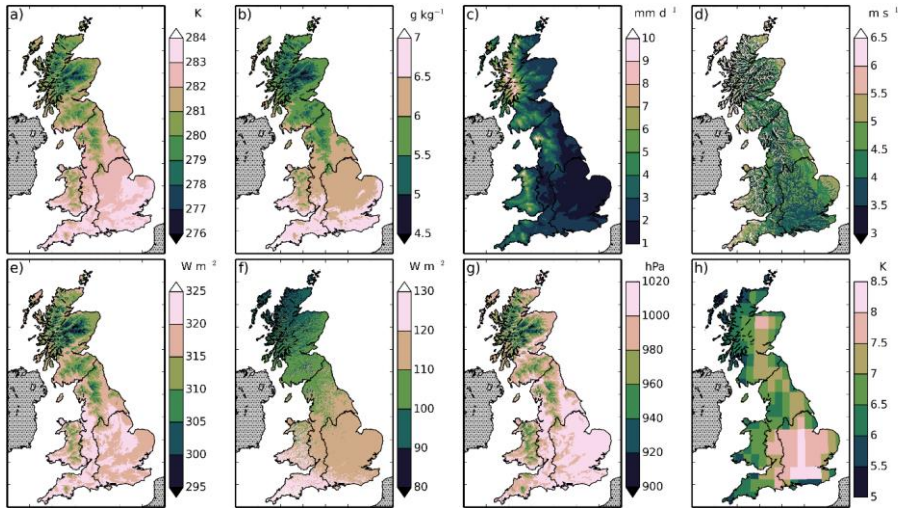
Site (ID)	Latitude	Longitude	Years	Land cover	Citation
Alice Holt (UK-Ham)	51.15	-0.86	2004-2012	Deciduous broadleaf woodland	(Wilkinson et al., 2012; Heinemeyer et al., 2012)
Griffin Forest (UK-Gri)	56.61	-3.80	1997-2001, 2004-2008	Evergreen needleleaf woodland	(Clement, 2003)
Auchencorth Moss (UK-AMo)	55.79	-3.24	2002-2006	Grass and crop	(Billett et al., 2004)
Easter Bush (UK-EBu)	55.87	-3.21	2004-2008	Grass	(Gilmanov et al., 2007; Soussana et al., 2007)

1430

1431 Table A2. Correlation statistics for meteorological variables with data from four sites.

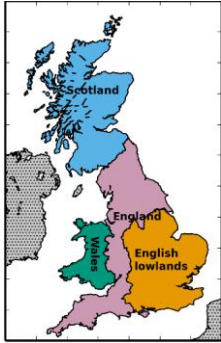
a) Air temperature			
Site	$r^2$	Mean bias	RMSE
Alice Holt	0.95	0.10 K	1.17 K
Griffin Forest	0.94	0.21 K	1.17 K
Auchencorth Moss	0.98	-0.02 K	0.78 K
Easter Bush	0.97	-0.46 K	0.96 K
b) Downward SW radiation			
Site	$r^2$	Mean bias	RMSE
Alice Holt	0.94	-3.01 W m <sup>-2</sup>	22.92 W m <sup>-2</sup>
Griffin Forest	0.85	-4.90 W m <sup>-2</sup>	31.29 W m <sup>-2</sup>
Auchencorth Moss	0.91	14.27 W m <sup>-2</sup>	27.96 W m <sup>-2</sup>
Easter Bush	0.88	5.73 W m <sup>-2</sup>	27.15 W m <sup>-2</sup>
c) Mixing ratio			
Site	$r^2$	Mean bias	RMSE
Alice Holt	0.90	-0.02 mmol mol <sup>-1</sup>	1.09 mmol mol <sup>-1</sup>
Griffin Forest	0.76	0.08 mmol mol <sup>-1</sup>	1.56 mmol mol <sup>-1</sup>
d) Wind speed			
Site	$r^2$	mean bias	RMSE
Alice Holt	0.88	1.24 m s <sup>-1</sup>	1.45 m s <sup>-1</sup>
Griffin Forest	0.59	1.36 m s <sup>-1</sup>	1.81 m s <sup>-1</sup>
Auchencorth Moss	0.63	-0.38 m s <sup>-1</sup>	1.37 m s <sup>-1</sup>
Easter Bush	0.82	0.44 m s <sup>-1</sup>	1.03 m s <sup>-1</sup>
e) Surface air pressure			
Site	$r^2$	Mean bias	RMSE
Griffin Forest	0.05	-0.42 hPa	1.38 hPa
Auchencorth Moss	0.01	-1.06 hPa	1.57 hPa
Easter Bush	0.03	0.01 hPa	1.33 hPa

1432



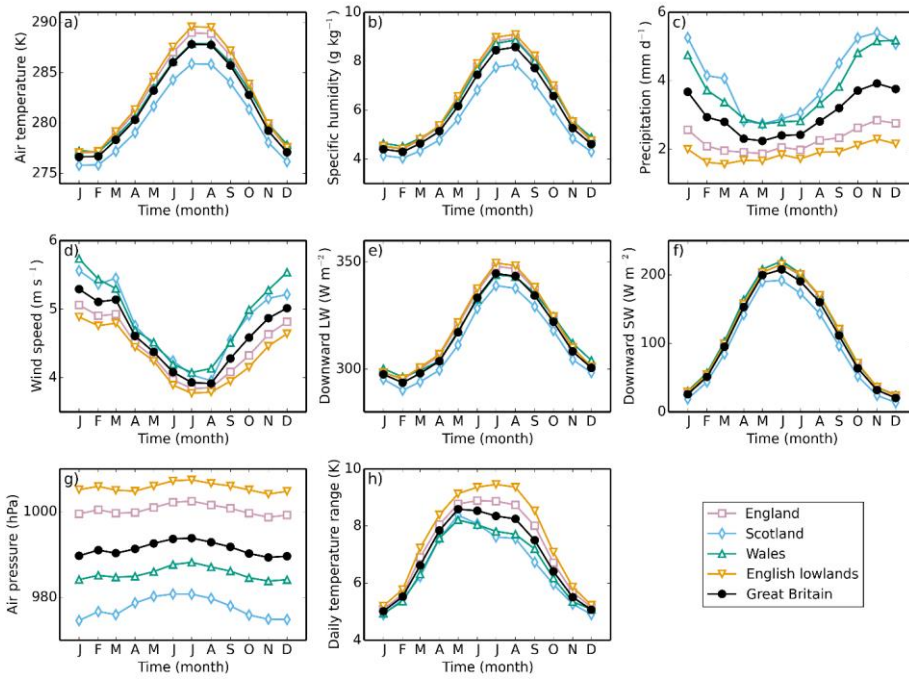
1433

1434 Figure 1. Means of the meteorological variables over the years 1961-2012. The variables are  
 1435 a) 1.2 m air temperature, b) 1.2 m specific humidity, c) precipitation, d) 10 m wind speed, e)  
 1436 downward LW radiation, f) downward SW radiation, g) surface air pressure, h) daily air  
 1437 temperature range.

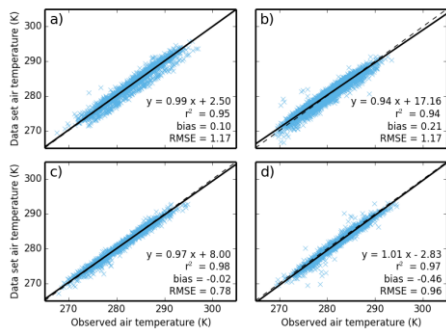


1438

1439 Figure 2. The regions used to calculate the area means. The English lowlands are a sub-  
1440 region of England. England, Scotland and Wales together form the fifth region, Great Britain.



1441  
 1442 Figure 3. Mean monthly climatology of meteorological variables, a) 1.2 m air temperature, b)  
 1443 1.2 m specific humidity, c) precipitation, d) 10 m wind speed, e) downward LW radiation, f)  
 1444 downward SW radiation, g) surface air pressure, h) daily air temperature range, for five  
 1445 different regions of Great Britain, calculated over the years 1961-2012.  
 1446



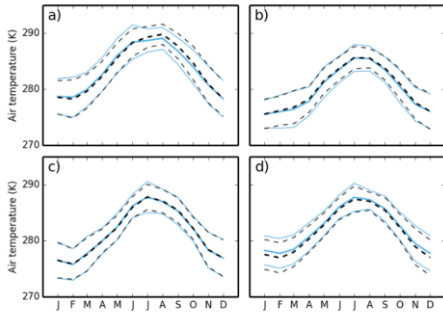
1447

1448 Figure 4. Plot of data set air temperature against daily mean observed air temperature at four  
 1449 sites. The dashed line shows the one to one line, while the solid line shows the linear regression,  
 1450 the equation of which is shown in the lower right of each plot, along with the  $r^2$  value, the mean  
 1451 bias and the RMSE. The sites are a) Alice Holt; b) Griffin Forest; c) Auchencorth Moss; d)  
 1452 Easter Bush.

1453



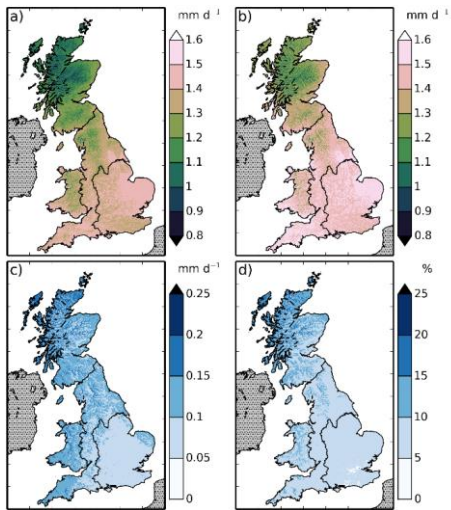
1454



1455

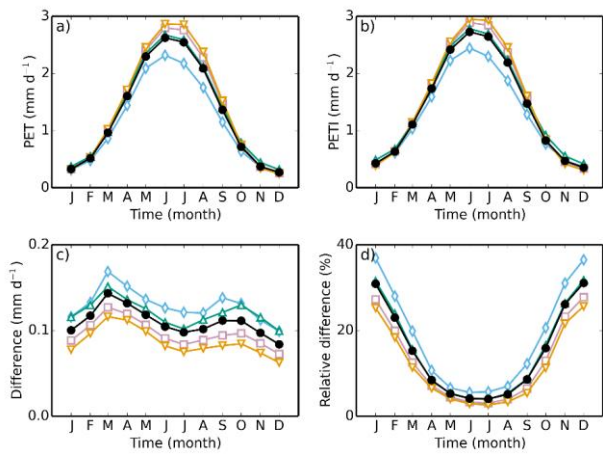
1456 Figure 5. Mean monthly climatology of the dataset (black, dashed lines) and observed (blue,  
1457 solid lines) air temperatures, calculated for the period of observations. The thicker lines show  
1458 the means, while the thinner lines show the standard errors on each measurement. Sites as in  
1459 Fig. 4.

1460



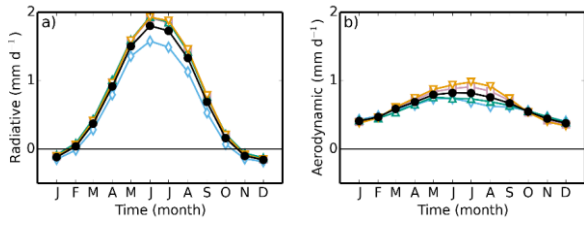
1461

1462 Figure 6. Mean a) PET, b) PETI, c) absolute difference between PETI and PET and d) relative  
 1463 difference calculated over the years 1961-2012.



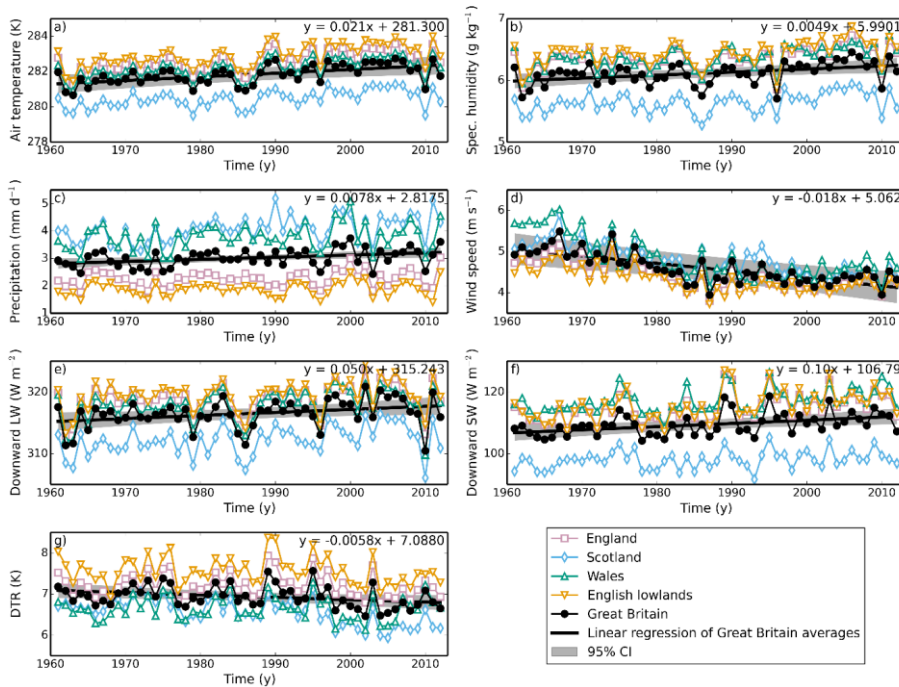
1464

1465 Figure 7. Mean monthly climatology of a) PET, b) PETI, c) absolute difference between PETI  
 1466 and PET, d) relative difference, for five different regions of Great Britain, calculated over the  
 1467 years 1961-2012. Symbols as in Fig. 3.



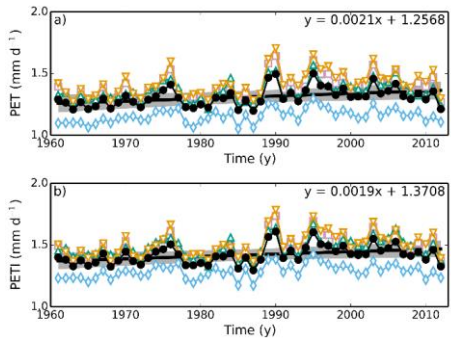
1468

1469 Figure 8. Mean-monthly climatology of the a) radiative and b) aerodynamic components of the  
 1470 PET for five different regions of Great Britain, calculated over the years 1961-2012. Symbols  
 1471 as in Fig. 3.



1472

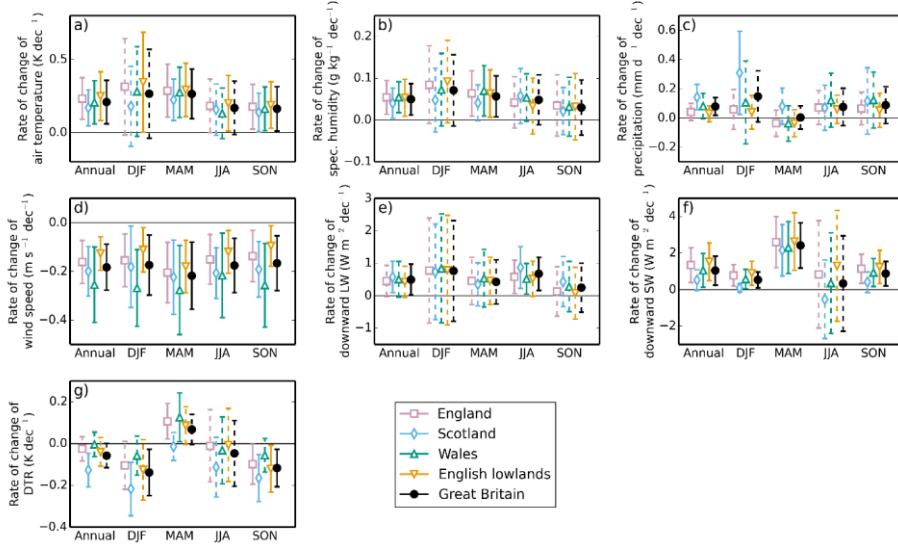
1473 Figure 9. Annual means of the meteorological variables, a) 1.2 m air temperature, b) 1.2 m  
 1474 specific humidity, c) precipitation, d) 10 m wind speed, e) downward LW radiation, f)  
 1475 downward SW radiation, g) daily air temperature range, over five regions of Great Britain. The  
 1476 solid black lines show the linear regression fit to the Great Britain annual means, while the grey  
 1477 strip shows the 95% CI of the same fit, assuming a non-zero lag-1 correlation coefficient. The  
 1478 equation of this fit is shown in the top right-hand corner of each plot.



1479

1480 Figure 10. Annual means of a) PET and b) PETI for five regions of Great Britain. Symbols as  
 1481 in Fig. 9.

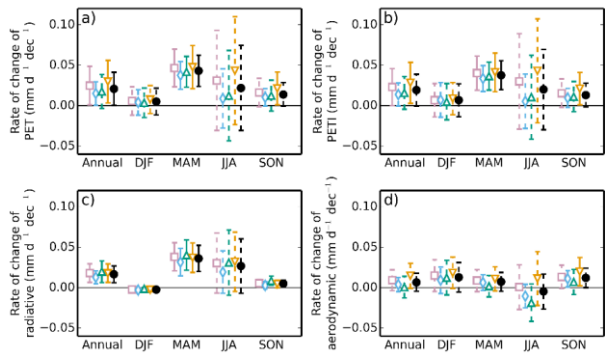
1482



1483

1484 Figure 11. Rate of change of annual and seasonal means of meteorological variables, a) 1.2 m  
 1485 air temperature, b) 1.2 m specific humidity, c) precipitation, d) 10 m wind speed, e) downward  
 1486 LW radiation, f) downward SW radiation, g) daily air temperature range, for five regions of  
 1487 Great Britain for the years 1961-2012. Error bars are the 95% CI calculated assuming a non-  
 1488 zero lag-1 correlation coefficient. Solid error bars indicate slopes that are statistically  
 1489 significant at the 5% level, dashed error bars indicate slopes that are not significant at the 5%  
 1490 level.

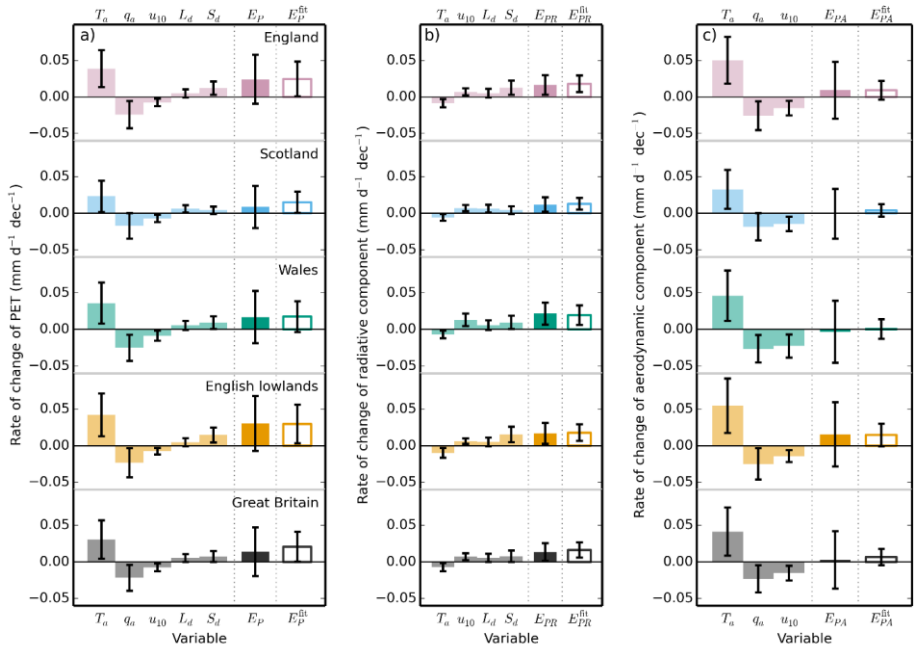
1491



1492

1493 Figure 12. Rate of change of annual and seasonal means of a) PET, b) PETI, c) the radiative  
 1494 component of PET and d) the aerodynamic component of PET for five regions of Great Britain  
 1495 for the years 1961-2012. Symbols as in Fig. 11.

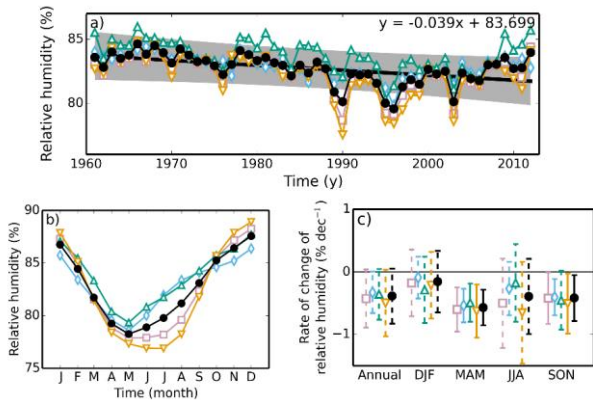




1496

1497 Figure 13. The contribution of the rate of change of each meteorological variable to the rate of  
 1498 change of a) PET, b) the radiative component and c) the aerodynamic component. The first five  
 1499 (four; three) bars are the contribution to the rate of change of annual mean PET from the rate  
 1500 of change of each of the variables, calculated per pixel, than averaged over each region. Each  
 1501 bar has an error bar showing the 95% CI on each value. Since the pixels are highly spatially  
 1502 correlated, we use the more conservative CI calculated by applying this analysis to the regional  
 1503 means. The next bar is the sum of the other bars and shows the attributed rate of change of  
 1504 annual mean PET. The final bar shows the slope and its associated CI obtained from the linear  
 1505 regression of the mean annual PET for each region.

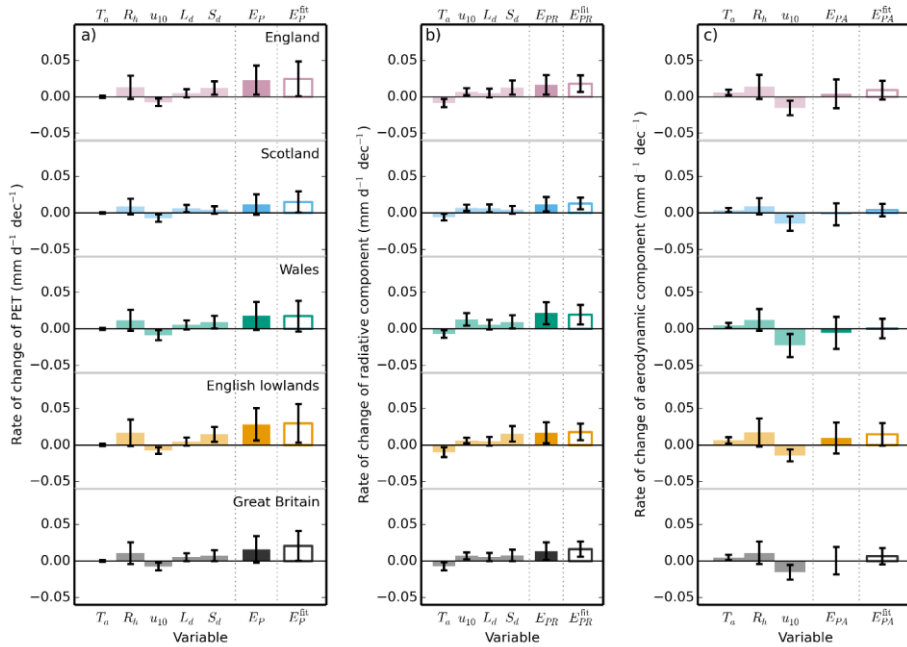
1506



1507

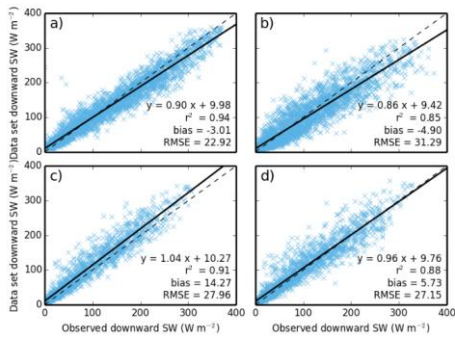
1508 Figure 14. Regional annual means (a), regional mean-monthly climatology (b) and regional  
 1509 rates of change of relative humidity for the years 1961-2012.

1510



1511  
 1512 Figure 15. The contribution of the rate of change of each meteorological variable to the rate of  
 1513 change of a) PET, b) the radiative component and c) the aerodynamic component, with relative  
 1514 humidity instead of specific humidity. The first five (four; three) bars are the contribution to  
 1515 the rate of change of annual mean PET from the rate of change of each of the variables,  
 1516 calculated per pixel, then averaged over each region. Each bar has an error bar showing the  
 1517 95% CI on each value. Since the pixels are highly spatially correlated, we use the more  
 1518 conservative CI calculated by applying this analysis to the regional means. The next bar is the  
 1519 sum of the other bars and shows the attributed rate of change of annual mean PET. The final  
 1520 bar shows the slope and its associated CI obtained from the linear regression of the mean annual  
 1521 PET for each region.

1522  
 1523

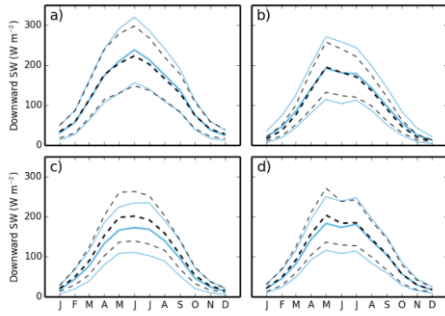


1524

1525 Figure A1. Plot of data set downward SW radiation against daily mean observed downward  
 1526 SW radiation at four flux sites. Symbols and sites as in Fig. 4.

1527

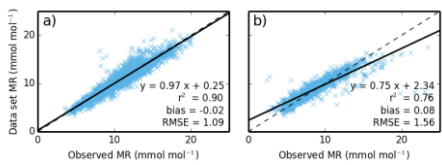
1528



1529

1530 Figure A2. Mean monthly climatology of the dataset (black, dashed lines) and observed (blue,  
1531 solid lines) downward SW radiation, calculated for the period of observations. Symbols as in  
1532 Fig. 5, sites as in Fig. 4.

1533

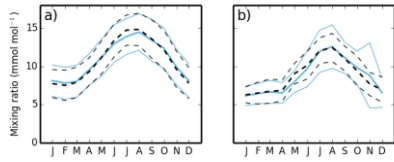


1534

1535 Figure A3. Plot of mixing ratio calculated using dataset meteorology against daily mean  
 1536 observed mixing ratio at four sites. Symbols as in Fig. 4. The sites are a) Alice Holt and b)  
 1537 Griffin Forest.

1538

1539

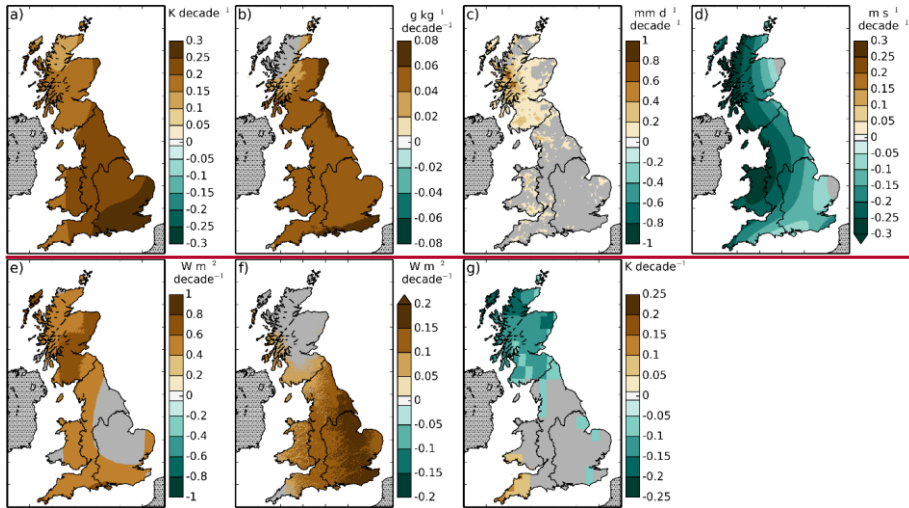


1540

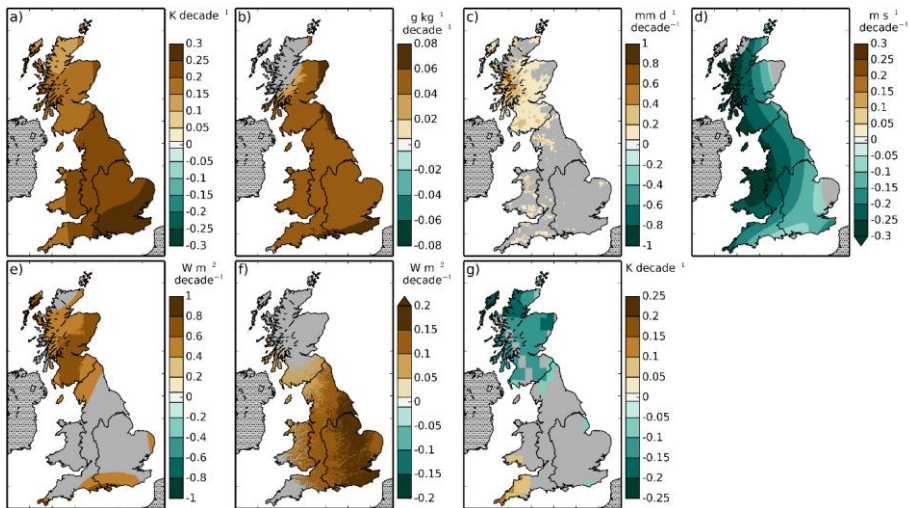
1541 Figure A4. Mean monthly climatology of the dataset (black, dashed lines) and observed (blue,  
1542 solid lines) mixing ratio, calculated for the period of observations. Symbols as in Fig. 5. Sites  
1543 as in Fig. A3.

1544

1545



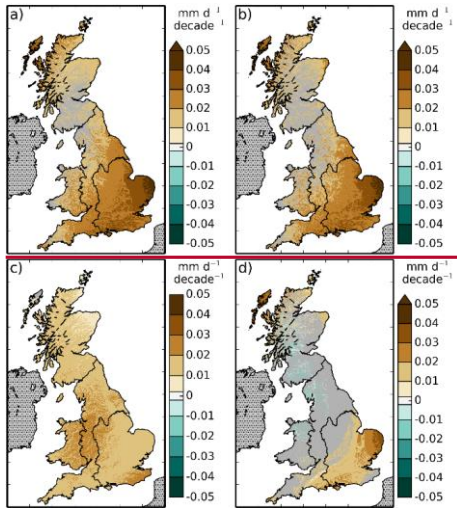
1546



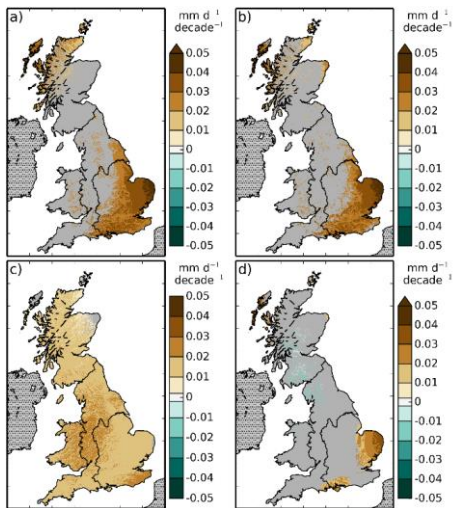
1547 Figure B1. Rate of change of the annual means of the meteorological variables, a) 1.2 m air  
1548 temperature, b) 1.2 m specific humidity, c) precipitation, d) 10 m wind speed, e) downward  
1549 LW radiation, f) downward SW radiation, g) daily air temperature range over the period 1961-  
1550 2012. Areas for which the trend was not significant are shown in grey.  
1551



1552

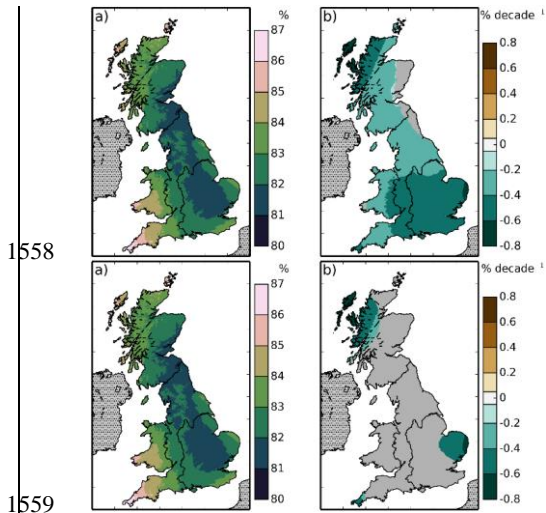


1553



1554 Figure B2. Rate of change the annual means of a) PET, b) PETI, c) the radiative component of  
1555 PET, d) the aerodynamic component of PET over the period 1961-2012. Areas for which the  
1556 trend was not significant are shown in grey.

1557



1558

1559

1560 Figure B3. ~~Mean~~Maps of a) mean and b) rate of change of annual mean of the relative humidity  
 1561 over the years 1961-2012. ~~(a). Rate of change of the annual mean of relative humidity (b).~~  
 1562 Areas for which the trend was not significant are shown in grey.

Formatted: Font color: Black

1563

1564